

Cosmic Rays and the Search for a Lorentz Invariance Violation

Wolfgang Bietenholz¹

John von Neumann Institut (NIC)
Deutsches Elektronen-Synchrotron (DESY)
Platanenallee 6, D-15738 Zeuthen, Germany

DESY-08-072

This is an introductory review about the on-going search for a signal of Lorentz Invariance Violation (LIV) in cosmic rays. We first summarise basic aspects of cosmic rays, focusing on rays of ultra high energy (UHECRs). We discuss the Greisen-Zatsepin-Kuz'min (GZK) energy cutoff for cosmic protons, which is predicted due to photopion production in the Cosmic Microwave Background (CMB). This is a process of modest energy in the proton rest frame. It can be investigated to a high precision in the laboratory, *if* Lorentz transformations apply even at factors $\gamma \sim O(10^{11})$. For heavier nuclei the energy attenuation is even faster due to photo-disintegration, again *if* this process is Lorentz invariant. Hence the viability of Lorentz symmetry up to tremendous γ -factors — far beyond accelerator tests — is a central issue.

Next we comment on conceptual aspects of Lorentz Invariance and the possibility of its spontaneous breaking. This could lead to slightly particle dependent “Maximal Attainable Velocities”. We discuss their effect in decays, Čerenkov radiation, the GZK cutoff and neutrino oscillation in cosmic rays.

We also review the search for LIV in cosmic γ -rays. For multi TeV γ -rays we possibly encounter another puzzle related to the transparency of the CMB, similar to the GZK cutoff, due to electron/positron creation and subsequent inverse Compton scattering. The photons emitted in a Gamma Ray Burst occur at lower energies, but their very long path provides access to information not far from the Planck scale. We discuss conceivable non-linear photon dispersions based on non-commutative geometry or effective approaches.

No LIV has been observed so far. However, even extremely tiny LIV effects could change the predictions for cosmic ray physics drastically.

An Appendix is devoted to the recent hypothesis by the Pierre Auger Collaboration, which identifies nearby Active Galactic Nuclei — or objects next to them — as probable UHECR sources.

¹Present address: Institut für Theoretische Physik, Universität Regensburg,
D-93040 Regensburg, Germany. E-Mail: bietenho@ifh.de

Preface : This overview is designed for non-experts who are interested in a cursory look at this exciting and lively field of research. We intend to sketch phenomenological highlights and theoretical concepts in an entertaining and self-contained form (as far as possible), avoiding technical details, and without claiming to be complete or rigorous.

Contents

1	Cosmic rays	3
1.1	Discovery and basic properties of cosmic rays	3
1.2	The Cosmic Microwave Background	7
1.3	The Greisen-Zatsepin-Kuz'min cutoff	8
1.4	Observations of super-GZK events	14
2	Lorentz Invariance and its possible violation	21
2.1	Link to the CPT Theorem	23
2.2	Status of experimental LI tests	24
2.3	Standard Model Extension (SME)	26
2.4	Maximal Attainable Velocities (MAVs)	29
2.5	Applications of distinct MAVs	31
2.5.1	Decay at ultra high energy	31
2.5.2	Vacuum Čerenkov radiation	31
2.5.3	Impact on the GZK cutoff	32
2.5.4	Impact on neutrino oscillation	35
3	Cosmic γ-rays	37
3.1	Another puzzle for high energy cosmic rays ?	37
3.2	γ -Ray-Bursts (GRBs)	40
3.3	Non-commutative (NC) field theory	41
3.3.1	The photon in a NC world	46
3.3.2	The NC photon revisited non-perturbatively	49
3.4	Analysis of GRB and blazar flare data	53
3.5	Effective Field Theory and vacuum birefringence	56
4	Conclusions	59
A	New development since Nov. 2007:	
	The AGN Hypothesis	62
A.1	Comments on the AGN Hypothesis	63
B	Table of short-hand notations	66

1 Cosmic rays

1.1 Discovery and basic properties of cosmic rays

Cosmic rays consist of particles and nuclei of cosmic origin with high energy. Part of the literature restricts this term to electrically charged objects, but in this review we adapt the broader definition, which also embraces cosmic neutrinos and photons.

The *discovery* of cosmic rays dates back to the beginning of the 20th century. At that time electroscopes and electrometers were developed to a point which enabled the reliable measurement of ionising γ -radiation. Around 1909 the natural radioactivity on the surface of the Earth was already well-explored, and scientists turned their attention to the radiation above ground. If its origin was solely radioactivity in the Earth, a rapid reduction would have been predicted with increasing height.

In 1910 first observations on balloons led to contradictory results: K. Bergwitz did report such a rapid decrease [1], whereas A. Gockel could not confirm it [2]. Still in 1910 Th. Wulf — who had constructed an improved electrometer — performed measurements on the Eiffel tower. He found some reduction of the γ -radiation compared to the ground, but this effect was clearly weaker than he had expected [3]. Although he admitted that the iron masses of the tower could affect the outcome, he concluded that either the absorption in the air is weaker than expected, or that there are significant sources above ground.

In 1912 V.F. Hess evaluated his measurements during seven balloon journeys [4]: he found only a very mild reduction of the radiation (hardly 10 %) for heights around 1000 m. Rising further he observed a slight increase, so that the radiation intensity around 2000 was very similar that that on ground. As he went even higher (up to 5350 m) he found a *significant increase*, which was confirmed in independent balloon-borne experiments by W. Kolhörster in 1913 up to 6300 m [5].

In Ref. [6] V.F. Hess presented a detailed analysis of his measurements in heights of (1000 . . . 2000) m, which were most reliable. These results agreed essentially with those by A. Gockel, who had also anticipated the observation of an intensified radiation when he rose even higher [2]. Hess ruled out the hypothesis of sources mainly inside the Earth. He added that sources in the air would require *e.g.* a RaC density in high sectors of the atmosphere, which exceeds the density measured near ground by about a factor of ≈ 20 . He concluded that a large fraction of the “penetrating radiation” does apparently *originate outside the Earth and its atmosphere*. In a specific test during an eclipse in 1912, and in the comparison of data that he obtained at day and at night, he did not observe

relevant changes. From this he inferred further that the sun is unlikely to be a significant source of this radiation [4],² which we now denote as *cosmic rays* (the earlier German term was “Höhenstrahlung”).

Another seminal observation was made by P. Auger in the Alps (1937) [7]. Several Geiger counters, which were separated by tens or hundreds of meters, detected an event at practically the same time. Such a correlation, in excess of accidental coincidence, was also reported in the same year by a collaboration in Berlin [8]. Later B. Rossi commented that he had made similar observations already in 1934. P. Auger gave the correct interpretation of this phenomenon, namely the occurrence of *extended air showers* caused by cosmic rays: a high energy primary particle of cosmic origin triggers a large cascade in the terrestrial atmosphere [7]. Based on the comparison of air shower measurements at sea level and on Jungfrauoch (in Switzerland, 3500 m above sea level), and some simple assumptions about the shower propagation, P. Auger *et al.* conjectured that primary particles occur at energies of at least 10^{15} eV [9].

Today we know that the primary particles carry energies of about $E \approx (10^9 \dots 10^{20})$ eV. The emerging cascades typically involve (in their maxima) $O(1)$ secondary particle for each GeV of the primary energy, so an air shower can include up to $O(10^{11})$ particles. The energy dependence of the flux is illustrated in Figure 1. Its intensity falls off with a power law $\propto E^{-3}$ (new fits shift the exponent to -2.7), up to minor deviations (“knee”³, “ankle”). We will come back extensively to the behaviour in the highest energy sector.

The *composition* of the rays depends on the energy. Here we are particularly interested in *ultra high energy cosmic rays (UHECRs)*, with energies $E \gtrsim 10^{18.5}$ eV, which are mostly of extragalactic origin. There one traditionally assumed about 90 % of the primary particles to be protons, about 9 % helium nuclei (α), plus small contributions of heavier nuclei. At lower energies these fractions change. In that regime, the magnetic field of $\sim 3 \mu\text{G}$ in our galaxy confines charged particles as diffuse radiation, so that the galactic component dominates [12]. In the range $(10^{15} \dots 10^{17})$ eV the rays mainly consist of heavier nuclei [13], and for $(10^{12} \dots 10^{15})$ eV there are $\sim 50\%$ protons, $\sim 25\%$ α and $\sim 13\%$ C, N and O nuclei, according to Ref. [10]. As we consider still lower energies, also leptons and photons contribute significantly, see Sections 2 and 3. We quote here typical numbers from the literature, but many aspects of the energy dependent composition are controversial [12].

²Radiation from the sun occurs at low energy, up to $O(10^8)$ eV. It won’t be addressed here, and we adapt a notion of cosmic rays starting at higher energy.

³In addition, a small “second knee” has been observed around $10^{17.5}$ eV. It is not visible in Figure 1, but we will comment on it in Subsection 1.3.

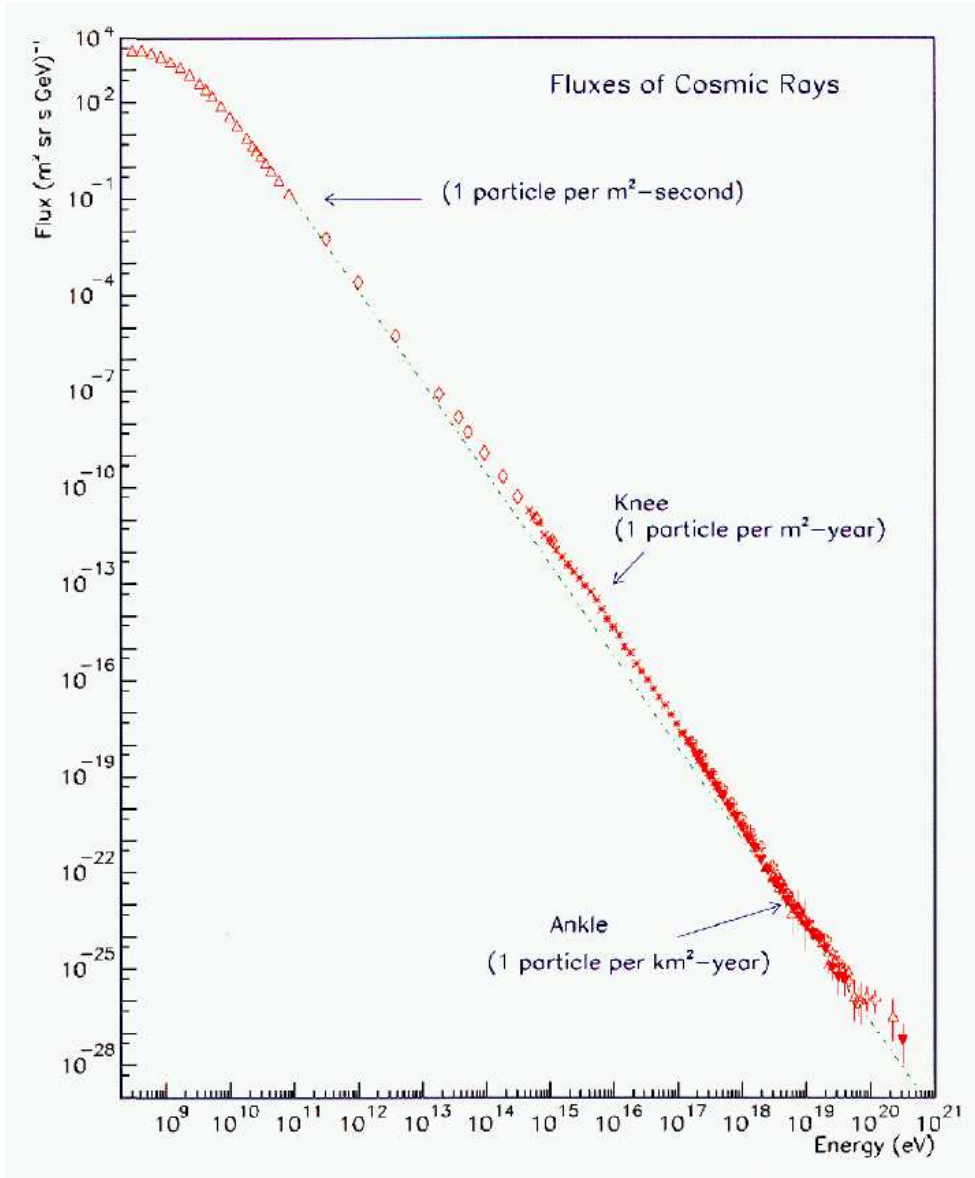


Figure 1: *The flux intensity of cosmic rays as a function of the energy (plot adapted from the HiRes Collaboration [10]). Over a broad energy interval it falls off essentially like flux $\propto E^{-3}$ (or $\propto E^{-2.7}$, according to recent high precision measurements). We are most interested in the UHECRs, with energies $E \gtrsim 10^{18.5}$ eV. Around $E = 6 \cdot 10^{19}$ eV an abrupt flux reduction is predicted. This is the GZK cutoff, to be discussed in Subsection 1.3 and beyond.*

The arrival directions of charged rays are essentially *isotropic*. This is explained by their deviation in interstellar magnetic fields: such fields occur at magnitudes of μG inside the galaxies, and of nG extragalactically, which is — over a large distance — sufficient for a sizable deflection. As a consequence the origin of charged rays from far distances can hardly be located.⁴

The *origin* of cosmic rays is still mysterious. The first proposal was the *Fermi mechanism* (“second order”), which is based on particle collisions in an interstellar magnetic cloud [14]. Collisions which are (almost) head-on are statistically favoured and lead to acceleration. A later version of the Fermi mechanism (“first order”) refers to shock waves in the remnant after a supernova [15]. However, these mechanisms can explain the cosmic rays at best in part; they cannot provide sufficient energies for UHECRs. In particular the first order mechanism could only attain about $E = O(10^{14})$ eV, and it predicts a flux $\propto E^{-2}$ — but the observed flux is close to a behaviour $\propto E^{-3}$, as Figure 1 shows. A variety of scenarios has been suggested later, for comprehensive reviews we refer to Refs. [16]. They can roughly be divided into two classes:

- Bottom-up scenarios : Certain celestial objects are equipped with some mechanism to accelerate particles to these tremendous energies (which can exceed the energies reached in terrestrial accelerators by at least 7 orders of magnitude). The question what these objects could be is puzzling. Pulsars⁵ [17] and quasars⁶ [18] are among the candidates that were considered, and recently Active Galactic Nuclei (AGN)⁷ attracted attention as possible UHECR sources, see Appendix A. However, a convincing explanation for the acceleration mechanism is outstanding (see Ref. [19] for a recent discussion, and Ref. [20] for a modern theory).

⁴Recent developments could change this picture for the UHECRs, see Appendix A. Of course, the approximately straight path length increases with the energy, so that UHECR directions may be conclusive if the source is nearby. As an example, a proton of $E = 10^{20}$ eV has in our galaxy a Larmor radius, $r_L[\text{kpc}] \approx E[\text{EeV}]/B[\mu\text{G}]$, which exceeds the galaxy radius ≈ 15 kpc ($1 \text{ EeV} = 10^{18}$ eV, cf. Appendix B).

⁵Pulsars are rotating magnetised neutron stars.

⁶A quasar, or quasi-stellar radio source, is an extremely bright centre of a young galaxy.

⁷An Active Galactic Nucleus is the environment of a super-massive black hole in the centre of a galaxy (its mass is estimated around $(10^6 \dots 10^{10})M_\odot$, where $M_\odot \simeq 2 \cdot 10^{30}$ kg is the solar mass). It absorbs large quantities of matter and emits highly energetic particles, in particular photons, electrons and positrons (we repeat that the acceleration mechanism is not known). Only a small subset of the galaxies have active nuclei. Our galaxy does not belong to them; the nearest AGN are located in Centaurus A and Virgo; this will be of importance in Appendix A.

- Top-down scenarios : The UHECRs originate from the decay or annihilation of super-heavy particles spread over the Universe. These particles were generated in the very early Universe, so here one does not need to explain where the energy comes from (see *e.g.* Refs. [21, 22]). One has to explain, however, what kind of particles this could be: magnetic monopoles have been advocated [23], while another community refers to exotic candidates called “wimpyzillas” [24] — but there are no experimental signals for any of these hypothetical objects. Moreover, this approach predicts a significant UHECR flux with γ and ν as primary particles, which is disfavoured by recent observations: in particular Ref. [25] established above 10^{19} eV an upper bound of 2 % for the photon flux. The negative impact on top-down scenarios is further discussed in Refs. [26, 27]. Ref. [28] had reported earlier measurements with similar conclusions.

1.2 The Cosmic Microwave Background

We proceed to another highlight of the historic development: in 1965 A.A. Penzias and R.W. Wilson discovered (rather accidentally) the Cosmic Microwave Background (CMB) [29], which gave rise to a breakthrough for the evidence in favour of the Big Bang scenario. It is estimated that the CMB emerged after about 380 000 years. At that time the cooling of the plasma reached a point where hydrogen atoms were formed. Now photons could scatter off these electrically neutral objects, so that the Universe became transparent (for reviews, see Refs. [30]). The CMB that we observe today — after a period of 13.7(2) Gyr of further cooling — obeys to a high accuracy Planck’s formula for the energy dependent photon density in black body radiation,

$$\frac{dn_\gamma}{d\omega} = \frac{1}{\pi^2} \frac{\omega^2}{\exp(\omega/(k_B T)) - 1} , \quad (1.1)$$

where ω is the photon energy (for $\hbar = 1$) and k_B is Boltzmann’s constant. This shape, plotted in Figure 2, is in excellent agreement with the most precise observation, which was performed by the Cosmic Background Explorer (COBE) satellite [31]. Any deviation from the black body formula (1.1) over the wave length range $\lambda \simeq (0.5 \dots 5)$ mm is below 0.005 % of the CMB peak.⁸ The temperature is identified as $T = 2.725(1)$ K [32].

⁸Sizable deviations seem to occur, however, at much larger wave length, $\lambda \gtrsim 1$ m, due to an additional *radio background*, the details of which are little known. We add that there is also a Cosmic Neutrino Background, which decoupled already about 2 s after the Big Bang, and its present temperature is estimated as $\lesssim 1.9$ K. We do not consider it here because it has no significant impact on cosmic rays.

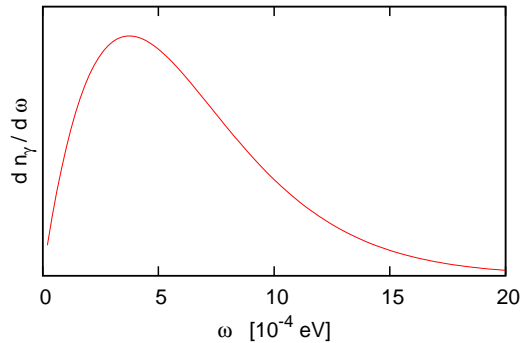


Figure 2: *The Planck distribution (1.1) of the black body radiation at the CMB temperature of $T = 2.725$ K. The CMB energy density agrees accurately with this Planck distribution — it is by far the most precise Planck radiation that has ever been measured.*

This implies that the mean photon energy and wave length are given by $\langle\omega\rangle \simeq 6 \cdot 10^{-4}$ eV and $\langle\lambda\rangle \simeq 1.9$ mm.⁹ The resulting photon density in the Universe amounts to $\int_0^\infty d\omega (dn_\gamma/d\omega) \simeq 410.4(5)$ cm⁻³. Interesting further aspects of the CMB — which are, however, not directly relevant for our discussion — are reviewed for instance in Ref. [33].

1.3 The Greisen-Zatsepin-Kuz’min cutoff

In the subsequent year the knowledge about cosmic rays *and* about the CMB led to an epoch-making theoretical prediction, which was worked out independently by K. Greisen at Cornell University [34], and by G.T. Zatsepin and V.A. Kuz’min at the Lebedev Institute [35]. They expected the flux of cosmic rays to drop abruptly when the energy exceeds the “*GZK cutoff*”¹⁰

$$\boxed{E_{\text{GZK}} \approx 6 \cdot 10^{19} \text{ eV}} . \quad (1.2)$$

The reason is that protons above this energy interact with background photons to generate pions. The dominant channel for this *photopion production* follows the scheme

$$p + \gamma \rightarrow \Delta(1232 \text{ MeV}) \begin{cases} \rightarrow p + \pi^0 \\ \rightarrow n + \pi^+ , \quad n \rightarrow p + e^- + \bar{\nu}_e . \end{cases} \quad (1.3)$$

⁹The term “microwave” usually refers to wave lengths in the range of about 1 mm . . . 10 cm, so it does apply to the CMB.

¹⁰Since this “cutoff” is not sharp, it is a bit arbitrary where exactly to put it. Eq. (1.2) gives a value which is roughly averaged over the literature, and which we are going to embed into phenomenological and theoretical considerations.

These two channels cover 99.4% of the $\Delta(1232)$ decays [32]. If even more energy than the threshold for this transition is available, excited proton states ($p^*(1440)$, $p^*(1520)$...) and higher Δ resonances ($\Delta(1600)$, $\Delta(1620)$, $\Delta(1700)$...) can contribute to the photopion production as well. In these cases one may end up with $p + \pi$ or also with $p + 2\pi$; at even higher energy the production of three pions is possible too.

It is obvious that a proton with energy $E_p > E_{GZK}$ loses energy under photopion production, until it drops below the threshold for this process.¹¹ We are now going to take a somewhat more quantitative look at transition (1.3) (in natural units, $\hbar = c = 1$).

We denote the proton energy E_p at the threshold for the $\Delta(1232)$ resonance as E_0 . In these considerations one refers to the Friedmann-Robertson-Walker metrics (see Appendix B) — which is co-moving with the expanding Universe — as the “laboratory frame” (we will call it the “FRW laboratory frame”).¹² We first consider the relativistic invariant

$$\begin{aligned} s &= (E_0 + \omega)^2 - (\vec{p}_p + \vec{p}_\gamma)^2 \\ &= E_0^2 - \vec{p}_p^2 + 2E_0\omega - 2\vec{p}_p \cdot \vec{p}_\gamma \overset{\text{head-on}}{\simeq} m_p^2 + 4E_0\omega \stackrel{!}{=} m_\Delta^2. \end{aligned} \quad (1.4)$$

\vec{p}_p and \vec{p}_γ are the 3-momenta of the proton and CMB photon. We arrived at the term $4E_0\omega$ by assuming a head-on collision (and $E_0 \gg m_p$). The last term refers to a Δ baryon at rest, which sets the energy threshold. Thus we obtain an expression for $E_0(\omega)$. As an exceptionally high photon energy we insert $\omega = 5\langle\omega\rangle = 3$ meV — photons with even higher energy are very rare due to the exponential decay of the Planck distribution (1.1). This leads to¹³

$$E_0 = \frac{m_\Delta^2 - m_p^2}{4\omega} \Big|_{\omega=5\langle\omega\rangle} \simeq 5.3 \cdot 10^{19} \text{ eV}. \quad (1.5)$$

Further kinematic transformations yield a simple expression for the inelasticity factor K , which represents the relative energy loss of the

¹¹In the original studies [34, 35] terms like “ Δ resonance” did not occur, but the authors knew effectively about the photopion production. They inferred this spectacular conclusion, although Ref. [34] only consists of 2 pages without any formula, and Ref. [35] is just a little more extensive. Its original Russian version has been translated but only few people have read (the page number is often quoted incorrectly). Nevertheless both works are of course top-cited on a renowned level.

¹²In terms of a CMB decomposition in spherical harmonics, the monopole contribution sets the temperature of 2.725(1) K. The dipole term is frame dependent; the requirement to make it vanish singles out the maximally isotropic frame [32], which we could also refer to in this context.

¹³In eq. (1.2) we increased this energy threshold slightly, which is consistent with the unlikelihood of exact head-on collisions.

proton under photopion production [36],

$$K := \frac{\Delta E_p}{E_p} = \frac{1}{2} \left(1 - \frac{m_p^2 - m_\pi^2}{s} \right). \quad (1.6)$$

This relative loss still refers to the FRW laboratory frame, but formula (1.6) holds for general proton-photon scattering angles.

Let us now change the perspective and consider the Mandelstam variable s in the rest frame of the proton, where we denote the photon 4-momentum as $(\omega', \vec{p}'_\gamma)$,

$$s = (m_p + \omega')^2 - \vec{p}'_\gamma{}^2 = m_p^2 + 2m_p \omega'. \quad (1.7)$$

The photon energy ω' is related to ω by the Doppler effect,

$$\omega' = \gamma \omega (1 - v_p \cos \vartheta). \quad (1.8)$$

v_p and ϑ are the proton velocity and the scattering angle in the FRW laboratory frame. The Lorentz factor γ can take a remarkable magnitude; for instance at the proton threshold energy $E_p = E_0$ it amounts to

$$\gamma = \frac{E_p}{m_p} \Big|_{E_p=E_0} \approx 10^{11}. \quad (1.9)$$

By averaging ω' over the angle ϑ one arrives at [36]

$$\bar{\omega} \simeq 180 \text{ MeV} \cdot \frac{E_p}{E_0}. \quad (1.10)$$

Hence a proton with $E_p \geq E_0$ perceives the CMB photons as quite energetic γ -radiation.¹⁴

Combining eqs. (1.6), (1.7) and (1.10) we can determine the inelasticity factor at a given proton energy (and averaged scattering angle),

$$\begin{aligned} K(\bar{\omega}) &= \frac{1}{2} \left(1 - \frac{m_p^2 - m_\pi^2}{m_p(m_p + 2\bar{\omega})} \right) \\ &= \begin{cases} 0.15 & \text{at } E_p = E_0, \quad \bar{\omega} = 180 \text{ MeV} \\ 0.20 & \text{at } E_p = 2E_0, \quad \bar{\omega} = 300 \text{ MeV} \end{cases}. \end{aligned} \quad (1.11)$$

We see that the inelasticity is significant already at the energy threshold, and beyond it (gradually) rises further.

¹⁴The velocity of the proton in the centre-of-mass frame is given by $\omega'/(\omega' + m_p)$. At $E_p \approx E_0$ it is small on the relativistic scale, hence the proton rest frame referred to above is not that far from the centre-of-mass frame.

We are now prepared to tackle the question which ultimately matters for the GZK cutoff: if a proton with $E_p > E_0$ travels through the Universe, how long is the *decay time* of its energy ?

This question was analysed by F.W. Stecker [36], who derived the following formula for the energy decay time τ ,

$$\frac{1}{\tau(E_p)} = -\frac{k_B T}{2\pi^2 \gamma^2} \int_{\bar{\omega}_0(E_p)}^{\infty} d\bar{\omega} \sigma(\bar{\omega}) K(\bar{\omega}) \bar{\omega} \ln \left(1 - e^{-\bar{\omega}/(2\gamma k_B T)} \right). \quad (1.12)$$

$\bar{\omega}_0$ is the photon threshold energy for photopion production in the rest frame of a proton (which has FRW laboratory energy E_p). The product of $\bar{\omega}$ with the logarithm emerges from the Planck distribution (1.1) after integration. $\sigma(\bar{\omega})$ is the total cross-section for the photopion production,¹⁵ which was explored experimentally already in the 1950's, so Refs. [34, 35, 36] could refer to it. The corresponding experiment with protons at rest, exposed to a γ -ray beam of about 200 MeV, had been reported for instance in Ref. [37]. The cross-section varies mildly with the energy, in the magnitude of $\sigma \approx 0.1$ mb. Its profile was reproduced in Ref. [36], along with the measured inelasticity factor $K(\bar{\omega})$. It is remarkable that this simple experiment at modest energy provides relevant information about the fate of UHECRs. Based on the knowledge about σ , Figure 2 in Ref. [36] displays the mean free path length for the proton, for instance

$$\ell_{E_p \approx 10 E_0}^{\text{free}} \approx 10 \text{ Mpc}. \quad (1.13)$$

A later fit to the experimental data, which refers directly to the product $\sigma(\bar{\omega})K(\bar{\omega})$, is worked out in Ref. [38]. It includes corrections like the higher photopion production channels, which still reduce the free path length a little.¹⁶

Refs. [34, 35] pointed out already that the corresponding *energy attenuation for heavier nuclei* is even stronger. The main reason here is the *photo-disintegration* into lighter nuclei due to interactions with CMB photons (see Ref. [39] for a detailed analysis). The fragments carry lower energies; the energy per nucleon remains approximately constant. Hence we are in fact dealing with an absolute limitation for the energy of cosmic rays consisting of nucleons.¹⁷ Numerous works have later reconsidered

¹⁵Strictly speaking it is cleaner to set the lower bound in this integral to zero and rely on the strong suppression below $\bar{\omega}_0$ due to $\sigma(\bar{\omega})$, but the form (1.12) is more intuitive. Moreover eq. (1.12) simplifies the energy attenuation to a continuous process — its discrete nature gives rise to minor corrections.

¹⁶The same is true for the somewhat higher CMB temperature in scattering processes long ago (although this effect is marginal). Various CMB temperatures have been considered in Ref. [35].

¹⁷Regarding non-nuclear rays, we stress that neutrinos are not subject to any theoretical energy limit in the CMB, but no UHECR neutrinos have been observed yet.

the attenuation of protons and heavier nuclei in the CMB in detail, see *e.g.* Refs. [40, 41] and references therein.

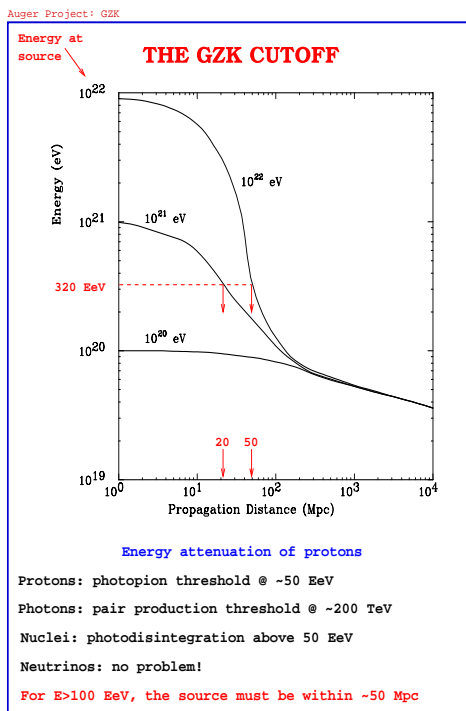


Figure 3: *The energy attenuation for protonic UHECRs due to photopion production with CMB photons (plot adapted from the Pierre Auger Collaboration [42]). Note that 1 EeV = 10¹⁸ eV (see Appendix B).*

At last one might object that protons may still travel very long distances with energies above E_{GZK} if they start at a much higher energy. However, at $E_p \gg E_{\text{GZK}}$ the attenuation is strongly intensified. (For instance the value of the lower integral bound $\bar{\omega}_0$ in eq. (1.12) decreases; once the integral captures the peak in Figure 2, many more photons can contribute to the photopion production). As a result, extremely high energies decrease rapidly, and the final super-GZK path does not exceed the corresponding path length at $E_p \approx E_0$ drastically. This feature is shown in a plot by the Pierre Auger Collaboration, which we reproduce in Figure 3.

It seems natural to assume a homogeneous distribution of UHECR sources in the Universe, both for bottom-up and for top-down scenarios (cf. Subsection 1.1). Then one could expect a pile-up of primary particles just below E_{GZK} . As a correction one should take into account another process, which dominates somewhat below E_{GZK} , and which enables the CMB to reduce the proton energy further: in the energy range

$5 \cdot 10^{17} \text{ eV} < E < E_{\text{GZK}}$ the *electron/positron pair production*

$$p + \gamma \rightarrow p + e^+ + e^- \quad (1.14)$$

causes this effect, though the inelasticity is much smaller than in the case of photopion production (consider the ratio in eq. (1.11)).

Ref. [41] presents an updated overview, which incorporates all relevant effects. This leads to Figure 4 for the *attenuation lengths* for various primary nuclei. For the proton it is composed as $\ell^{-1} \simeq \ell_{p\pi}^{-1} + \ell_{ee}^{-1}$, which refers to photopion production and e^-/e^+ pair creation (at even lower energy adding also the inverse attenuation length due to the redshift becomes significant).

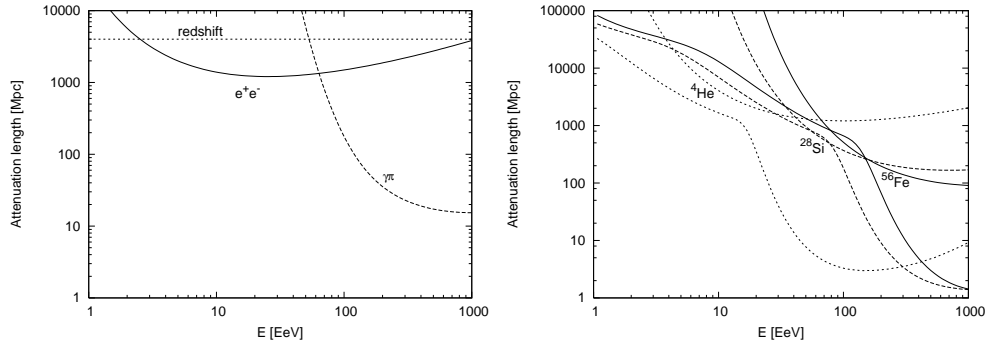


Figure 4: *Illustration of the energy attenuation of UHECRs due to photopion production with CMB photons for protons (on the left), and due to photo-disintegration of heavier nuclei (on the right). In both cases also e^-/e^+ pair production is considered (upper curves at high energy). The plot on the left even captures the redshift, which is, however, not really important at the ultra high energies that we are interested in. These plots are adapted from Ref. [41].*

All in all, one concludes the following: if protons — or heavier nuclei — hit our atmosphere with energies $E > E_{\text{GZK}}$, they are expected to come from a distance of maximally

$$\boxed{\ell_{\text{max}} \approx 100 \text{ Mpc}} . \quad (1.15)$$

If we rise the “cutoff” to 10^{20} eV (cf. footnote 10) the range decreases to $\ell_{\text{max}} \approx 50 \text{ Mpc}$. For instance this distance reaches out to the Virgo cluster of galaxies (its centre is about 20 Mpc from here). ℓ_{max} is a large distance compared to our galaxy (or Milky Way) — our galactic plane has a diameter of about 30 kpc. But ℓ_{max} is short compared to the

(co-moving) radius of the visible Universe. On that scale the sources of super-GZK radiation should be *nearby*,

$$(R_{\text{Milky Way}} \simeq 15 \text{ kpc}) \ll \ell_{\text{max}} \ll (R_{\text{visible Universe}} \simeq 14 \text{ Gpc}) . \quad (1.16)$$

Despite the e^+/e^- pair production, some pile-up seems to occur at energies $E \lesssim E_{\text{GZK}}$ (cf. footnote 23). The status of the subsequent dip is discussed in Refs. [43]. As we mentioned in footnote 3, a “second knee” in the cosmic flux was observed by various collaborations around $10^{17.5}$ eV. As a possible interpretation it could be the pile-up at the lower end of the pair creation threshold [12].

However, in this review we want to focus on the issue of super-GZK energies in cosmic rays. Not even in our vicinity — given by the range (1.15) — we know of any acceleration mechanism, which could come near such tremendous energies. Therefore the detection of *super-GZK events* could represent a mystery — and perhaps a hint for new physics. So let us now summarise the actual observations in this respect.

1.4 Observations of super-GZK events

Even before the GZK cutoff was established from the theoretical side, one spectacular event had been reported by the Volcano Ranch Observatory in the desert of New Mexico [44]. The energy of the cosmic particle that triggered this event was estimated at 10^{20} eV, which exceeds already the GZK cutoff (1.2). Refs. [34, 35] both quoted this report and commented that they do not expect any events at even higher energies (Greisen added that he found even that event “surprising”). In fact, identifying the energy of the primary particle is a delicate issue — which we will address below — and the corresponding techniques were at an early stage.

In any case this initiated a long-standing and controversial challenge to verify the validity of the GZK cutoff. In 1971 yet another super-GZK event was reported from an air shower detected near Tokyo [45].¹⁸ This inspired a large-scale installation in Akeno (170 km west of Tokyo), which is known as *AGASA* (Akeno Giant Air Shower Array); a historic account is given in Ref. [46].

Meanwhile also the *Fly’s Eye* project in Utah went into operation, and in 1991 it reported an event with $3 \cdot 10^{20}$ eV primary particle energy [47]. Up to Ref. [45], this is the highest cosmic ray energy ever reported. In macroscopic units it corresponds to 48 J.¹⁹

¹⁸For that event the energy was estimated even as $4 \cdot 10^{21}$ eV, but it is not often quoted in the literature.

¹⁹It is popular to compare this to the kinetic energy of a tennis balls. Its mass is typically 57.6 g, so that these 48 J are the kinetic energy for a speed of 147 km/h, which is somewhat below the speed attained in a professional game.

Up to the 21st century numerous new super-GZK events were detected, in particular by AGASA. According to the data of this collaboration, the spectrum — *i.e.* the flux of UHECR rays — continues to follow the power-like decrease in the energy that we saw in Figure 1, with hardly any extra suppression as E_{GZK} is exceeded. This contradiction to the theoretical expectation triggered an avalanche of speculations. The AGASA results have been considered essentially consistent with the data of further air shower detectors in *Yakutsk* (Russia, at Lake Baikal) [48] and in *Haverah Park* (England, near Leeds) [49]. An overview of their super-GZK statistics is given in Figure 5.

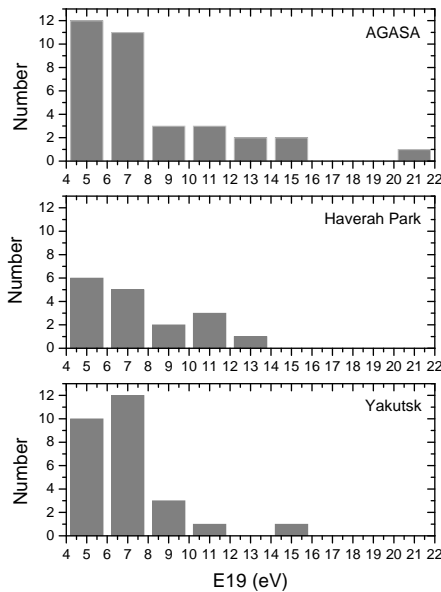


Figure 5: *The statistics of GZK and super-GZK events reported by the observatories AGASA, Haverah Park and Yakutsk, against the energy in units of 10^{19} eV (Figure adapted from Ref. [50]).*

This observation *disagrees*, however, with the data of the *HiRes* (High Resolution Fly’s Eye) observatory, which concludes that the cosmic rays do respect the GZK cutoff [51]. HiRes is the successor experiment of Fly’s Eye since 1994, with a refined technology.²⁰

A comparison of the cosmic ray spectra as determined by AGASA (1990 - 2004) and by HiRes (1997 - 2006) is shown in Figure 6. Commented overviews over the results of these collaborations are included in Ref. [40, 52]. Figure 5 also shows that the overall statistics of these

²⁰Initially the HiRes results seemed to agree as well, but here and in the following we refer to the results presented later by this Collaboration.

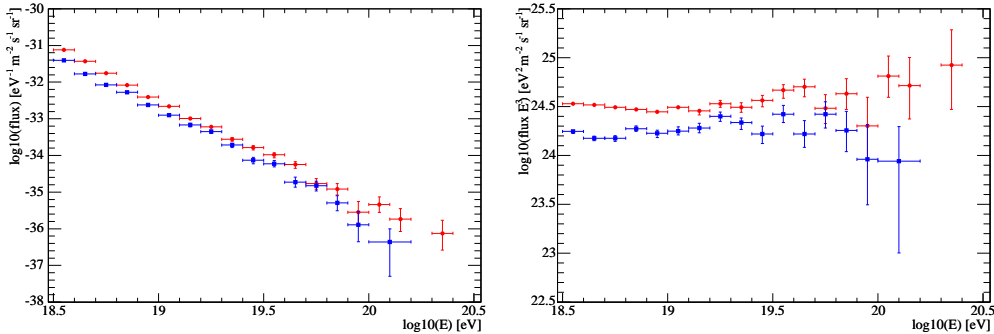


Figure 6: A direct comparison of the cosmic flux at ultra high energy as measured by the Observatories AGASA (upper symbols) and HiRes (lower symbols). The plot on the left shows the flux as a function of the energy E . On the right it is rescaled by a factor E^3 (cf. Figure 1), which renders it approximately constant up to E_{GZK} . We see that the continuation beyond E_{GZK} is controversial (plots adapted from Ref. [53]).

UHECR observations is modest. Note that the flux above 10^{12} eV is around 10 primary particles per minute and m^2 , but above $10^{18.5}$ eV it drops to $O(1)$ particle/ $(\text{km}^2 \text{ year})$ (as indicated in Figure 1), so the search for UHECR takes patience. One may question if there is really a significant contradiction between HiRes and the other groups mentioned above. In fact, an analysis in Ref. [54] concludes that this discrepancy between AGASA and HiRes might also be explained by statistical fluctuations, if the energy scale is corrected in each case by 15% (which is well below the systematic uncertainty).

Nevertheless a large community assumed that a contradiction is likely and wondered about possible reasons. An obvious suspicion is that this may actually be a discrepancy between *different methods*.

- To sketch these two methods, we first address the air shower, which is illustrated in Figure 7. At an early stage the huge energy transfer of an UHECR primary particle onto the molecules in the atmosphere generates — among other effects — a large number of light mesons (pions, kaons . . .), which rapidly undergo leptonic (or photonic) decays. Of specific interest for the observer are the muons emerging in this way: thanks to the strong time dilation they often survive the path of about 25 km to the surface of the Earth (although their mean life time is only $2 \cdot 10^{-6}$ s). Another consequence of the extremely high speed is that the air shower is confined to a narrow cone — typically the directions of motion of the secondary particles deviate by less than 1° from the primary particle direction

in the shower maximum (a few hundred meters from the core). The method applied by AGASA, Yakutsk and Haverah Park is an array of numerous Čerenkov detectors — spread over a large area on ground — which identify the trajectories and energies of highly energetic secondary particles. They use tanks with pure water, where Čerenkov radiation is amplified by photomultipliers. Detecting in particular a set of leptons μ^\pm , e^\pm (and photons) belonging to the same shower — with precise time of arrival, speed and direction — provides valuable information about the shower. Its evolution in the atmosphere, and ultimately the primary particle energy, are reconstructed by means of sophisticated numerical methods. (Of course, the information recorded on Earth is still insufficient for a unique reconstruction, so that maximal likelihood methods²¹ have to be applied to trace back the probable scenario.)

- The method used by HiRes — and previously by Fly’s Eye — observes the showers in the atmosphere, before they arrive at Earth. The showers excite N_2 molecules of the air, which subsequently emit UV or bluish light when decaying to their ground state (with wave lengths $\lambda \approx (220 \dots 440)$ nm). Although this light is weak, it is visible from Earth to powerful telescopes, along with light collecting mirrors, at least in nights with hardly any moonshine or clouds. (These telescopes are structured in a form similar to the compound eye of an insect.) In 1976 Volcano Ranch achieved the first successful observation, which was confirmed by the detection of the same air shower on ground. This *air fluorescence light*²² is emitted isotropically. It is also illustrated in Figure 7, along with the Čerenkov radiation in the air as a further effect. The direct nature of this observation is a valuable virtue, but an obvious disadvantage is the limitation of the detection time to $\approx 10\%$. In this method, the observable height grows with the energy of the primary particle, which complicates the interpretation of the data [52].

We add a couple of qualitative remarks, without going into details. An obvious question is how protons as primary particles can be distinguished from heavier nuclei. For the latter the air showers arrive at the maximal number of particles at a higher point. The depth D_{\max} in the atmosphere

²¹A synopsis of this method is given in Ref. [32].

²²We adapt this term from the literature, although it actually suggests that the primary particle must be a photon. The appropriate term for this effect would be “scintillation”, or more generally “luminescence”.

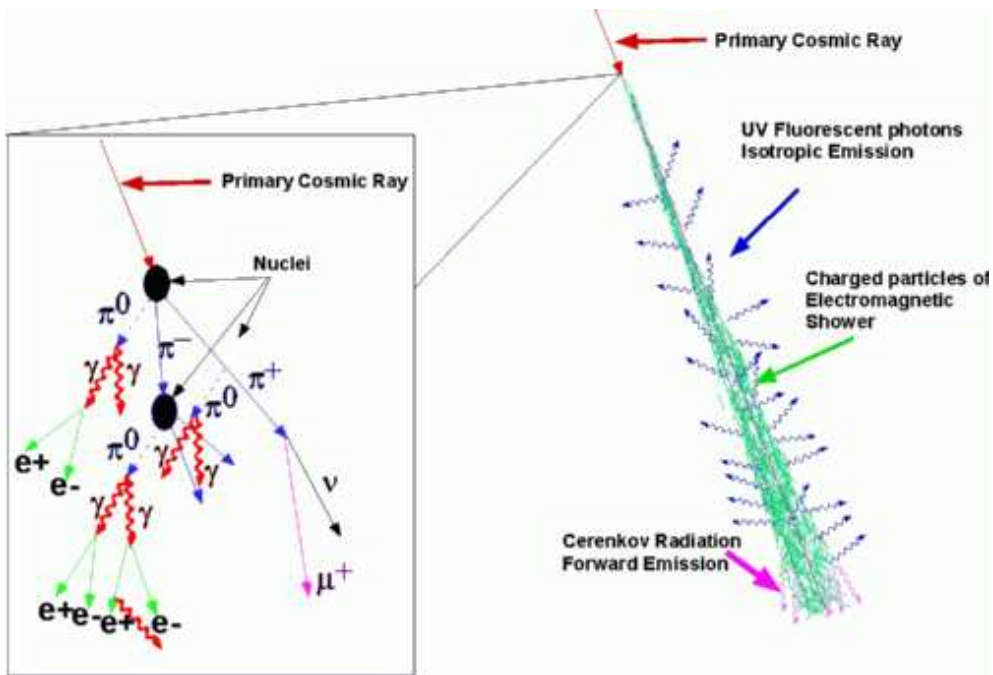


Figure 7: *The evolution of an air shower, as illustrated by the HiRes Collaboration [10]. We recognise the fluorescence light (UV or blue), the Čerenkov radiation in the air, and the production of light mesons, which rapidly decay into leptons and photons (see zoom on the left).*

to that point can be parametrised as [55, 27]

$$[D_{\max}(\text{proton}) - D_{\max}(A)] \propto \ln A , \quad (1.17)$$

where A is the atomic mass number. This point can approximately be identified by either of these two methods: for the fluorescence method this observation is quite direct, and on ground it is characterised by the electron/muon ratio. Further criteria — such as the time profile of the signal and the curvature of the shower front — are reviewed in detail in Refs. [56], and summarised in Ref. [12].

In particular the Fly’s Eye record of $3 \cdot 10^{20}$ eV seemed to originate from a quite heavy primary nucleus, such as oxygen. However, the identification is not easy at all, and in practice the criteria are not always consistent. Only cosmic γ -rays can be distinguished quite clearly from other primary particles (they penetrate much deeper into the atmosphere, hence the air shower maximum is closer to Earth).

In the course of a long flight through the CMB, heavy nuclei are expected to break apart (photo-disintegration), as we mentioned before. Therefore a dominance of protons in the UHECRs suggests that the primary particles come from relatively far distances, and vice versa.

The status of UHECR observations to this point is reviewed in detail in Refs. [16, 40]. In light of the dilemma between the results obtained with these two techniques, the *Pierre Auger Collaboration* designed a new project in Argentina (near Malagüe, province of Mendoza) with the goal to clarify the situation [42]. Its planning started in 1992 and it is in stable operation since January 2004, while part of the equipment has still been installed. The concept of the Pierre Auger project is the combination of *both* techniques described above:

- On Earth it involves 1600 detectors with 12 tonnes of water, where three photomultipliers monitor the Čerenkov light caused by air showers. The installation of these tanks has been terminated in 2008. They are distributed over an area of 3000 km² on a triangular grid of spacing 1.5 km (for comparison: air showers due to UHECRs have diameters of about 6 km at the terrestrial surface).
- In addition 24 telescopes are searching for fluorescence light from 4 well-separated sites — all of them have already been operating since 2004.

The Čerenkov array is suitable for collecting large statistics, while the telescopes are important for a reliable calibration of the energy measurement. This can be achieved best based on the data from air showers, which are observed in both ways, *hybrid events*, by evaluating a variety of correlations [57]. With a single detection technique the energy calibration has been notoriously problematic.

In Refs. [57, 58, 11] the Pierre Auger Collaboration presented data collected until the middle of 2007, which we reproduce in Figure 8. The exposure to this point already exceeds the total exposure which was accumulated by HiRes and AGASA by about a factor of 2 resp. 4. The systematic uncertainty in the energy measurement is estimated around 22% and the statistical error around 6% (which is rather harmless in this context). The vertical arrows in this plot mark the upper limits for the energy bins with 84% C.L. [11], based on the Feldman-Cousins method for Poisson distributions [59]. The small labels indicate the number of events detected in the corresponding bin, and the error bars represent the statistical uncertainty of the flux. Below E_{GZK} (as given in eq. (1.2)) we recognise the power-like behaviour of the energy spectrum. In the intervals $4 \cdot 10^{18} \dots 4 \cdot 10^{19}$ eV, and beyond $4 \cdot 10^{19}$ eV its slope was measured $\propto E^{-2.69(6)}$ resp. $\propto E^{-4.2(2)}$, which rules out a single power law by 6 standard deviations. Hence for $E > E_{\text{GZK}}$ the flux drops clearly below the extrapolated power law. Nevertheless a considerable number of

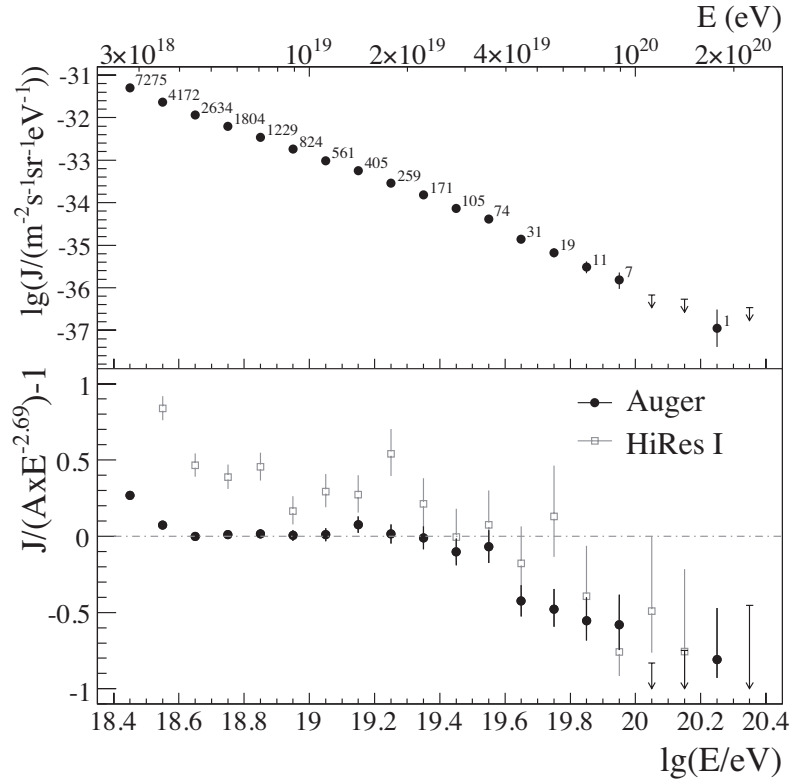


Figure 8: *The UHECR spectrum according to the data by the Pierre Auger Collaboration collected from January 2004 until August 2007 (plots adapted from Ref. [11]). The lower panel reveals a clear reduction of the rescaled flux beyond E_{GZK} , roughly consistent with the HiRes data and the predicted GZK cutoff. Nevertheless there is a considerable number of new super-GZK events (the upper panel displays the number of events).*

new super-GZK events have been observed.²³ Confronted with the fluxes measured earlier by AGASA and HiRes, these new data are closer to the latter. They are certainly consistent with an extra damping once the energy threshold for the Δ resonance is exceeded. On the other hand, the sizable number of super-GZK cosmic rays asks for an explanation and keeps the door open for speculations. An interesting interpretation of the UHECR arrival directions was published by the Pierre Auger Collaboration in November 2007, see Appendix A.

In this review we focus on Lorentz Invariance Violation (LIV) as one attempt to explain a possible excess of UHECRs compared to the theoretical prediction. We should add, however, that the “boring” outcome of full consistency with the GZK cutoff is by no means disproved — recently that scenario has actually been boosted, see again Appendix A.

2 Lorentz Invariance and its possible violation

So far we have assumed Lorentz Invariance (LI) to hold. In fact, it played a key rôle in the derivation of the GZK cutoff: the transformation of the scattering process of an UHECR proton and a CMB photon to the rest frame of the proton established the link to the experimentally known cross-section. Also the determination of the inelasticity factor for the proton under photopion production depends on LI, since it refers again to the proton rest frame (regardless whether one relies on theory, as in eq. (1.11), or on laboratory experiments). The same holds for the photo-disintegration of heavier nuclei, and for electron/positron pair creation.

LI was therefore crucial for the analysis of the energy attenuation of super-GZK cosmic rays. Here we relied on Lorentz transformations with extreme Lorentz factors of the magnitude

$$\gamma = \frac{1}{\sqrt{1-v^2}} \gtrsim 10^{11} , \quad (2.1)$$

see eq. (1.9) (we still set $c = 1$). There are no direct experimental tests if LI still holds without any modifications for such extreme boosts; accelerator experiments are limited to Lorentz factors $\gamma \lesssim O(10^5)$. If the validity of the GZK cutoff will ultimately be confirmed, then this observation may be considered an indirect piece of evidence for LI under tremendous boosts. If, on the other hand, the final analysis reveals a

²³If one rescales the flux with the factor E^3 — as in Figure 6 — the shape turns into a small peak below E_{GZK} (which could be interpreted as a pile-up, as we mentioned in Subsection 1.3), and the suppression beyond the threshold appears weaker.

mysterious excess of super-GZK events, it might indicate new physics. In that case, one point to question about the standard picture is LI — so let us take a closer look at it.

LI is a central characteristic of relativity:

- In *Special Relativity Theory* (SRT) LI holds as a *global* symmetry. The transformation rules were derived by H.A. Lorentz (1899 and 1904), H. Poincaré declared them a Law of Nature, A. Einstein provided a consistent physical picture (1905) and H. Minkowski embedded it into the geometry of a 4d space (1907).
- In *General Relativity Theory* (GRT) LI holds as a *local* symmetry (A. Einstein, around 1915). In each space-time point the frame can be chosen so that locally the metrics takes the Minkowski form $g = \text{diag}(1, -1, -1, -1)$, which holds globally in SRT. It is therefore tempting — and possible — to write GRT in the terminology of a gauge theory (see for instance Ref. [60], Section 6.4). However, as a quantum field theory this formulation is not renormalisable: the renormalisation group flow does not lead to a conformal field theory (*i.e.* to scale invariance) at high energy, as reviewed recently in Ref. [61]. Therefore our established description of particle physics (local quantum field theory) is incompatible with GRT, which applies to very low energy and describes long-range gravity successfully.

Hence LI plays an essential rôle in both, SRT and GRT, although this rôle is not the same. In this review we mostly address high particle energies up to the maximum that has been observed, hence SRT is in general the appropriate framework. At specific points, however, we are also going to comment on conceivable connections to GRT — this becomes relevant in view of speculations up to the Planck scale.²⁴

In general it is untypical for global symmetries to hold exactly, so in SRT one could puzzle why this should be the case for LI (and the related CPT invariance, see Subsection 2.1).²⁵ On the other hand, gauge symmetries are exact, hence in this respect the GRT picture appears helpful (as long as no violation of LI is observed).

Nevertheless for our further discussion the framework of SRT is essential, since it allows us to apply particle physics as described by quantum

²⁴For approaches to quantum gravity, which discuss in particular the rôle of LI and its possible violation, see *e.g.* Refs. [62, 63, 64, 65].

²⁵In this spirit, the Standard Model of particle physics appears more natural in the now established form, which incorporates neutrino masses, and therefore only approximate chiral symmetry.

field theory. In field theory, the manifestation of LI as a global symmetry is well established. Some field $\Phi(x)$, which may represent a scalar, a spinor, a 4-vector or some tensor, transforms in a (finite dimensional) representation D of the Lorentz group $SO(1,3)$,

$$\begin{aligned} \Phi(x) &\longrightarrow U(\Lambda)^\dagger \Phi(x) U(\Lambda) = D(\Lambda) \Phi(\Lambda^{-1}x) \\ U &\text{ unitary , } \Lambda \in SO(1,3) , \end{aligned} \tag{2.2}$$

see for instance Ref. [60]. In particular scalar quantities — like the Lagrangian of a relativistic field theory — are Lorentz invariant ($D(\Lambda) = 1$).

In contrast to the rotation group, the Lorentz group is *non-compact*. The extrapolation of LI to arbitrarily high energy leads to the generic UV divergences in quantum field theories. The formulation on non-commutative spaces — to be addressed in Subsection 3.3 — was originally motivated as an attempt to weaken these UV divergences. Further early suggestions to deviate from LI in quantum field theories include Refs. [66].

2.1 Link to the CPT Theorem

According to the *CPT Theorem*, particle physics is invariant if three discrete transformations are performed simultaneously:

C : flips particles into the corresponding anti-particles and vice versa.

This changes the signs of all couplings to gauge fields, hence C is denoted as *charge conjugation*.

P : *parity*, space reflection, $\vec{x} \rightarrow -\vec{x}$.

T : inversion of the time direction, $t \rightarrow -t$.

The CPT Theorem states that, assuming *locality and LI*, CPT invariance is inevitable. This was recognised first by W. Pauli and G. Lüders [67] and put on a rigorous basis by R. Jost [68].

The basic idea is an analytic continuation of the Lorentz group to imaginary time (Wick rotation), so one arrives at a reflection at the origin of 4d Euclidean space. This reflection captures P and T, and the Wick rotation implies that C is included as well. The combination amounts to an anti-unitary symmetry transformation. Applying the CPT transformation twice, one also obtains a derivation of the Spin-Statistics Theorem. (A historically and mathematically precise account is given in Ref. [69]).

Only recently O.W. Greenberg turned the consideration around and proved the following Theorem [70]: *Any breaking of CPT invariance necessarily entails a Lorentz Invariance Violation (LIV)*.

This Theorem is very general, it applies whenever CPT invariance breaks in any Wightman function.

On the other hand, if we only assume LIV, then CPT symmetry may be broken or not, *i.e.* there are many ways to break LI while leaving CPT symmetry intact. The leading LIV terms are linear in the energy resp. momenta, and these terms break CPT too; they are CPT odd. If we only admit LIV terms starting quadratically in the energy, then CPT can be preserved [71], so it is natural to assume

$$\text{LIV}|_{\text{CPT odd}} \propto E, \quad \text{LIV}|_{\text{CPT even}} \propto E^2. \quad (2.3)$$

2.2 Status of experimental LI tests

According to Greenberg’s Theorem, LI tests can be performed indirectly by verifying CPT invariance. Experiments probe in particular the CPT prediction of identical masses for particles and their anti-particles. This holds for instance for e^+ , e^- up to $8 \cdot 10^{-9}$, and for p , \bar{p} up to 10^{-8} (in both cases this is the bound for the relative deviation with 90 % C.L.) [32]. On-going tests investigate the strangeness driven oscillation $K_0 \leftrightarrow \bar{K}_0$ and conclude [73]

$$|M_{K_0} - \bar{M}_{K_0}| < 5.1 \cdot 10^{-10} \text{ eV} \quad (95 \% \text{ C.L.}), \quad (2.4)$$

which corresponds to a remarkable relative precision of $O(10^{-18})$.

Similar high precision LI tests via CPT measure the magnetic moments of elementary particles and anti-particles [74]. A further indirect method to test LI in part deals with the equivalence principle [75]. However, direct tests are even more powerful, and we will explain below why we are more interested in *CPT-conserving* LIV parameters.

The status of numerous experimental LI tests by means of a variety of methods has been reviewed extensively in Refs. [72, 76, 77]. Atomic physics gives access to excellent precisions for specific LIV parameters. Such parameters describe, for instance, a particle spin coupling to a conceivable “tensor background field”. We will come back to these objects in the following Subsection. Here we anticipate that a large number of such parameters can be introduced as additional couplings in the Standard Model. In light of the discussion in Subsection 2.1, we stress that these LIV terms are local, but they can be even or odd under CPT transformation. According to Ref. [78] they are all bounded by $O(10^{-27})$, in a form which factors out the Planck scale (2.6).

These precisions are impressive, and all results are in agreement with LI — *no LIV has ever been observed*. One may wonder if even higher precision is still of interest, or if it is already sufficient for all phenomenological purposes. In the following we would like to argue that this is not necessarily the case. The precision achieved so far may be insufficient

with respect to scenarios, which could drastically affect physics on the Planck scale, or even the propagation of cosmic rays.

- We first address the CPT conserving class of LIVs, which exclude terms of $O(E)$ [71], so we can assume the violation effect to be $\propto E^2$, as in relation (2.3). Let us consider the case where LI is violated dramatically on the Planck scale, where one expects both, gravity effects and quantum effects to be strong. For instance the magnitude of (dimensionless) LIV effects at such energies could be

$$\text{LIV}(E = M_{\text{Planck}}) = O(1) , \quad (2.5)$$

where M_{Planck} is the Planck mass, *i.e.* the energy scale set by the gravitational constant G ,

$$M_{\text{Planck}} = 1/\sqrt{G} \simeq 1.2 \cdot 10^{28} \text{ eV} \simeq 22 \mu\text{g} . \quad (2.6)$$

Accelerator experiments reach energies $E \leq O(10^{13})$ eV, so they could only be confronted with such LIV effects $< O(10^{-30})$. It is therefore conceivable that a CPT conserving LIV has been overlooked up to now, although it plays an essential rôle on the Planck scale.

- We move on to the case where LI *and* CPT are violated. Then we expect LIV effects $\propto E$. Let us assume that even a surprisingly strong LIV parameter of this kind, say with a magnitude of $O(10^{-23})$, has been overlooked. It would be amplified to $O(10^{-8})$ on the Planck scale, so even there it would be of minor importance.

Therefore the *CPT conserving LIV terms* are more interesting. In addition to this estimate of magnitudes one might also argue that breaking one fundamental law of standard quantum field theory — which has been a principal pillar of physics since the 20th century — is a very daring step already. Hence it appears reasonable to study this step in detail, rather than damaging yet another highly established principle on top of it.

Cosmic rays represent indeed a unique opportunity to observe effects not too far below the Planck scale. The point is not only that they carry the *highest particle energies* in the Universe, but — even more importantly — their extremely *long flight*, which could accumulate tiny effects of new physics also at low or moderate energy (we will sketch examples in Subsection 3.4). If there is any hope to find experimental hints related to

theoretical approaches like string theory²⁶ or (loop) quantum gravity,²⁷ then it is likely to involve cosmic rays (although also LHC might have a chance [85]).²⁸ These hypothetical theories tend to install new fields in the vacuum, in addition to the Higgs field of the Standard Model. We are now going to glimpse at the mechanism how such new background fields could lead to spontaneous LIV.

2.3 Standard Model Extension (SME)

A systematic approach to add local LIV terms to the Standard Model has been worked out by A. Kostelecký and collaborators starting 10 years ago [87]. This collaboration provides a kind of encyclopedia of such terms, which is reviewed — along with its experimental bounds — in Ref. [88]. The original motivation emerged from string theory [89], which is, however, not needed for the resulting *Standard Model Extension* (SME).

We take a look at a prototype of a LIV term in this extension. Consider (in a short-hand notation) the Lagrangian of some fermion field $\psi(x)$, which may represent a quark or a lepton,

$$\mathcal{L} = i\bar{\psi}\gamma_{\mu}\partial^{\mu}\psi - g\bar{\psi}\phi\psi - ig'G_{\mu\nu}\bar{\psi}\gamma^{\mu}\partial^{\nu}\psi + \dots \quad (2.7)$$

We start with the free kinetic term, followed by the Yukawa coupling g to the Higgs field ϕ . The Standard Model assumes ϕ to undergo Spontaneous Symmetry Breaking (SSB), so that one of its components takes a non-vanishing expectation value, say $\langle\phi_0\rangle > 0$. This leads to the fermion mass $g\langle\phi_0\rangle$. A mass term cannot be written into the Lagrangian directly

²⁶String theories start from a higher dimension and first need a spontaneous LIV in that space to explain why we experience only 4 extended dimensions. This requires a non-perturbative mechanism, which is not well understood. One attempt to formulate string theory beyond perturbation theory is the 10d IIB matrix model (or IKKT model) [79]; a possible spontaneous splitting into extended and compact directions is discussed in Refs. [80], and for its 4d counterpart in Refs. [81].

As a different aspect, LIV effects on the Casimir force in a 5d brane world are discussed in Ref. [82].

²⁷Conceivable loop quantum gravity effects on cosmic rays are discussed in Refs. [83]. So far we can restrict parameters in specific quantum gravity approaches based on the bounds on LIV parameters [84].

²⁸We mention at the side-line that the scattering of UHECR primary particles on atmospheric molecules takes place at higher energies in the centre-of-mass frame than any scattering in accelerator experiments. In particular the proton-proton collisions at LHC (with 7 TeV per beam) will be equivalent in the centre-of-mass energy to the scattering of a 10^{17} eV proton on a fixed target. This happens about $2.5 \cdot 10^5$ times per second in the terrestrial atmosphere, in addition to the cosmic rays hitting other astronomical bodies, which obviously invalidates popular concerns about the safety of LHC [86]. Here, however, we are interested in interactions of UHECRs with CMB photons, which involve modest centre-of-mass energies, see Subsection 1.3.

if we want to keep the freedom to couple the left- and the right-handed chirality components of the fermion field independently to a gauge field; this is the situation in the electroweak sector of the Standard Model.²⁹

Let us now consider the third term in the Lagrangian (2.7), which is one of the possible extensions beyond the Standard Model. The Yukawa-type coupling $g' \in \mathbb{R}$ is another free parameter, which couples the fermion to a new background field of the Higgs-type, albeit with a tensor structure. Again we assume SSB, which could, for instance, lead to

$$\langle G_{00} \rangle > 0, \quad \langle G_{\mu\nu} \rangle = 0 \quad (\text{otherwise}) . \quad (2.8)$$

This additional term will obviously distort the fermion dispersion relation compared to the Standard Model, which amounts to a spontaneous LIV.

In contrast to the Higgs field we are now confronted with the question if new background fields — which may have a vector or a tensor structure — are Lorentz transformed as well. For a simple change of the observer’s inertial frame, all fields — including the background fields — are transformed, and \mathcal{L} remains invariant. However, the question if particles, which are described by fields like ψ , really perceive LI depends on a transformation of these fields only in a constant background [90, 72]. Kostelecký *et al.* denote this as an “active” (or “particle”) Lorentz transformation, and in this respect LI may break *spontaneously*, as in eq. (2.8).³⁰

In this way we can construct a non-standard dispersion relation for any particle, depending on its coupling to the tensor field $G_{\mu\nu}$ or further new background fields. The inclusion of gauge interactions proceeds in the familiar way (one promotes some global symmetries to local ones by means of covariant derivatives).

Of course the LIV parameter g' is just one example — the mass term and kinetic term in the Lagrangian (2.7) could both be extended by including a background field for each element of the Clifford algebra (further terms are written down in Section 3.5). Another example, which was considered earlier [91], is the addition of an extra gauge term of the Chern-Simons type to modify QED,³¹

$$\mathcal{L}_{\text{CS}} = -\frac{1}{4}\epsilon^{\mu\nu\rho\sigma} p_\mu A_\nu F_{\rho\sigma} = \frac{\mu}{2} \vec{B} \cdot \vec{A}, \quad (p_\mu p^\mu = \mu^2 > 0) . \quad (2.9)$$

²⁹On the other hand, a fermion mass term $-m\bar{\psi}\psi$ is allowed in a vector theory like QCD, where both chirality components of a quark couple to the gluons in the same manner.

³⁰Here one re-introduces a distinction, which one had hoped to overcome since the historic work by Einstein.

³¹In non-Abelian gauge theory, LIV through Chern-Simons-type terms is studied in Refs. [92].

Here p_μ is a vector of dimension mass (and $\vec{B} = \nabla \times \vec{A}$). Each component has vanishing covariant derivatives in all frames. This vector introduces a “preferred direction”, where also all the ordinary derivatives $\partial_\nu p_\mu$ vanish — Ref. [91] associates it with the preferred frame in a galaxy. It identifies an astrophysical bound of $\mu < O(10^{-33})$ eV based on radio galaxies (the method will be sketched in Subsection 3.5). Recently there have been attempts to achieve even higher precision for this bound based on the rotation of CMB photon polarisation vectors [93].

Note that \mathcal{L}_{CS} breaks also CPT invariance spontaneously. Examples for CPT conserving LIV terms in the fermionic and gauge part of the extended Lagrangian are the LIV term in eq. (2.7), or $K_{\mu\nu\rho\sigma} F^{\mu\nu} F^{\rho\sigma}$ (where K is another background tensor field). Kostelecký *et al.* have identified more than 100 LIV parameters in this way, including CPT breaking terms [94]. The resulting model preserves a number of properties of the Standard Model, like energy and momentum conservation, gauge invariance and locality. For massive fermions at low energy, and small LIV parameters, also energy positivity and causality are safe [95]. In the framework of SRT the photon is identified with the Nambu-Goldstone boson of the SSB of Lorentz symmetry. That collaboration also discussed various scenarios for an interpretation in the GRT framework [87, 64, 88].

In this parametrisation, the current status is summarised in Ref. [78] as follows: all (dimensionless) LIV coefficients are $< 10^{-27}$ (as we mentioned before). For those which break CPT the upper bound is as tiny as 10^{-46} , which further motivates our focus on CPT even terms. A detailed overview of the various bounds is given in Ref. [77].

An obvious question is why LIV should become manifest only at huge energies, although SSB is typically a low energy phenomenon. In principle even a LIV detected a low energy would not necessarily imply LIV at high energies. Of course we are interested in the opposite situation, where LIV is significant only at high energies, so we have to assume the SSB to persist over all energies that we consider. This setting requires *tiny* LIV parameters multiplying momenta of the fields (as in the examples above). Then the deviation from LI is only visible at huge momenta and a contradiction to known phenomenology can be avoided.

Although consistent, this scenario implies a severe *fine tuning problem*. On tree level one might hope for a somehow natural suppression of the LIV parameters by a factor $m_{\text{ew}}/M_{\text{Planck}} \sim 10^{-17}$ (where m_{ew} is the electroweak mass scale) [96]. If one includes 1-loop radiative corrections, however, this effect is lost and the magnitude of LIV effects is just given by $O(g_{\text{ew}}^2)$ (g_{ew} being an electroweak Yukawa coupling) [97], which is far from the suppression needed. If we consider LIV nevertheless, we have to add this problem to the list of unsolved hierarchy problems, like the small

vacuum angle θ in QCD, the small particle masses (on Planck scale) or the small cosmological constant. On the other hand, the Standard Models of particle physics and cosmology are well established, despite the presence of these unsolved problems.

2.4 Maximal Attainable Velocities (MAVs)

Within the same framework we now switch to the pragmatic perspective of Ref. [71]. We saw in the previous Subsection that LIV can be arranged for. Now we assume that this mechanism has been at work, and we proceed to an *effective Lagrangian*, which includes explicit LIV terms. Such an effective Lagrangian may also capture hadrons as composite particles (like Chiral Perturbation Theory).

Following Ref. [71] we leave, however, other Standard Model properties intact as far as possible. We therefore require CPT and gauge invariance to persist, and $SO(3)$ rotation symmetry to hold in a “preferred frame”.³² Moreover we do not break power counting renormalisability, *i.e.* we only add terms of mass dimension ≤ 4 .

Let us outline which terms are admitted by these conditions. For a bosonic field $\vec{\Phi}$ we can add a purely spatial kinetic term

$$\mathcal{L}_{\text{eff}} = \dots + \frac{1}{2} \sum_{i=1}^3 \sum_{a,b} (\partial_i \phi^a) \varepsilon_{ab} (\partial_i \phi^b) , \quad (\varepsilon_{ab} = \varepsilon_{ba}) . \quad (2.10)$$

(Equivalently we could add a term with only time derivatives instead). For a fermion field we insert a spatial kinetic term as well, where the LIV parameters can be distinct for positive or negative chirality,

$$\mathcal{L}_{\text{eff}} = \dots + i\bar{\psi} \vec{\gamma} \cdot \vec{\partial} [\varepsilon_+(1 + \gamma_5) + \varepsilon_-(1 - \gamma_5)] \psi . \quad (2.11)$$

Gauge interactions require covariant derivatives also in these non-standard terms. For the pure gauge part we first consider the Abelian gauge group $U(1)$, where the electric and the magnetic field are given by $E^i = -F^{0i}$, $B^i = \frac{1}{2}\epsilon^{ijk}F_{jk}$. The above conditions allow for three independent terms,³³

$$\vec{E}^2 - \vec{B}^2 , \quad \vec{E} \cdot \vec{B} , \quad \vec{B}^2 . \quad (2.12)$$

³²In contrast to Ref. [91], the following considerations on cosmic rays can hardly employ the preferred frame in a galaxy, because the primary particle paths extend over much larger distances. One might refer to the frame which renders the CMB maximally isotropic, cf. footnote 12.

³³Without insisting on CPT invariance, the Chern-Simons term (2.9) would be added to this list.

The first two among these terms are LI, so we work with the third one. Also in Yang-Mills gauge theories Ref. [71] uses the corresponding term

$$\mathcal{L}_{\text{eff}} = \cdots + g'' \sum_a \vec{B}^a \vec{B}^a, \quad (2.13)$$

where the index a runs over the generators of the Abelian factors in the gauge group.

In this way one obtains a quasi-Standard Model with 46 LIV parameters. In view of the above list the large number may come as a surprise at first sight, but it can be understood by the numerous new fermion generation mixings (for one case, the phenomenological impact on neutrino oscillation will be discussed in Subsection 2.5.4). Coleman and Glashow verified that all these parameters preserve the vanishing gauge anomaly, so that the model remains gauge invariant on quantum level.

We proceed to another prototype illustration and consider a neutral scalar field [71]. In some background the renormalised propagator G is written as

$$-iG^{-1} = (p^2 - m_0^2)f(p^2) + \varepsilon \vec{p}^2 g(p^2). \quad (2.14)$$

Geometrically we assume the usual Minkowski space with $c = 1$, $p^2 = E^2 - \vec{p}^2$, and m_0 is the renormalised mass at $\varepsilon = 0$. The functions f and g are not specified, but f obeys the conventional normalisation, and g is adapted to it, $f(m_0^2) = g(m_0^2) = 1$ (both functions are smooth in this point).

Let us now turn on a tiny LIV parameter ε and consider its leading order. The poles in the propagator are shifted to

$$\begin{aligned} E^2 &\simeq \vec{p}^2 + m_0^2 - \varepsilon \vec{p}^2 \simeq \vec{p}^2 c_{\text{P}}^2 + m^2 c_{\text{P}}^4 \\ \text{with} \quad m &= \frac{m_0}{1 + \varepsilon}, \quad c_{\text{P}} = 1 - \varepsilon \quad (\text{to } O(\varepsilon)). \end{aligned} \quad (2.15)$$

The renormalised mass is modified, $m_0 \rightarrow m$. However, we are more interested in the feature of the dispersion relation (2.15): the parameter c_{P} takes the rôle, which is usually assigned to c . From the group velocity

$$\frac{\partial E}{\partial |\vec{p}|} = \frac{|\vec{p}|}{\sqrt{\vec{p}^2 + m^2 c_{\text{P}}^2}} c_{\text{P}} \quad (2.16)$$

it is obvious that this is the speed that the particle approaches asymptotically at large $|\vec{p}|$.

Following this pattern, each particle type P can pick up its own *Maximal Attainable Velocity (MAV)* c_{P} ; it might slightly deviate from the speed c , which establishes the Minkowski metrics. A tiny value of the

dimensionless parameter ε justifies the above linear approximations, and it is compatible with the desired setting where LIVs only become noticeable at huge momenta. We mentioned before that this imposes a new hierarchy problem (which we have to live with) and that we are referring here to an effective approach, which captures composite particles, unlike Subsection 2.3.

2.5 Applications of distinct MAVs

Let us now address some applications that we are led to if we assume certain particles to possess MAVs distinct from c . We still follow Ref. [71] and focus on applications of potential interest in cosmic ray propagation.³⁴

2.5.1 Decay at ultra high energy

We consider the possibility that some particle with index 0 decays into a set of particles with indices $a = 1, 2, \dots$. At ultra high energy all masses are negligible, but we assume individual MAVs for the particles involved, c_0, c_a . We further define c_{\min} as the minimal MAV among the decay products. Then the energetic decay condition reads

$$\begin{aligned} |\vec{p}^{(0)}| c_0 &= \sum_a |\vec{p}^{(a)}| c_a \geq c_{\min} \sum_a |\vec{p}^{(a)}| \geq c_{\min} |\vec{p}^{(0)}| \\ \Rightarrow c_0 &\geq c_{\min} := \min_a c_a . \end{aligned} \quad (2.17)$$

The interesting observation is that tiny differences in the MAVs can be arranged such that a usual decay cannot take place anymore if the primary particle carries ultra high energy. This happens when the condition (2.17) is violated, *i.e.* if c_0 is smaller than any of the c_a .

On the other hand, new decays could be allowed at high energy, such as the photon decay $\gamma \rightarrow e^+ + e^-$, see Subsections 2.5.2 and 3.5, or the radiative muon decay $\mu^- \rightarrow e^- + \gamma$. A further example is the inverse β -decay $p \rightarrow n + e^+ + \nu_e$, which tightens the bounds on specific LIV parameters [99] based on the new results for UHECR that we review in Appendix A.

2.5.2 Vacuum Čerenkov radiation

Next we consider a particle with a MAV that slightly exceeds the speed of light, *i.e.* it exceeds the MAV of the photon in vacuum,

$$\frac{c_P}{c_\gamma} = 1 + \varepsilon > 1 . \quad (2.18)$$

³⁴It has also been suggested to test MAVs in air showers [98].

This particle can be accelerated to a speed $v > c_\gamma$. Then it will emit *vacuum Čerenkov radiation*, so it slows down intensively. The energy required for vacuum Čerenkov radiation has to fulfil

$$E > \frac{m}{\sqrt{1 - (c_\gamma/c_P)^2}} \simeq \frac{m}{\sqrt{2\varepsilon}} , \quad (2.19)$$

where m is the particle mass, and we consider the leading order in ε .

As we discussed in Section 1, we know from cosmic rays that *protons* support an energy up to $O(10^{20})$ eV over a considerable path, hence this energy does not fulfil inequality (2.19). Coleman and Glashow infer

$$\varepsilon_p < \frac{m_p^2}{2E^2} \Big|_{E=10^{20} \text{ eV}} \approx 5 \cdot 10^{-23} , \quad (2.20)$$

where m_p and ε_p are the mass and the ε -parameter (see eq. (2.18)) of the proton.

Cosmic *electrons and positrons* are observed only up to $E \approx 1$ TeV, hence the Čerenkov constraint on their ε -parameter is much less stringent, $\varepsilon_e < 10^{-13}$. On the other hand, the absence of the photon decay $\gamma \rightarrow e^- + e^+$ constrains ε_e from below [100]. In total one arrives at

$$-10^{-5} < \left(\frac{c_e}{c_\gamma} - 1 \right) < 10^{-13} . \quad (2.21)$$

2.5.3 Impact on the GZK cutoff

In this generalised framework we now reconsider the head-on collision $p + \gamma \rightarrow \Delta(1232)$ of relation (1.3). For the MAVs we could check all kinds of scenarios — they are all conceivable in the effective ansatz of Subsection 2.4. Here we pick out the particularly interesting option that only the proton has a slightly slower MAV,

$$c_\gamma = c_\Delta = 1 , \quad c_p = 1 - \varepsilon < 1 , \quad (2.22)$$

(in the notation of eq. (2.20): $\varepsilon = -\varepsilon_p$). The condition for a Δ resonance in the scattering on a CMB photon was written down before in eq. (1.4). The following requirement still holds,

$$m_\Delta^2 \leq (E_p + \omega)^2 - (p - \omega)^2 \simeq E_p^2 - p^2 + 2\omega(E_p + p) , \quad (2.23)$$

where E_p , $p = |\vec{p}|$ are the proton energy and momentum, and ω is the photon energy, all in the FRW laboratory frame. The evaluation of

the right-hand-side is now modified due to the non-standard dispersion relation of the proton,

$$E_p^2 - p^2(1 - \varepsilon)^2 = m_p^2(1 - \varepsilon)^4 \quad \rightarrow \quad E_p^2 - p^2 \simeq m_p^2 - 2\varepsilon E_p^2, \quad (2.24)$$

where we assumed $E_p \gg m_p$ and $|\varepsilon| \ll 1$. If we additionally make use of $E_p \gg \omega$, we arrive at a new energy threshold condition, where one term is added compared to eq. (1.4),

$$m_\Delta^2 - m_p^2 + \underline{2\varepsilon E_p^2} \leq 4\omega E_p. \quad (2.25)$$

Once more, the extra term is suppressed by the factor ε , but it can become powerful at very large energies. The consequence of this modification is illustrated in Figure 9: the right-hand-side increases linearly with the proton energy E_p and reaches the standard threshold (for $\varepsilon = 0$) at the value E_0 given in eq. (1.5). A small $\varepsilon > 0$ leads to an increased threshold energy, and above a critical value ε_c the Δ resonance is avoided,

$$\varepsilon_c = \frac{\omega}{2E_0} \simeq \frac{2\omega^2}{m_\Delta^2 - m_p^2} \Big|_{\omega=5 \langle \omega \rangle = 3 \text{ meV}} \simeq 3 \cdot 10^{-23}. \quad (2.26)$$

Hence the critical parameter ε_c is tiny indeed, and this is all it takes to remove the GZK cutoff, at least in view of the dominant channel of photopion production.³⁵ (This is of course compatible with the condition (2.20), which only requires $\varepsilon > -5 \cdot 10^{-23}$.) The experimental bounds for the LIV parameters in the fundamental SME Lagrangian are below 10^{-27} (cf. Subsection 2.3). However, it is not obvious how this translates into bounds on effective MAV differences (remember that here we started from a renormalised propagator).³⁶

Let us stress once more that this is not in contradiction to the fact that this Δ resonance is observed at low energy — in that case the masses contribute significantly to the energies and the above approximations are not valid any longer.

For $\varepsilon > \varepsilon_c$ the dominant candidate for a photopion production channel is an excited proton state,

$$p + \gamma \rightarrow p^*(1435) \rightarrow p + \pi^0. \quad (2.27)$$

But at ultra high energy p^* can only decay if $c_p \geq c_\pi$, according to condition (2.17).³⁷ With a suitable choice of the MAVs we could close that channel too, and so on.

³⁵The idea that LIV could invalidate the GZK cutoff was first expressed in Refs. [101]. Later it has also been discussed in the SME framework [102].

³⁶A possible transition from SME parameters to hadrons by means of a parton model was discussed in Ref. [103].

³⁷Bounds on c_π based on UHECR are discussed in Refs. [65, 104].

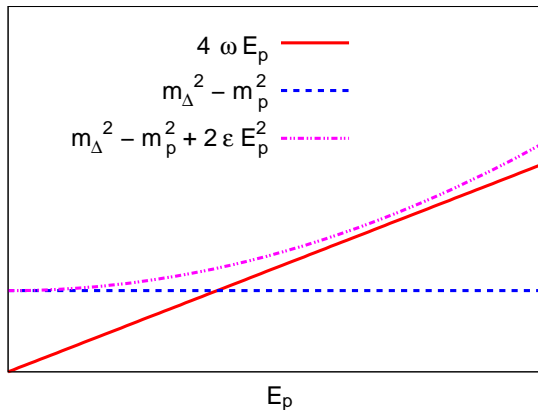


Figure 9: An illustration of the threshold for the term $4\omega E_p$ to enable photopion production through the $\Delta(1232)$ resonance: in the standard situation (all MAVs are 1) this threshold is constant, $m_\Delta^2 - m_p^2 \simeq (807 \text{ MeV})^2$. For $\varepsilon > 0$ the threshold squared picks up a contribution $\propto E_p^2$, see eq. (2.25), which requires a higher proton energy, and $\varepsilon > \varepsilon_c$ (illustrated by the dashed-dotted line) closes this channel for photopion production.

Just before Ref. [71] appeared, Ref. [18] attracted attention to the observation that the top 5 super-GZK events known at that time all arrived from the direction of a quasar (cf. footnote 6). This inspired Coleman and Glashow to suggest an unconventional hypothesis: the super-GZK primary particles could be *neutrons*. Assuming particle specific MAVs, the following arguments yield a consistent picture (see also Ref. [105]):

- For $c_n < c_{\min}$ (where c_{\min} refers to the β -decay products in the sense of relation (2.17)) the decay of the neutron can be avoided.
- Since we already assumed a slightly reduced neutron MAV, we might add $c_n < c_\Delta$ to protect the neutron from the GZK cutoff.
- Unlike the proton, the neutron is hardly deflected by interstellar magnetic fields, hence the scenario of an approximately straight path — which is required to make sense of the observation in Ref. [18] for quasars at large distances — becomes realistic.

This suggestion is currently not discussed anymore, but its consistency is beautiful enough to be reviewed nevertheless. Nowadays $O(100)$ super-GZK events have been reported (see Section 1), and the quasar hypothesis is out of fashion as well. However, the hypothesis of clustered UHECR directions has recently been revitalised, see Appendix A. Also the idea of electrically neutral primary particles is still considered, see

e.g. Refs. [106].³⁸ They include pions π^0 [65], photons [107] (though Ref. [25] puts a narrow bound on their UHECR flux), neutrinos [108] and hadrons of (u, d, s) quarks, which could be stable in SUSY theories [109].

2.5.4 Impact on neutrino oscillation

If the MAVs can deviate from c , there are *three* bases for the neutrino states:

- the flavour basis with the states $|\nu_e\rangle, |\nu_\mu\rangle, |\nu_\tau\rangle$,
- the basis of the neutrino masses,
- the basis of the MAVs.

In this framework neutrino oscillation could occur even at vanishing neutrino masses, due to a flavour mixing in the MAV basis.³⁹ However, in light of experimental data this scenario has soon been discarded [111, 112], so we start here from the usual point of view that the observed neutrino oscillation is evidence for non-vanishing neutrino masses.

We do consider, however, the possibility that the mass driven oscillation could still be modified as a sub-leading effect by additional MAV mixing. This scenario was investigated [113] based on the data by the MACRO Collaboration in Gran Sasso (Italy). The study can be simplified by focusing on the oscillation $\nu_\mu \leftrightarrow \nu_\tau$, which is most relevant for the observation of cosmic neutrinos. In this 2-flavour picture the two parameters

$$\begin{aligned} \Delta v &:= |\text{MAV}(\nu_1) - \text{MAV}(\nu_2)| \\ \theta_v &:= \text{mixing angle of } |\nu_\mu\rangle \text{ and } |\nu_\tau\rangle \text{ in the MAV basis} \end{aligned} \quad (2.28)$$

modify the life time of ν_μ .

As an example, Figure 10 shows the survival probability of ν_μ over a distance of 10^7 m (roughly a path across the Earth passing near the centre) at $\Delta v = 2 \cdot 10^{-25}$ (still in natural units, $c = 1$). The three curves refer to the MAV mixing angles with $\sin 2\theta_v = 0, \pm 1$. We see that the effect of such a mixing is very significant for neutrino energies of $O(100)$ GeV. If we assume neutrino masses $m \lesssim 1$ eV, this corresponds to a Lorentz factor $\gamma \gtrsim 10^{11}$, similar to the primary proton in a UHECR (see eq. (1.9)). Cosmic neutrinos in this energy range occur,⁴⁰ and their behaviour is again suitable for a sensitive test of LI at ultra high γ -factors.

³⁸However, neutral primary particles are not required for the hypothesis discussed

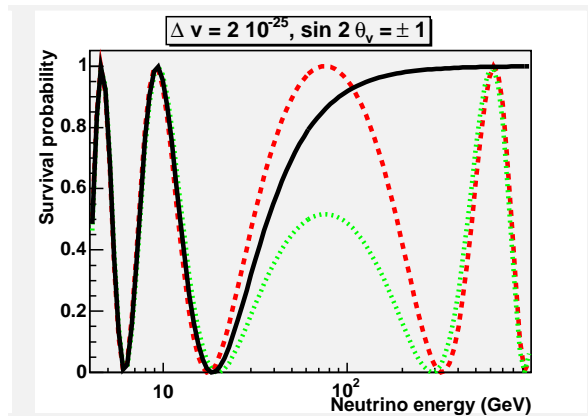


Figure 10: *The survival probability for a neutrino ν_μ over a distance of 10^7 m, for a MAV difference $\Delta v = 2 \cdot 10^{-25}$ (see eq. (2.28)). The plot is adapted from Ref. [113]. It shows the curves for mixing angles $\theta_v = 0$ (only mixing due to the neutrino masses) and $\theta_v = \pm\pi/4$ (red dashed line and green dotted line), where θ_v parameterises a mixing with ν_τ in the MAV basis. We see a strong effect on neutrinos of $O(10^{11})$ eV.*

The MACRO Collaboration detected upward directed muons generated by neutrinos in the $|\nu_\mu\rangle$ state through the scattering on a nucleon,

$$\nu_\mu + n \rightarrow \mu^- + p \quad \text{or} \quad \nu_\mu + p \rightarrow \mu^+ + n . \quad (2.29)$$

By monitoring multi-Coulomb scattering they reconstructed the energy E_μ and finally E_{ν_μ} . They observed 58 events with $E_{\nu_\mu} \gtrsim 130$ GeV and compared this flux to the one of ν_μ at low energies. It turned out that the oscillation curve obtained solely by mass mixing (corresponding to the curve for $\sin 2\theta_v = 0$ in Figure 10) works very well. Including the additional parameters (2.28) does not improve the fits to the data. Therefore the scenario of additional $\nu_\mu \leftrightarrow \nu_\tau$ mixing due to different MAVs is not supported, and Ref. [113] concludes

$$\Delta v < 6 \cdot 10^{-24} . \quad (2.30)$$

Of course the exact bound on Δv depends on the mixing angle — it becomes even more stringent when $|\sin 2\theta_v|$ approaches 1.

in Appendix A, since it assumes *nearby* UHECR sources.

³⁹A discussion in the SME terminology is given in Ref. [110].

⁴⁰One suspects that there are cosmic neutrinos at much higher energies as well — they are not restricted by any GZK-type energy cutoff (cf. footnote 17) nor deviated by magnetic fields, so they could open new prospects to explore the Universe. Several projects are going to search for them systematically, see Section 4.

This result is in agreement with similar analyses based on the Super-Kamiokande K2K data [112, 114]. Ref. [112] introduced a parameter n to distinguish scenarios for the origin of neutrino mixing as follows:

$$n = \begin{cases} -1 & \text{mass mixing (standard)} \\ 0 & \text{energy independent mixing} \\ 1 & \text{LIV resp. violated equivalence principle.} \end{cases} \quad (2.31)$$

The fit to the K2K data led to $n = -0.9(4)$, supporting the standard picture and strongly constraining the alternatives. Similarly Ref. [114] generalised the scenario corresponding to $n = 1$ by admitting vector and tensor background fields — as in Subsection 2.3 — and arrived qualitatively at the same conclusion.

Regarding the SME mixing parameters, a phenomenological test with $\bar{\nu}_e \leftrightarrow \bar{\nu}_\mu$ data has been presented in Ref. [115]. On the theoretical side the $\nu_\mu \leftrightarrow \nu_\tau$ oscillation of *Majorana neutrinos* is discussed in Ref. [116].

3 Cosmic γ -rays

In this section we are going to consider the photons themselves as they appear in cosmic rays — so far they entered our discussion only in the background. Their identification as primary particles is on relatively safe grounds (cf. Section 1).

3.1 Another puzzle for high energy cosmic rays ?

The highest energies in cosmic γ -rays were observed around $E_\gamma \gtrsim 50$ TeV (see *e.g.* Refs. [117]). They originate from the *Crab Nebula*, which is the remnant of a supernova — recorded by Chinese and Arab astronomers in the year 1054 — at a distance of 2 kpc.

The sources of the strongest γ -rays reaching us from *outside* our galaxy are *blazars*. Blazars are a subset of the AGN, see footnote 7.⁴¹ A few hundred blazars are known. A prominent example is named *Markarian 501*; in 1997 the High Energy Gamma Ray Astronomy (HEGRA) satellite detected γ -rays with $E_\gamma \gtrsim 20$ TeV from an outburst that this blazar had emitted [118]. It is located at a distance of 157 Mpc — this can be determined from the redshift ($z \simeq 0.034$). Here also the direction of the source is known, in contrast to far-travelling charged cosmic rays (gravitational deflections are small). Another example, which is noteworthy in this context, is *Markarian 421*, at a distance of 110 Mpc, which emitted photons that arrived with ~ 10 TeV [119].

⁴¹Appendix A addresses the hypothesis that AGN could emit UHECRs as well.

It was suggested that the observation of these highly energetic γ -rays could pose a new puzzle, which is similar to the GZK cutoff [120]. Again the question is why the CMB can be transparent for rays of such high energies. In this case, one expects electron/positron pair creation of an UV photon in the ray and an IR photon in the background,

$$\gamma_{\text{UV}}(E) + \gamma_{\text{IR}}(\omega) \rightarrow e^+ + e^- , \quad (3.1)$$

if sufficient energy is involved. This pair creation is followed by inverse Compton scattering on further CMB photons, triggering a cascade. In the centre-of-mass frame both photons in the transition (3.1) have the energy

$$\bar{\omega} = \frac{E}{\gamma} = \omega\gamma , \quad (3.2)$$

where γ is the Lorentz factor between centre-of-mass and FRW laboratory frame (cf. Section 1). The condition for pair creation is obvious,

$$\bar{\omega}^2 \equiv E\omega \geq m_e^2 . \quad (3.3)$$

If we insert once more the exceptionally large CMB photon energy that we referred to before in Sections 1 and 2, $\omega \approx 0.003 \text{ eV} \approx 5 \langle \omega \rangle$, the threshold for E is almost 10 TeV. If we repeat the considerations about the CMB photon density and the cross-section for this pair creation, in analogy to Subsection 1.3, also the observed energies E of photons coming from far distances (outside our galaxy) might be puzzling [121]. The mean free path length $\ell_{\gamma\gamma}$ is given by a formula similar to eq. (1.12),

$$\frac{1}{\ell_{\gamma\gamma}(E)} = \frac{1}{8E^2} \int_{\omega_{\min}(E)}^{\infty} d\omega \frac{dn_{\gamma}/d\omega}{\omega^2} \int_{(2m_e)^2}^{4E\omega} ds s \sigma_{\gamma\gamma}(s) . \quad (3.4)$$

As in eq. (1.4), s is one of the (LI) Mandelstam variables. The differential photon density of the CMB follows Planck's formula (1.1). The minimal CMB photon energy is $\omega_{\min}(E) = m_e^2/E$, see eq. (3.3). The boundaries for the angular integral over s are also obvious, and $\sigma(s)$ is the cross-section. It peaks just above the threshold $s = (2m_e)^2$, and at high energy ($s \gg m_e^2$) it decays as [21]

$$\sigma_{\gamma\gamma} \propto \frac{1}{s} \ln \frac{s}{2m_e^2} . \quad (3.5)$$

Ref. [122] evaluated this formula and found for instance for $E = 10 \text{ TeV}$ a path length $\ell_{\gamma\gamma} \approx 10 \text{ Mpc}$, so that the radiation from Markarian 421 and 501 appears amazing. Ref. [122] suggested a generalisation of formula (3.4) to a LIV form, inserting *ad hoc* a deformed photon dispersion

relation, which extends $\ell_{\gamma\gamma}$. However, the question if this puzzle persists in the LI form, after taking all corrections into account, is controversial [123, 124, 76]. One issue is our poor knowledge about the radio background radiation, which dominates over the CMB at wave lengths $\gtrsim 1$ m (cf. footnote 8). Ref. [21] studied the effective penetration length ℓ_{cascade} of the photon cascade under different assumptions for the extragalactic magnetic field and the radio background. Over a broad interval for these two parameters, Figure 14 in that work implies

$$\ell_{\text{cascade}} \approx \begin{cases} 100 \text{ Mpc} & \text{at } E = 30 \text{ TeV} \\ 300 \text{ Mpc} & \text{at } E = 10 \text{ TeV} . \end{cases} \quad (3.6)$$

In light of these numbers the observations of Markarian 421 and 501 appear less puzzling, but the issue is still under investigation. As in the case of the GZK cutoff we discuss possible solutions for such a puzzle — if it exists — based on LIV.

Also this *multi-TeV* γ -puzzle could in principle be solved by assuming different MAVs (cf. Sections 2.4, 2.5) for the two particle types involved [125],

$$c_e = c_\gamma + \varepsilon_e . \quad (3.7)$$

For a head-on collision the condition (3.3) is modified to

$$E\omega > m_e^2 + \varepsilon_e E^2 + O(\varepsilon_e^2) , \quad (3.8)$$

in analogy to eq. (2.25). Therefore a parameter $\varepsilon_e > 0$ could increase the energy threshold and — if ε_e reaches a critical value ε_c — exclude the electron-positron pair creation. Then the Universe becomes transparent for photons of higher energy. At the energies that we considered above, this happens for

$$\varepsilon_e > \varepsilon_c = 2 \frac{E\omega - m_e^2}{E^2} \Big|_{E=20 \text{ TeV}, \omega=5 \langle\omega\rangle=0.003 \text{ eV}} \simeq 2 \cdot 10^{-15} . \quad (3.9)$$

This critical value is much larger than the one for the proton in eq. (2.26). However, what matters is that ε_c is well below the upper bound on ε_e that one obtains from the absence of vacuum Čerenkov radiation, given in eq. (2.21). Therefore the MAV scenario could provide a conceivable solution to the (possible) multi-TeV γ -puzzle as well.

Ref. [126] contains a discussion in the spirit of SME and finds that LIV, in addition to modifying the minimal energy threshold, could also imply an *upper* energy bound for this pair production.

3.2 γ -Ray-Bursts (GRBs)

We now consider cosmic γ -rays of lower energy and focus on *γ -Ray-Bursts* (GRBs). These bursts are emitted in powerful eruptions over short periods, usually of a few seconds or minutes (in extreme cases of $0.1 \dots 10^3$ s). They typically include photons with energies $E_\gamma \approx (10^4 \dots 10^8)$ eV. Temporarily they are the brightest spots in the sky. The size of these sources is rather small. About the GRB origin we only have speculations, such as the merger of two neutron stars, or of two black holes, or of a neutron star and a black hole, or hypernovae (a theoretically predicted type of supernova, where an exceptionally massive star collapses). There are, however, sophisticated models for the GRB generation, dealing in particular with fireball shock scenarios or a gravitational core collapse [127].⁴²

GRBs have been observed since 1967. Most of them were discovered first by satellites (such as Hubble); subsequently ground-based telescopes could focus on them and identify the distance to the source. Today also the initial detection from Earth is possible, in particular from the observatory in La Silla (Chile) [130], which enables an immediate evaluation of the redshift. A spectacular GRB was observed in 2005 from the satellite SWIFT: it came from a distance of ~ 4 Gpc; these photons travelled to us directly from the Universe when it was only $9 \cdot 10^8$ years old.

The very long journey of photons with different energies but similar emission times is suggestive for a test of the *photon dispersion relation*. This test probes if the group velocity v_γ is really independent of the momentum [120]. The simplest approach for a deviation of this standard assumption is the introduction of a photon mass $m_\gamma > 0$ (which requires a modification of the Higgs mechanism). This obviously leads to

$$v_\gamma(p) = \frac{p}{\sqrt{p^2 + m_\gamma^2}} \neq \text{const.} \quad (3.10)$$

as sketched in Figure 11 ($c = 1$ is still the photon MAV). From the observation that the photons in a GRB arrive at approximately the same time one can deduce $m_\gamma < 10^{-6}$ eV [120]. However, the bound obtained in the laboratories is superior by many orders of magnitude, $m_\gamma < 10^{-17}$ eV [32].

Therefore the option of introducing a photon mass is not attractive in this context — even if it exists below the experimental bound, its effect would be invisible to us in GRBs. In the following we stay with $m_\gamma = 0$. The MAV ansatz $E^2 = p^2 c_\gamma^2$ does not help as a theoretical basis for a possible momentum dependence of the speed of photons. On the effective

⁴²It has also been proposed that the sources of GRB and UHECR could coincide [128, 129].

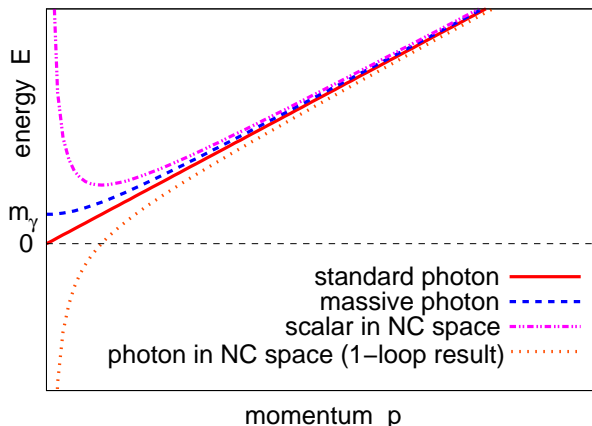


Figure 11: *Qualitative comparison of various dispersion relations in the IR regime: standard photon (mass zero in commutative space), massive photon (in commutative space), massless scalar particle in an NC space and massless photon in an NC space. The latter corresponds to the 1-loop result, but its feature changes non-perturbatively, see Subsection 3.3.2.*

level one can still study LIV modified Maxwell equations and evaluate the dispersion together with the rotation of the polarisation plane [131, 132], see Subsection 3.5. However, we now proceed to another theoretical approach for new physics, including a non-linear photon dispersion relation, which is highly fashionable. That approach is basically different from the effective action concepts that we considered in Section 2.⁴³

3.3 Non-commutative (NC) field theory

As a brief introduction, we embed this booming field of research into a historic perspective. Galilei’s system of coordinate transformation did not have any constant of Nature (hence it was in some sense more relativistic than the relativity theory of the 20th century). Einstein did introduce the speed of light c as such an invariant; it is a corner stone of both, Special and General Relativity Theory. Now there are speculations that there might be yet another constant of Nature in addition to c . Ref. [134] denotes this line of thought as “Doubly Special Relativity” (according to Ref. [133] it emerged as an effective model for “varying speed of light” in a quantum space-time). This second constant is usually assumed to be a large, observer-independent energy.

One often refers to gravity effects becoming important in field theory

⁴³A further alternative are “varying speed of light theories”, which are reviewed in Ref. [133].

at very large energy. This is supposed to be a generic property, which is likely to hold even though we do not have an established theory of quantum gravity [61]. Therefore it appears natural to relate this second constant to the Planck mass (2.6) (though there may be alternatives [135]). Geometrically this means the absence of sharp points, but a space where points are washed out on the scale of the Planck length

$$L_{\text{Planck}} = M_{\text{Planck}}^{-1} \simeq 1.6 \cdot 10^{-35} \text{ m} . \quad (3.11)$$

(J. von Neumann dubbed it “pointless geometry”, though this term applies to the phase space in standard quantum mechanics as well).

It can be compared to the lattice regularisations, which truncates short distances *ad hoc*. For numerous quantum field theories this is the only regularisation scheme, which works beyond perturbation theory.⁴⁴ It is not only a basis for the numerical measurement of observables, but it actually *defines* these theories on the non-perturbative level. Nevertheless hardly anyone would assume a lattice structure to be physical — it could at best mimic the geometry on the Planck scale. A more subtle way to introduce a geometric UV cutoff places field theory on a space with a *non-commutative geometry*. Let us briefly review the historic construction in the first publication on this subject [138].

We know that quantum mechanics is endowed with a natural discretisation of angular momenta based on the uncertainty relation. The idea is now to make use of this mechanism for space coordinates as well: the coordinate components should be described by operators with discrete spectra, as it is familiar for the angular momentum components. This can be achieved from a higher dimensional perspective. We start from a 5d Minkowski-type space with the invariant quantity

$$S = x_0^2 - x_1^2 - x_2^2 - x_3^2 - x_4^2 . \quad (3.12)$$

We specify a surface $S = \text{const.} > 0$, which is a 4d de Sitter space inside the 5d light cone. Now we list the generators of transformations that leave S invariant,⁴⁵

$$\begin{aligned} L_3 &= \frac{\hbar}{i}(x_1\partial_2 - x_2\partial_1) , & \text{invariant} & : x_1^2 + x_2^2, x_0, x_3, x_4 , \\ M_1 &= i\hbar(x_0\partial_1 - x_1\partial_0) , & \text{invariant} & : x_0^2 - x_1^2, x_2, x_3, x_4 , \\ X_1 &= \frac{a}{i}(x_1\partial_4 - x_4\partial_1) , & \text{invariant} & : x_1^2 + x_4^2, x_0, x_2, x_3 , \\ T &= ia(x_0\partial_4 - x_4\partial_0) , & \text{invariant} & : x_0^2 - x_4^2, x_1, x_2, x_3 . \end{aligned}$$

⁴⁴The “fuzzy sphere” [136] has recently been considered as a possible alternative, but numerical work in that regularisation [137] is at an early stage.

⁴⁵In general we use natural units, but at this point it is instructive to make an exception and write \hbar explicitly.

The operators L_1, L_2, M_2, M_3 and X_2, X_3 are analogous. They all conserve 5d LI. L_i and M_i generate the familiar rotations and Lorentz boosts, so they preserve in addition also 4d LI (at $x_4 = 0$). The latter is broken, however, by the X_i and T . Here a parameter a enters in a rôle similar to \hbar in the 4d transformations.

To show that the spectra of X_i are discrete, we follow the procedure which is well-known from quantum mechanics. We write the rotated plane in polar coordinates, $(x_1, x_4) = r(\sin \varphi, \cos \varphi)$, so that $X_1 = -ia\partial_\varphi$. For an eigenfunction ψ , $X_1\psi = \lambda\psi$, we make the ansatz

$$\psi \propto \exp(i\varphi\lambda/a) , \quad \text{and} \quad \psi(\varphi) = \psi(\varphi + 2\pi) \Rightarrow \lambda = na \quad (n \in \mathbb{Z}) .$$

As another property that is familiar from the angular momentum algebra, these position operators are *non-commutative (NC)*

$$[X_i, X_j] = \frac{ia^2}{\hbar} \epsilon_{ijk} L_k , \quad [T, X_i] = \frac{ia^2}{\hbar} M_i . \quad (3.13)$$

That property obviously implies *new uncertainty relations* for these space-time coordinate operators (without involving momenta !)

$$\Delta X_i \Delta T , \Delta X_i \Delta X_j \geq O(a^2) , \quad (i \neq j) . \quad (3.14)$$

In this sense a takes indeed the rôle of a minimal length, and thus of a new constant of Nature. A field theory living on this space is necessarily *non-local* over the characteristic extent a . LI is violated in the 4d subspace, though its 5d version is preserved. The latter property shows that this way to implement a minimal length is far more subtle than a crude space-time lattice⁴⁶: some facet of relativity persists, and the mechanism is organically embedded into the general framework of quantum physics.⁴⁷

⁴⁶Alternatively, a discrete 4d space-time with Poisson distributed random sites can be compatible with local LI [139]. The LI dispersion relation can be reproduced exactly, even on regular lattices, if one implements a “perfect lattice action” based on the renormalisation group (see *e.g.* Ref. [140] and refs. therein).

⁴⁷Based on such considerations, it is tempting to speculate that extra dimensions could in fact have a physical meaning. The literature on this issue is tremendous; we do not try to review it here, but we only mention one point:

Further arguments for extra dimensions deal with the *mass hierarchy problem*, *i.e.* the question why the known particle masses are so far below the Planck mass (2.6) (or in QCD: $m_{u,d} \ll \Lambda_{\text{QCD}}$). For instance, fermions naturally undergo a renormalisation, which puts their mass *non-perturbatively* on the cutoff scale (unless some artificial fine-tuning of the bare mass is performed). An extra dimension helps to some extent to implement approximate chirality and therefore a small fermion mass [141]. If one is willing to assume SUSY in addition, then this mechanism is transmitted to the boson masses as well.

Snyder constructed the 4-momentum as [138]

$$P_\mu = \frac{\hbar}{a} \frac{x_\mu}{x_4} \quad (\mu = 0 \dots 3), \quad (3.15)$$

which is consistent with $L_k = \epsilon_{ijk}(X_i P_j - X_j P_i)$, $M_i = X_i P_0 + T P_i$. The commutators

$$[X_i, P_j] = i\hbar \left[\delta_{ij} + \left(\frac{a}{\hbar} \right)^2 P_i P_j \right] \quad (3.16)$$

yield Heisenberg uncertainties, which are modified to $O(a^2 P_i P_j / \hbar)$. For a tiny parameter a we have — *on tree level* — again the situation that the modification is only visible at huge momenta.

Based on the uncertainty relations (3.14), the identification of a as the Planck length now leads to a consistent picture of the space-time uncertainty range as the event horizon of a mini black hole [142]. In fact, a (hypothetical) measurement of a length of $O(L_{\text{Planck}})$ requires (according to the Heisenberg uncertainty) an enormous energy density, which gives rise to such an event horizon — the notion of detectable events then requires inequalities (3.14) to hold with $a \sim L_{\text{Planck}}$. This *Gedankenexperiment* suggests that points should indeed be washed out over a range of $O(L_{\text{Planck}})$. If several directions are involved, as in relation (3.14), this is practically equivalent to non-commutativity.

As a variant we may just combine the uncertainty over the gravitational radius $\Delta x / 2 \sim L_{\text{Planck}}^2 \cdot \Delta p$ with Heisenberg's uncertainty to arrive at a modification of the latter, even in one dimension [143],

$$\Delta x \gtrsim \max\left(\hbar / (2\Delta p), 2L_{\text{Planck}}^2 \Delta p / \hbar\right) \gtrsim L_{\text{Planck}}. \quad (3.17)$$

However, this modification can lead to dangerous processes, setting in at the 1-loop level, where it is not obvious how to avoid a contradiction to known phenomenology [144]. We now return to the NC space — although it is plagued by dangers of this kind as well — keeping in mind that basic progress in physics has been repeatedly related to the realisation that specific quantities are “unspeakable” [145].

Above we followed the historic path to non-commutativity. The currently popular version (for a review, see *e.g.* Ref. [146]) inserts for the coordinate commutators a constant “tensor field”,⁴⁸

$$[X_\mu, X_\nu] = i\Theta_{\mu\nu}, \quad \min(\Delta X_\mu, \Delta X_\nu) = \frac{1}{2} |\Theta_{\mu\nu}|. \quad (3.18)$$

⁴⁸It is a tensor under a twisted Poincaré group, and the action can be called LI if one also adapts a twisted particle statistics [147].

Thus we have the case of an “*active LIV*” (see Subsection 2.3), and agreement with the general scope of DSR. The question of its CPT invariance is discussed in Refs. [148, 149, 150].

The original motivation for introducing NC coordinates was the hope to tame the notorious UV divergences in quantum field theory. In fact, they are removed in the non-planar diagrams, but in the planar diagrams they persist [151]. Moreover, the non-planar diagrams give rise to new divergences in the IR sector [152], which causes the dangerous processes that we announced.

A famous example is the one-particle irreducible 2-point function $\langle\phi(-p)\phi(p)\rangle$ in the 4d NC $\lambda\phi^4$ model. The planar 1-loop contributions diverges $\propto \Lambda^2$ as in the commutative case (Λ being a UV cutoff), whereas the non-planar diagram picks up an additional phase factor,

$$\langle\phi(-p)\phi(p)\rangle_{1\text{-loop, non-planar}} = \frac{\lambda}{6} \int \frac{d^4k}{(2\pi)^4} \frac{e^{ik_\mu\Theta^{\mu\nu}p_\nu}}{k^2 + m^2}. \quad (3.19)$$

The exponential phase factor is generic for each crossing between lines of external propagators and loops. At finite $\Theta^{\mu\nu}$ and p_ν the integral $\int dk_\mu$ converges now thanks to the rapid oscillation at large $|k_\mu|$. As a consequence, for this non-planar diagram the UV cutoff turns into [152]

$$\Lambda_{\text{eff}}^2 = \frac{1}{1/\Lambda^2 - p_\mu(\Theta^2)^{\mu\nu}p_\nu}. \quad (3.20)$$

The UV limit $\Lambda \rightarrow \infty$ can in fact be taken in this term, as long as the field momentum p remains finite. In addition to the IR divergence due to the latter condition, we also see that the limit $\|\Theta\| \rightarrow 0$ is *not smooth*.

So far no systematic solution has been found for the treatment of multi-loop diagrams, which involve such singularities at both ends of the momentum scale. Hence renormalisation does not become easier but even more complicated due to non-commutativity. This problem is known as *UV/IR mixing*. Intuitively this is not too surprising in view of the uncertainty relation (3.18).

Part of the literature deals with a truncated expansion in small $\|\Theta\|$, which allows for instance for a generalised formulation of the Standard Model [153]. This generalisation may be of interest by itself, but due to the UV/IR mixing effects — and the related discontinuous transition to standard commutativity, $\|\Theta\| \rightarrow 0$ — it is *fundamentally different* from complete quantum field theory on a NC space; for instance, locality is restored in that truncated expansion. Ref. [154] also refers to such a truncated expansion to embed NC field theory into the SME (cf. Subsection 2.3). However, since this alters basic properties, the SME — or

other low energy effective field theory approaches to include LIV terms — and (full-fledged) NC field theory are basically different.

Despite — or because of — the amazing UV/IR mixing effects, NC field theory has attracted a lot of attention; over the last 10 years, about 2500 works have been written about it. This boom was triggered by the observation that it can be mapped onto certain string theories at low energy [155]. In that framework one could also relate the non-locality range $\sqrt{|\Theta|}$ to the string extent; this was the inspiration of Refs. [143]. A general analysis of the spatial uncertainty in string theory is given in Ref. [156], and Ref. [157] presents numerical results related to the emerging geometry in the IIB matrix model (cf. footnote 26).

NC field theory can be viewed as the second main theoretical framework for LIV, in addition to the approach described in Subsections 2.3 and 2.4. In both cases it was string theory which inspired a new concept in particle physics,⁴⁹ but the way that the formulations are elaborated now they can be introduced and studied as modifications of standard field theory without any reference to strings.

3.3.1 The photon in a NC world

Due to non-commutativity, gauge transformations and translations are intertwined. As a consequence, even the pure $U(1)$ gauge field picks up a Yang-Mills type self-interaction term, *i.e.* the $U(1)$ gauge field becomes NC as well.

This can be seen easily if we switch to the alternative formulation, which uses ordinary coordinates, but all field multiplications are performed with the *star product* (or Groenewold-Moyal product) [159]

$$\phi(x) \star \psi(x) := \phi(x) \exp\left(\frac{i}{2} \overleftarrow{\partial}_\mu \Theta^{\mu\nu} \overrightarrow{\partial}_\nu\right) \psi(x) . \quad (3.21)$$

Its equivalence to the formulation referred to above can be shown by a plane wave decomposition, which allows for a transition between fields and Weyl operators (see *e.g.* Ref. [160]). The star-commutator $[x_\mu, x_\nu]_\star = i\Theta_{\mu\nu}$ makes this link plausible. In case of a pure $U(N)$ gauge action,

$$S[A] = -\frac{1}{4} \int d^d x \operatorname{Tr} F_{\mu\nu} \star F^{\mu\nu} , \quad F_{\mu\nu} = \partial_\mu A_\nu - \partial_\nu A_\mu + ig[A_\mu, A_\nu]_\star$$

the commutator term does not vanish, even if the gauge group is $U(1)$, since it is promoted to a star-commutator, $[A_\mu, A_\nu]_\star := A_\mu \star A_\nu - A_\nu \star A_\mu$.

This formulation applies to all NC $U(N)$ gauge theories, but for the gauge groups $SU(N)$ it fails: in commutative spaces the algebra of the

⁴⁹The history is reviewed from this perspective in Ref. [158].

generators A^a closes thanks to the identity $\text{Tr}[A^a, A^b] \equiv 0$, which does not hold, however, for the star-commutator. In view of phenomenology, the group $U(1)$ is therefore of primary interest.

The Yang-Mills type self-interaction in NC spaces leads to a distorted photon dispersion relation. On tree level the non-commutativity only affects very short distances and therefore the UV behaviour of dispersion relations. But on quantum level it causes in addition IR singularities, as we pointed out before. Ref. [161] performed a 1-loop calculation of the effective potential in NC $U(1)$ gauge theory and derived a dispersion relation of the form

$$E^2 = \bar{p}^2 + C \frac{g^2}{p \circ p} + O(g^4),$$

$$p \circ p := -\Theta^{\mu\nu} p_\nu \Theta_\mu^\sigma p_\sigma > 0, \quad C = \text{const.} \quad (3.22)$$

This suggests that a small non-commutativity has a stronger impact than a large one, and based on GRB data one could therefore be tempted to claim a *lower* bound [162],⁵⁰ which is large compared to the Planck length scale,

$$\|\Theta\| > 10^{-44} \text{ m}^2 \simeq (10^{13} \cdot L_{\text{Planck}})^2. \quad (3.23)$$

However, one should better not insist on this apparently spectacular inequality (as Ref. [162] also noticed) for a number of reasons:

- First we stress that this does not rule out the standard commutative world, $\Theta = 0$, where no extra term of this kind occurs. Eq. (3.22) shows again that the transition $\|\Theta\| \rightarrow 0$ is not smooth.

Part of the literature deals with an expansion in $1/\|\Theta\|$, which does have a smooth limit to a commutative field theory at $\|\Theta\| \rightarrow \infty$ — at least in perturbation theory around the free field vacuum — because the extra phase factor $\exp(ik_\mu \Theta^{\mu\nu} p_\nu)$ (for the crossing of propagator lines, see eq. (3.19)) cancels the non-planar diagrams at finite external momentum p . However, that commutative limit does not coincide with the standard setting $\Theta = 0$. Moreover, in case of SSB the above perturbative argument collapses, because it does not refer to an expansion around a vacuum state anymore, and therefore NC effects may persist [164].

- Such a strong non-commutativity is well above the upper bound established from other observations [162]. Does this mean that NC field theory is ruled out already?

Further aspects make this issue more complicated.

⁵⁰Ref. [163] presents a similar consideration based on 1-loop effects in the potential for NC scalars, which becomes strong for very small $\|\Theta\| > 0$.

- A careful evaluation [165] revealed that the NC term in eq. (3.22) is actually *negative*,

$$C = -\frac{2}{\pi^2} . \quad (3.24)$$

Therefore the system appears *IR unstable*, as illustrated in Figure 11. In string theory there are attempts to interpret such systems (a key word is “tachyon condensation” [166]), but in simple terms of quantum physics a system without a ground state does not have an obvious meaning. Hence this observation looks like a disaster for NC field theory — it seems to be in straight contradiction to everyday’s experience.

The behaviour with a *positive* IR divergence can be realised for instance for NC scalar particles. This feature was indeed measured numerically in the 3d $\lambda\phi^4$ model with a NC spatial plane [167], as sketched in Figure 11. A condensation of the finite mode of minimal energy then gives rise to a “stripe pattern” formation, *i.e.* some non-uniform periodic order dominates the low energy states, which corresponds to SSB of Poincaré invariance. In perturbation theory the negative IR energy for the NC photon emerges from the requirement to fix the gauge.

There is extensive literature about electrodynamics with star products on tree level, ignoring this problem. However, the question is in which regime non-commutativity effects could be manifest while quantum corrections are not visible. Here the surprises on quantum level are even more striking than in the case of LIV parameters entering effective field theory [97] because of the UV/IR mixing. Most people who were concerned with this severe problem moved on to a supersymmetric version, where the negative IR divergence is cancelled by a positive one due to the fermionic partner of the gauge field, with an opposite loop correction [165, 168]. Does this mean that non-commutativity is only sensible if one puts SUSY as yet another hypothetical concept on top of it ?

Even then the corresponding $\mathcal{N} = 4$ super-Yang-Mills theory suffers from a hierarchy problem for the SUSY breaking scale [149].

- From our point of view, the apparent quest for multiple hypotheses (NC geometry plus SUSY) to cancel the IR instability makes NC field theory less attractive. However, if the 1-loop result has such amazing features one may wonder if it should be trusted to extract qualitative properties of the system. We therefore reconsidered this question on the *non-perturbative* level [169].

3.3.2 The NC photon revisited non-perturbatively

A truly non-perturbative investigation of the NC photon — at finite non-commutativity and finite self-coupling — has to be carried out numerically. This requires a Euclidean metrics. If we introduce a NC Euclidean time, reflexion positivity (as one of the Osterwalder-Schrader axioms [170]) is lost. Then it is not known how to achieve a transition to Minkowski signature, so we keep the Euclidean time commutative.⁵¹

Moreover we need the (anti-symmetric) tensor Θ to be invertible on the NC subspace,⁵² hence we only introduce a NC spatial plane (x_1, x_2) with a single non-commutativity parameter θ

$$[\hat{x}_i, \hat{x}_j] = i\theta \epsilon_{ij} \quad (i, j = 1, 2) , \quad (3.25)$$

while the plane (x_3, x_4) is kept commutative. (Once the Euclidean time x_4 commutes, this form can always be obtained by means of rotations.) This is the only conceptually clean non-perturbative NC setting available, and it can be viewed as a minimally NC formulation.

Next we need a regularisation to a finite number of degrees of freedom in order to enable a numerical treatment. As in commutative field theory the lattice is suitable for this purpose. Here we review the NC lattice formulation briefly, details are explained in Ref. [160]. Although we do not have sharp points for the lattice sites at hand, a lattice structure can be imposed by requiring the operator identity

$$\exp\left(i\frac{2\pi}{a}\hat{x}_i\right) = \hat{\mathbb{1}} . \quad (3.26)$$

The length a is now the (analog of a) lattice spacing, *i.e.* the spacing in the spectra of the operators \hat{x}_i (which cannot be diagonalised simultaneously). Again in the spirit of minimal non-commutativity we let the momentum components commute (as in Snyder's formulation (3.15)). Their usual periodicity over the Brillouin zone has remarkable consequences,

$$\begin{aligned} e^{ik_i\hat{x}_i} &= e^{i(k_i+2\pi/a)\hat{x}_i} \quad \Rightarrow \\ \hat{\mathbb{1}} &= e^{i(k_i+2\pi/a)\hat{x}_i} e^{-ik_j\hat{x}_j} \\ &= \exp\left(i\left(k_i + \frac{2\pi}{a}\right)\hat{x}_i - ik_j\hat{x}_j + \frac{1}{2}\left(k_i + \frac{2\pi}{a}\right)k_j[\hat{x}_i, \hat{x}_j]\right) \\ &= \hat{\mathbb{1}} \exp\left(\frac{i\pi}{a}\theta(k_2 - k_1)\right) \quad \Rightarrow \quad \frac{\theta}{2a}k_i \in \mathbb{Z} . \end{aligned} \quad (3.27)$$

⁵¹The opposite case with $[\hat{x}_i, \hat{t}] = \frac{1}{\kappa}\hat{x}_i$, $[\hat{x}_i, \hat{x}_j] = 0$ [171] is known as κ -Minkowski space. Work on its impact on dispersion relations is summarised in Ref. [124].

⁵²If this is the case, two operators \mathcal{O} at distinct points can be multiplied as [160] $\mathcal{O}(x)\mathcal{O}(y) = \pi^{-d}(\det\Theta)^{-1} \int d^d z \mathcal{O}(z) \exp[-2i(\Theta^{-1})_{\mu\nu}(x-z)_\mu(y-z)_\nu]$, where d is the dimension of the NC subspace, which has to be even.

In the exponent on the right-hand-side we had to keep track of the Baker-Campbell-Hausdorff term, which we evaluated by inserting relation (3.25). For fixed parameters θ and a we infer from this exponential factor that the momentum components in the NC lattice are discrete, so that this lattice is automatically *periodic*. Of course, this property is in contrast to lattices in a commutative space. Here we inevitably obtain an *UV and IR regularisation* at the same time.

If our lattice is periodic over N sites in each of the NC directions, the momentum components are integer multiples of $2\pi/(aN)$, which — along with relation (3.27) — implies

$$\theta = \frac{1}{\pi}Na^2 . \quad (3.28)$$

This shows that the extrapolation of interest is the *Double Scaling Limit* (DSL), which leads simultaneously to the continuum and to infinite volume at fixed θ ,

$$\left. \begin{array}{l} a \rightarrow 0 \quad (\text{continuum limit}) \\ Na \rightarrow \infty \quad (\text{infinite volume}) \end{array} \right\} \text{ at } Na^2 = \text{const.} \quad (3.29)$$

The requirement to take this simultaneous UV and IR limit is again specific to NC field theory and related to the UV/IR mixing. Any deviation from this balanced condition can lead to a limit, which is not really NC (it may lead to $\theta \rightarrow 0$ or ∞). This can cause confusion, and in other regularisation schemes it is less obvious how to control this equilibrium between UV and IR effects.

In view of lattice simulations, the construction of link variables in the NC plane appears difficult — note that a compact link variable should now be star-unitary, $U \star U^\dagger = U^\dagger \star U = \mathbb{1}$. However, there is an exact mapping [172] onto a $U(N)$ matrix model in one point, the so-called twisted Eguchi-Kawai model [173], which is numerically tractable.

The DSL of $U(1)$ lattice gauge theory on a NC plane has been studied in Refs. [174]. Wilson loops of *small* areas are real and they follow the Gross-Witten area law of commutative 2d $U(N \rightarrow \infty)$ gauge theory [175]. Wilson loops of *large* area A are shape dependent. For most shapes they have a complex phase A/θ , which corresponds to an Aharonov-Bohm effect, if one formally interprets $1/\theta$ as a magnetic field across the plane. The same interpretation was suggested long ago based on simple tree level considerations [176], and it is also inherent in the famous Seiberg-Witten map [155] onto open bosonic string theory.

Let us return to the 4d $U(1)$ gauge theory and its formulation on a regular lattice in the commutative plane, and a lattice as constructed

above in the NC plane. In each direction there is (approximately) the same number N of lattice sites.

In the NC plane the self-interaction and the gauge transformations are again non-local. As a consequence, there are *gauge invariant open Wilson lines*, in contrast to gauge theory in commutative spaces. Due to the separation of their end-points they carry non-vanishing momenta, so these open Wilson lines are suitable order parameters to probe if translation and rotation symmetry is spontaneously broken (we refer to the discrete translation and rotation symmetry on the lattice, resp. the continuous version in the DSL). In Mean Field Approximation, active Poincaré symmetry will always appear broken because of the constant tensor $\Theta_{\mu\nu}$. However, the question whether SSB really sets in or not is dynamical. We verified it by measuring the expectation values of open Wilson lines.

Numerical simulations at varying gauge coupling and different lattice sizes N revealed that a number of observables — Wilson loops and lines and their correlators, matrix spectra as extent of a dynamically generated space — stabilise (to a good approximation) for [169]

$$\beta \equiv \frac{1}{ag^2} \propto \sqrt{N} . \quad (3.30)$$

This defines the scale for the lattice spacing, up to a proportionality constant, which corresponds to the choice of θ . Now the DSL is well-defined and it can be explored by increasing N and β , while keeping the ratio $N/\beta^2 = \text{const.}$ Thus we extrapolate to the continuum and to infinite volume at fixed θ .

Our simulation results led to the phase diagram shown in Figure 12: at strong coupling, $\beta \lesssim 0.35$ we find for any N a symmetric phase, and at weak coupling again, but in between (at moderate coupling) there is a phase of spontaneously broken Poincaré symmetry.⁵³ Apparently the strong fluctuations at small β avoid SSB on one side, and at weak coupling the correlation length exceeds the scale of the mode of minimal energy, so that SSB only occurs at moderate coupling. The transition line between the weak and moderate coupling roughly follows the behaviour $\beta_c \propto N^2$, which means that the DSL curve (3.30) always ends up in the *broken phase*. So this is the phase that actually describes the NC continuum limit. Since it stabilises all observables that could be measured, the NC photon could be IR stable after all.

Figure 13 shows the numerically measured dispersion relations of the photon in a NC space. In the symmetric phase at weak coupling it is

⁵³This observation agrees qualitatively with later simulations of the 4d twisted Eguchi-Kawai model, which were performed with different motivations [177].

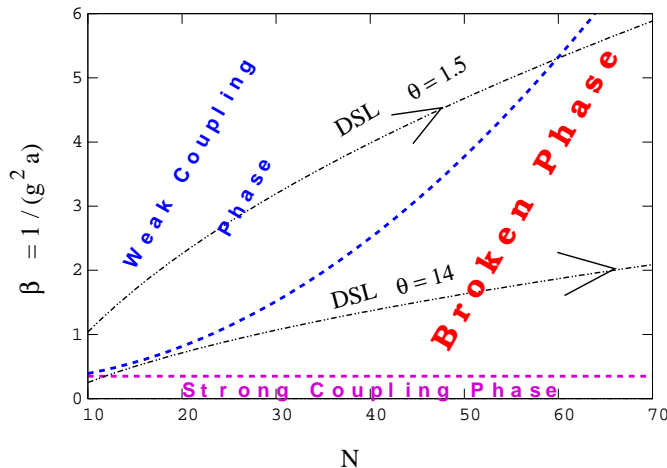


Figure 12: *The phase diagram for NC QED (pure $U(1)$ gauge theory) based on numerical results [169]. At strong coupling ($\beta \lesssim 0.35$), and also at weak coupling, translation and rotation symmetry is intact. In between, at moderate coupling, there is a phase where it is spontaneously broken. Perturbation theory perceives the weak coupling phase. The DSL (3.29), however, leads to the broken phase, which is therefore physically relevant.*

fully consistent with the IR instability found in perturbation theory, cf. Figure 11. Hence we agree with that calculation, but it does not capture the phase which is really relevant for the NC photon. The limit to a continuous, infinite NC space (the DSL) takes it to the broken phase, and there Figure 13 shows that the linear dispersion relation is restored.

This linear dispersion relation is consistent with *IR stability* and with the interpretation of the photon as a Nambu-Goldstone boson of the SSB of Poincaré symmetry (as it was also suggested in the SME [87]). This dispersion relation $E(p)$ was measured in the commutative plane, $p_1 = p_2 = 0$, $p = p_3$, where the exponential decay of the correlation function of open Wilson lines is clearly visible.

Once IR stability holds, the next step would be to elaborate also explicit non-perturbative results for a NC deformation of the dispersion in the DSL. Such a study should address finite momentum components of the NC directions in the broken phase dispersion relation. This could then be confronted with phenomenological data to set bounds on θ . A NC deformation in the IR sector could also be highly relevant for cosmic rays in view of the background radiation: the GZK cutoff and the multi-TeV γ -puzzle both depend on the CMB (and radio background) photons.⁵⁴

⁵⁴Moreover the CMB anisotropy (cf. footnote 12 and Ref. [33]) might be affected by NC effects, if they were sizable in the early Universe [178].

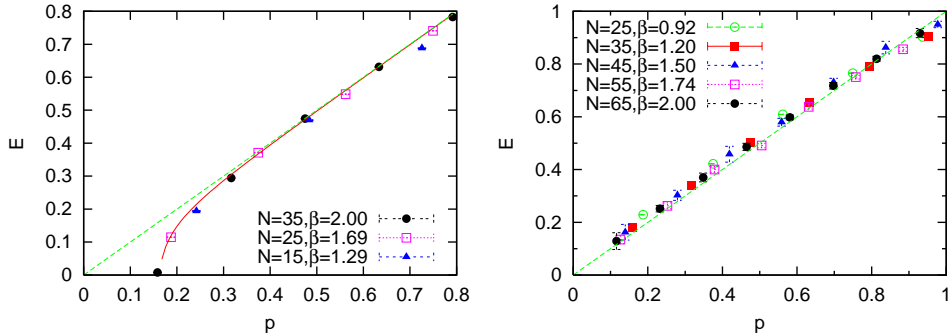


Figure 13: *The dispersion relation of the NC photon in the symmetric phase (on the left) and in the phase of spontaneously broken Poincaré symmetry (on the right). The behaviour on the left matches the 1-loop result, which is IR unstable, and which we also sketched in Figure 11. The behaviour on the right was measured in the broken phase, which describes an IR stable NC continuum and infinite volume limit [169].*

The results obtained already [169] suggest the important feature that *the photon may survive in a NC world* after all, without the necessity of SUSY to cancel a negative IR divergence. Hence NC QED *is* an option for new physics. Of course, the version with a constant Θ is probably still just a mimic of a realistic fuzzy quantum space.

3.4 Analysis of GRB and blazar flare data

From the preceding discussion we extract the message that a theoretical basis for a deformed photon dispersion is conceivable. Similar to Subsection 2.4 we now turn to a pragmatic point of view and just assume some *effective* deformation. We adapt an obvious parameterisation ansatz [120] for the photon energy E at some momentum \vec{p} ,

$$\vec{p}^2 = E^2 \left(1 + \frac{E}{M} \right) \quad \rightarrow \quad v_\gamma(E) \simeq 1 - \frac{E}{M}. \quad (3.31)$$

M is a very large mass, which emerges *somehow*, for instance from some kind of “quantum gravity foam”.⁵⁵ We keep track of $O(E/M)$, and v_γ is the photon speed (which turns into $c = 1$ for $M \rightarrow \infty$).

Ref. [181] performed a systematic analysis of the GRB data collected

⁵⁵A general discussion of possible power series corrections to dispersion relations and their constraints based on requirements like positivity, causality and rotation symmetry is given in Ref. [179]. Ref. [180] studies the impact on the thermodynamics of a photon gas.

by three satellites named SWIFT, BATSE and HETE⁵⁶ and confronted the data with ansatz (3.31). In fact there is a distinction in the time of arrival: photons with higher energy tend to arrive earlier (which would naively suggest $M < 0$). However, the analysis has to verify if this could also be explained without new physics. We do not know if the photons of different energies in a GRB were emitted exactly at the same time (we repeat that we have to refer to hypotheses and models for the origin of GRBs [127]). We consider photons in energy bins which differ by ΔE . Without new physics, the delay in the time of arrival can be described as

$$\Delta t = d_{\text{source}} (1 + z) \quad (z : \text{redshift}) , \quad (3.32)$$

where d_{source} is the parameter for the possible time-lag at the source. This delay is further enhanced on the way to Earth by the factor $(1 + z)$.

Then the question is if the data can be fitted better when we add a LIV parameter. This leads to the extended parameterisation ansatz

$$\frac{\Delta t}{1 + z} = d_{\text{source}} + a_{\text{LIV}} K(z) , \quad a_{\text{LIV}} := \frac{\Delta E}{MH_0} , \quad (3.33)$$

where H_0 is the Hubble parameter and $K(z)$ is a correction factor, which is derived in Ref. [181]. Figure 14 (on the left) shows the left-hand-side of eq. (3.33) on the vertical axis, so the question is if the data⁵⁷ are compatible with a constant, and therefore with LI. Although the best linear fit — shown in the plot — has a slight slope, it is obvious that a constant behaviour is not excluded. The outcome of a precise evaluation is reproduced in Figure 14 on the right. The inner (outer) depicted area captures the parameters d_{source} and a_{LIV} with 68 % (95 %) C.L. The crucial point is that $a_{\text{LIV}} = 0$ (absence of LIV) is included in the permitted region, and a_{LIV} is strongly constrained, which leads to the cautious conclusion

$$|M| > 1.4 \cdot 10^{25} \text{ eV} \approx 0.0012 M_{\text{Planck}} \quad (3.34)$$

with 95 % C.L. In some sense this is a negative result: once again the data do not give evidence for new physics. However, it is impressive that these observations allow for robust phenomenological insight about an energy regime, which is not that far below the Planck scale.

We add that there are further analyses of GRB data along these lines, which do not find evidence for LIV either. In some studies the bound

⁵⁶For instance HETE distinguished for the GRB photons 4 energy bins and detected them in time intervals of $6.4 \cdot 10^{-3}$ s.

⁵⁷The error bars were enhanced by the authors of Ref. [181] compared to the satellite data, until they became compatible with a consistent picture.

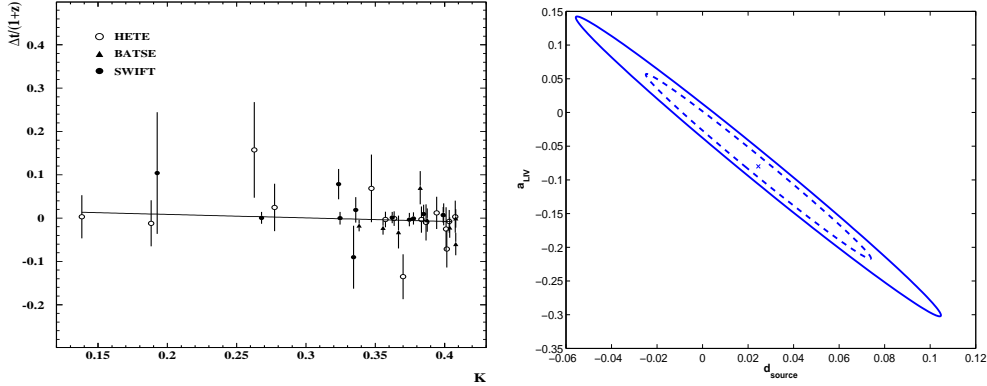


Figure 14: *Illustrations of the GRB data analysis in Ref. [181]: on the left the left-hand-side of eq. (3.33) is plotted against the function $K(z)$. The question is if the fit requires a non-zero LIV parameter a_{LIV} , i.e. if there is a slope with respect to $K(z)$. On the right the window for the parameters d_{source} (for a lag at the source) and a_{LIV} is shown for 68% resp. 95% C.L. A strong deviation from the LI scenario $a_{\text{LIV}} = 0$ is ruled out, which implies the bound (3.34) (plots adapted from Ref. [181]).*

for $|M|$ is set even higher, e.g. Refs. [182, 183] analysed the data of single GRBs and concluded $|M| > 0.015 M_{\text{Planck}}$ resp. $|M| > 0.0066 M_{\text{Planck}}$.

Very similar investigations are also carried out based on the γ -rays emitted in *blazar flares*. Recently the MAGIC Collaboration used the Imaging Atmospheric Čerenkov Telescope to analyse a flare of Markarian 501 (cf. Subsection 3.1) and arrived even at $|M| > 0.022 M_{\text{Planck}}$ [184]. The Gamma-ray Large Area Space Telescope (GLAST) [185] is now going to search systematically for photons from GRBs and blazar flares in the energy interval of 8 keV to 300 GeV, which is promising in view of further insight even above these bounds [186]. GLAST has arrived in orbit in June 2008.

If we assume some quantum space-time background, then it is natural that it is subject to fluctuations, which may affect the speed of photons also stochastically [187]. A consequence of this additional effect could be the broadening of a flare width, which increases with the distance.

At last we add that GRBs are also accompanied by a burst of neutrinos, which may lead to additional prospects for LIV tests [188].

3.5 Effective Field Theory and vacuum birefringence

After discussing NC field theory as a LIV approach in Subsection 3.3, we returned to the Effective Field Theory (EFT) framework in Subsection 3.4. This is the theoretical framework that we had already employed in Section 2. It includes the LIV terms, which are not excluded by symmetries, in an energetic hierarchy. This concept works successfully in many branches of physics — for instance in Chiral Perturbation Theory — but the example of NC field theory shows that it is not without alternative (in the latter case, the IR divergences are incompatible with EFT).

A systematic EFT analysis has to distinguish the mass dimensions n of the LIV operators. We summarise this approach briefly, following the excellent discussion in Ref. [76]. We require rotation symmetry and gauge invariance, and we introduce a time-like unit vector u . Then an extended QED Lagrangian includes the renormalisable terms

$$\begin{aligned} n = 3 & : b\bar{\psi}\gamma_5 u_\mu \gamma^\mu \psi & (3.35) \\ n = 4 & : K_{\mu\nu\rho\sigma} F^{\mu\nu} F^{\rho\sigma} + i\bar{\psi}u_\mu u_\nu \gamma^\mu D^\nu (c + d\gamma_5)\psi, \quad (b, c, d : \text{const.}) . \end{aligned}$$

We encountered the $n = 4$ terms before in Section 2: note that $K_{\mu\nu\rho\sigma} = u_{[\mu}g_{\nu][\rho}u_{\sigma]}$ has to obey rotation symmetry, which renders it equivalent to the term (2.13), and the last term above is equivalent to (2.11) (we proceed to covariant derivatives D^ν).

Refs. [189, 190] explored the possibilities to add LIV operators of mass dimension $n = 5$, which are quadratic in the fields (of one kind) and not reducible to lower dimensions or total derivatives by applying the equations of motion. They assumed these (CPT odd) terms to be $O(1/M_{\text{Planck}})$ suppressed.⁵⁸ In the pure gauge action, Ref. [189] identified only one (independent) term,

$$\frac{\xi}{M_{\text{Planck}}} u^\mu F_{\mu\nu} (u \cdot \partial) (u_\rho \tilde{F}^{\rho\nu}), \quad (\tilde{F}^{\rho\nu} := \frac{1}{2} \epsilon^{\rho\nu\alpha\beta} F_{\alpha\beta}). \quad (3.36)$$

The LIV parameter ξ affects the photon dispersion relation as

$$E_\pm^2 = k^2 \pm \frac{\xi}{M_{\text{Planck}}} k^3 \quad (k = |\vec{k}|), \quad (3.37)$$

where \pm refers to left/right-handed circular polarisation.⁵⁹

⁵⁸Of course, extending this rule to lower dimensions n leads to another manifestation of the unsolved hierarchy problem, which we commented on before.

⁵⁹Actually radiative corrections amplify the LIV term, leading to a fine-tuning problem even for this dimension 5 term [191].

A perturbative quantisation for the corresponding scalar model — where the Lagrangian involves second order time derivatives — was constructed in Ref. [192].

The LIV modified fermion dispersion is similar, if we assume $m \ll E \ll M_{\text{Planck}}$ (where m is the fermion mass). Then we can choose the spinor field to be an approximate eigenvector of γ_5 resp. of the chiral projectors, and we obtain [189]

$$E^2 = p^2 + m^2 + \eta_{\pm} \frac{p^3}{M_{\text{Planck}}} \quad (p = |\vec{p}|) , \quad (3.38)$$

with $\eta_{\pm}^{\text{fermion}} = -\eta_{\mp}^{\text{anti-fermion}}$ [193]. Ref. [76] discusses new QED phenomena, which may occur due to this modification, including the transitions

$$\begin{aligned} e^- &\rightarrow e^- + \gamma && \text{vacuum Čerenkov radiation} \\ \gamma &\rightarrow e^+ + e^- && \text{photon decay} \\ e^{\pm} &\rightarrow e^{\pm} + e^+ + e^- && \text{pair emission} \\ \gamma &\rightarrow 2\gamma , 3\gamma \dots && \text{photon splitting.} \end{aligned} \quad (3.39)$$

In Subsection 2.5 we already addressed vacuum Čerenkov radiation and the photon decay. In contrast, lepton pair emission and photon splitting cannot be arranged for by different MAVs, but by suitable SME parameters [95, 194]. Moreover we have discussed in Subsection 3.1 that the photon absorption $\gamma + \gamma \rightarrow e^+ + e^-$ — which occurs in standard QED as well — may be altered by LIV terms, in particular in view of the energy threshold.

A careful analysis has to keep track of angular momentum conservation, which can be achieved *e.g.* in the photon decay above the energy threshold, since the momenta do not need to be collinear. Thus all the three LIV parameters, ξ , η_+ and η_- , are involved. This decay (as well as the pair emission) would occur rapidly above threshold, so that the observed high energy photons, in particular from the Crab Nebula and from blazars (with lower energy but longer time of flight, see Subsections 3.1 and 3.2) set combined constraints on these three parameters [76].

If the GZK cutoff attenuates ultra high energy protons as predicted by standard field theory, this should also generate high energy photons,

$$p + \gamma_{\text{IR}} \rightarrow \Delta^+ \rightarrow p + \pi^0 \rightarrow p + 2\gamma_{\text{UV}} . \quad (3.40)$$

Since it is not observed that UHECRs are accompanied by such UV photons [25], Ref. [195] concludes that they are also subject to the expected attenuation, and derived a tiny bound for $|\xi|$, for the case $\eta_{\pm} = 0$. Ref. [196] generalised this study to obtain combined constraints for ξ and η_{\pm} , considering in particular the processes $\gamma \rightarrow e^+ + e^-$ and $\gamma \rightarrow 3\gamma$.

Based on the Crab Nebula photons up to ≈ 50 TeV one obtains extremely stringent constraints, if one relies on the standard assumption about the origin of its γ -radiation (synchrotron emission of high

energy electrons and positrons, and inverse Compton scattering of the synchrotron photons) [76, 197].

However, at this point we would like to be as economic as possible with our assumptions. Without any hypothesis about the mechanism causing the radiation, nor any assumption about the interactions in a LIV modified QED (which is needed for the transitions in the list (3.39)) we can still address *purely kinematic effects*.⁶⁰

In this regard we have already discussed the energy dependence of the photon speed in Subsection 3.4. In addition the dispersion relation (3.37) also implies a *helicity dependence* for plane waves of the same momentum k . Over a distance ℓ it leads to a relative delay Δt_h ,

$$v_{\pm} = \frac{\partial E_{\pm}}{dk} \simeq 1 \pm \frac{\xi}{2M_{\text{Planck}}} k \quad \rightarrow \quad \Delta t_h \simeq \frac{|\xi| \ell k}{M_{\text{Planck}}} . \quad (3.41)$$

It is a virtue of this formula that it is not affected by the uncertainty about a relative time-lag in the photon emission of different momenta k (unlike the studies reviewed in Subsection 3.4). However, one needs of course the (mild) assumption that there is no relative delay between the helicities at the source.

As we mentioned before, Markarian 421 and 501 are the two known blazars which emitted photons that arrived with energies $E \gtrsim 10$ TeV. The quasi-simultaneous arrival of both helicity states implies [193]

$$|\xi| < 126 \quad \rightarrow \quad |M| > 0.008 M_{\text{Planck}} , \quad (3.42)$$

where M refers to the notation used in Subsection 3.4. This bound is in the same magnitude as those derived from the energy dependence.

Birefringence : The helicity dependent energy (3.37) yields yet another purely kinematic effect, which leads to a much stronger bound on the parameter ξ [76].⁶¹ In addition to the group velocity v_{\pm} there are also distinct phase velocities. As a consequence, the polarisation plane of *linearly* polarised γ -radiation of momentum k is rotated after time t by the angle

$$\alpha(t) = \frac{t}{2}(E_+ - E_-) \simeq \frac{\xi k^2 t}{M_{\text{Planck}}} . \quad (3.43)$$

⁶⁰Also in this respect there are attempts to go beyond the EFT approach and motivate the corresponding (parity breaking) modification of the Maxwell eqs. from quantum gravity [198].

⁶¹Further studies address possible LIV birefringence effects in gravitational waves [199] and on the electron self-energy [63].

Most useful for our purposes is the effect that a linearly polarised burst covering momenta $k_{\min} \dots k_{\max}$ will be depolarised. The net polarisation is lost completely when the difference in the polarisation planes arrives at

$$\alpha_{\max} - \alpha_{\min} = \frac{\xi t}{M_{\text{Planck}}} (k_{\max}^2 - k_{\min}^2) \approx \frac{\pi}{2}. \quad (3.44)$$

We mentioned in Section 2 that this effect has been used to constrain the $n = 3$ Chern-Simons term (2.9) [91], and it has also been applied to establish bounds on $n = 4$ LIV terms in the SME [200]. For the $n = 5$ term that we are discussing here, this birefringence property was studied by Gleiser and Kozameh [131]. They referred to γ -rays originating from galaxies at a distance of 300 Mpc. For wave lengths ranging from 400 nm to 800 nm a linear polarisation was observed, within $< 10^\circ$ deviation of the polarisation plane. As a final highlight, let us quote that this yields a *trans-Planckian* bound of

$$|\xi| \lesssim 10^{-4} \quad \rightarrow \quad |M| > 10^4 M_{\text{Planck}}. \quad (3.45)$$

Of course this refers to a specific order in the EFT framework.⁶² If we restrict the consideration to CPT even terms — returning to the concept outlined in Section 2 — such operators of dimension $n = 5$ are excluded. In the EFT scheme we would then naturally proceed to $n = 6$ operators causing LIV effects of $O(E^2/M_{\text{Planck}}^2)$. For these terms helicity dependent photon velocities are still possible, but not required anymore [76]. Here the absence of vacuum Čerenkov radiation for protons of energies up to $\sim 10^{20}$ eV (see Subsection 2.5.2) becomes most powerful. As we anticipated in footnote 36, Ref. [103] discusses a link between SME parameters and hadronic effects by employing the parton model, though this connection is not ultimately clarified.

4 Conclusions

Cosmic rays involve particles at the highest energies in the Universe. Their flux is small at ultra high energies, which makes measurements difficult, but there is on-going progress in the techniques and extent of the corresponding observatories. In addition to the ultra high energy, we can also take advantage of their extremely long path to extract information, which is inaccessible otherwise — that property is even more powerful in view of conclusions about scenarios for new physics. Therefore cosmic rays provide a unique opportunity to access phenomenology

⁶²Returning to NC field theory, Ref. [201] discusses how UV/IR mixing (see Subsection 3.3) could affect birefringence. As for the laboratory, Ref. [202] proposed a high precision experiment on vacuum birefringence.

at tremendous energies. We have seen in the last Subsections that this can reach out to energies only two or three orders of magnitude below the Planck scale, and for specific parameters one even attains trans-Planckian magnitudes. Hence predictions in this regime have now arrived at *falsifiability*, which is a basic criterion for a scientific theory [203]. Although this only leaves a small window for possible LIV parameters, there is a wide-spread consensus that this scenario deserves attention — over the past 10 years a preprint on this subject appeared on average about once a week, and at least 52 are top-cited.

We have discussed the challenges to verify the GZK cutoff for UHE-CRs, and the multi-TeV γ -puzzle. The question is: why is the Universe — with its Cosmic Background Radiation (CBR) — so transparent for protons, or heavier nuclei, with energies $E_p \gtrsim 6 \cdot 10^{19}$ eV, and for photons with $E_\gamma \gtrsim 10$ TeV ? In both cases it is still controversial if the puzzle really persists.

The photopion production of UHECR protons with CMB photons is actually a process of harmlessly low energy (around 200 MeV) in the rest frame of the proton. It can be studied in detail in our laboratories. However, the application of the results for the cross-section etc. to UHE-CRs requires boosts with Lorentz factors of the order $\gamma \sim O(10^{11})$. The applicability of such extreme Lorentz transformations cannot be tested in the laboratories (which are limited to $\gamma \lesssim O(10^5)$). Hence the viability of LI under extreme boosts is a central issue. If a puzzle persists at last, LIV provides a possible solution. In Section 2 we discussed a theoretical basis of LIVs (SME and in particular MAVs), and its impact on cosmic rays physics — a tiny LIV could remove the GZK cutoff.

As an alternative theoretical framework for LIV, Section 3 addressed field theory in a NC space. This approach is fundamentally different from the effective action concepts that we considered in Section 2. We focused in particular on the dispersion relation of the photon in a NC world. A possible distortion of the photon dispersion can be probed best by the observation of GRBs or blazar flares. We also discussed the Effective Field Theory approach to LIV terms for cosmic photons and stringent limits on leading terms, based on momentum or helicity dependent photon velocities.

Up to now, *no experimental evidence for LIV has been found* anywhere, despite more and more precise tests. As examples we reviewed attempts with cosmic neutrinos and photons (other high precision tests are performed in atomic physics [72, 77, 78]). However, a large number of LIV parameters are conceivable. For some of them the tested precision may still be insufficient to rule out interesting scenarios for new physics, which could shed completely new light on the open issues mentioned

above. If the GZK cutoff is indeed confirmed — as the data by the collaborations HiRes and Pierre Auger suggest — then this could be viewed as *indirect evidence in favour of the validity of LI even at $\gamma \sim O(10^{11})$* .

New projects to detect *UHECRs* are on the way. As examples we mention Telescope Array (TA) [204] (another hybrid approach with an air shower array on ground and fluorescence telescopes), the Extreme Universe Space Observatory (EUSO) [205] and the Orbiting Wide-angle Light-collectors (OWL) [206] (both are going to search for air fluorescence light from satellites). The general prospects for observatories in space are discussed in Ref. [207].

High energy γ -rays are detected by satellite-based telescopes in the AGILE Observatory [208] (Astro-rivelatore Gamma a Immagini Leggero), and in the GLAST Observatory [185] (systematic observation of cosmic photons over a broad energy). On ground there are suitable Čerenkov detector arrays, such as the High Energy Stereoscopic System H.E.S.S. in Namibia [209] and MAGIC [184] (we have already referred to GLAST and MAGIC in Section 3). Ref. [210] gives a recent overview. Regarding GRBs, the Chinese-French Space-based multi-band astronomical Variable Objects Monitor mission (SVOM) [211] plans to detect about 80 bursts a year.

As for the upcoming search for high energy cosmic *neutrinos* (outlined *e.g.* in Ref. [128]) we mention the IceCube Neutrino Observatory [212], which detects Čerenkov light in the antarctic ice, as well as ANITA (Antarctic Impulse Transient Antenna, balloon-borne), ANTARES (Astronomy with a Neutrino Telescope and Abyss environmental REsearch, at sites deep in the Mediterranean Sea) and NESTOR (Neutrino Extended Submarine Telescope with Oceanographic Research) [213].

Let us also mention a completely new technique, which is currently under investigation [214]: the idea is to measure the synchrotron radiation of air shower leptons in the magnetic field of the Earth, in particular radio flashes, with an array of 30 dipole antennae.

Finally we should emphasise once more that the Pierre Auger Observatory is still at an early stage; it is operating successfully since the beginning of the year 2004, but the final Čerenkov detectors have been installed in 2008. Moreover that Collaboration plans another observatory in the northern hemisphere [42].

This is a very active field of research with exciting open questions. We may expect enlightening new data in the near future. They could lead to new insight in outstanding issues like LIV — or to new puzzles and *perhaps* to evidence for new physics.

A New development since Nov. 2007: The AGN Hypothesis

In November 2007 the Pierre Auger Collaboration published a spectacular report [215], which is relevant for the issues that we discussed in Section 1. They analysed the arrival directions of the UHECRs that they had detected so far. We denote their observation as the *AGN Hypothesis*:

The UHECRs directions are clustered and correlated with the locations of nearby Active Galactic Nuclei (AGN).

This is clearly in contrast to the traditional assumption of an isotropic distribution (see Section 1.1).⁶³ The possibility that the AGN — or other objects located next to them — could be the UHECR sources appears consistent because they refer to AGN *nearby*: then the UHECR may be little deflected by magnetic fields, and attenuated only mildly by the CMB. In this scenario one could assume also AGN far away to emit UHECRs, but they would arrive with energies below the GZK cutoff at Earth. Therefore the AGN Hypothesis agrees with the validity of the GZK cutoff; it disfavours the possibility that UHECRs indicate new physics. In particular Ref. [218] deduces an upper bound for the MAV difference $c_\pi - c_p < 5 \cdot 10^{-23}$. On the other hand, it could be the starting point of a new epoch of *cosmic ray astronomy*.

The Pierre Auger Collaboration started from the UHECR data collected in the period from January 2004 to May 2006. Their analysis involved 3 parameters

E_{\min} : threshold energy to be counted as an UHECR

ψ : angular interval around an UHECR direction

R_{\max} : maximal distance to a “nearby AGN”.

Thanks to the analysis of hybrid events, which were detected by the extended air shower *and* by the fluorescence telescopes, the energy has a relatively small uncertainty around 22% (cf. Subsection 1.4), and the angular accuracy is about 1° [11]. E_{\min} and R_{\max} were of course assumed in the order of the GZK cutoff and the predicted super-GZK path length (eqs. (1.2) and (1.15)). The distance to the AGN is known from the redshift of their γ -radiation.

⁶³For the characteristic of AGN we refer to footnote 7, and for an earlier suggestion that they could be the UHECR source to Ref. [216]. The question if they could be endowed with a sufficiently powerful acceleration mechanism has recently been reconsidered in Refs. [217].

These 3 parameters were tuned to the values

$$(E_{\min}, \psi, R_{\max}) = (5.6 \cdot 10^{19} \text{ eV}, 3.1^\circ, 75 \text{ Mpc}), \quad (\text{A.1})$$

which gave maximal support for the AGN Hypothesis: it captures 12 out of 15 UHECRs, whereas only 3.2 would be expected for hypothetical isotropic rays (although in that case one could question if one should keep these three parameters fixed).

As a clean test this Collaboration then analysed — still with fixed parameters (A.1) — the UHECRs that they detected later, in the period May 2006 to August 2007. In that case it captures 8 out of 13 UHECRs. So the ratio went down, but the number 8 is still large compared to 2.8, which would be the expectation for isotropic rays.

The ensemble of UHECR directions observed by the Pierre Auger Collaboration in the whole period January 2004 to August 2007 is shown in the Figure 15; it covers their 27 top UHECRs ($E > 5.7 \cdot 10^{19}$ eV). The black circles mark the range within 3.1° of their directions of arrival, and the asterisks correspond to the 472 known nearby AGN (up to the distance R_{\max} in eq. (A.1), which corresponds to redshift $z = 0.018$), according to the Véron-Cetty & Véron Catalogue [219]. The alternative use of the Swift BAT Catalogue leads qualitatively to the same results [220]. In further investigations Ref. [221] (Ref. [222]) reports a correlation between these 27 UHECR directions and the locations of spiral galaxies (extended nearby radiogalaxies) by using the HIPASS Catalogue (several catalogues).

A.1 Comments on the AGN Hypothesis

The AGN Hypothesis consists actually of two parts, and we consider it worthwhile discussing them separately:

- (a) Clustering of the UHECR directions.
 - (b) Correlation of the clustered directions with locations of nearby AGN.
- Part (b) depends on (a), but the validity of (a) only could be an option.

Ref. [215] reports 99% C.L. for part (a) and here only two tuned parameters enter, E_{\min} and ψ . Still this new UHECR statistics is in the same magnitude as the total previous world data (and the same holds for the total exposure so far, *i.e.* [detection time] \times [area]; a comparative Table is given in Ref. [52]). Hence one may wonder why this clustering did not become obvious earlier. Of course, previous data were also analysed with this respect, and some indication for clustering was found in the world data available in 1995 (from Volcano Ranch, Haverah Park, Yakutsk and AGASA at an early stage) [223]. This inspired

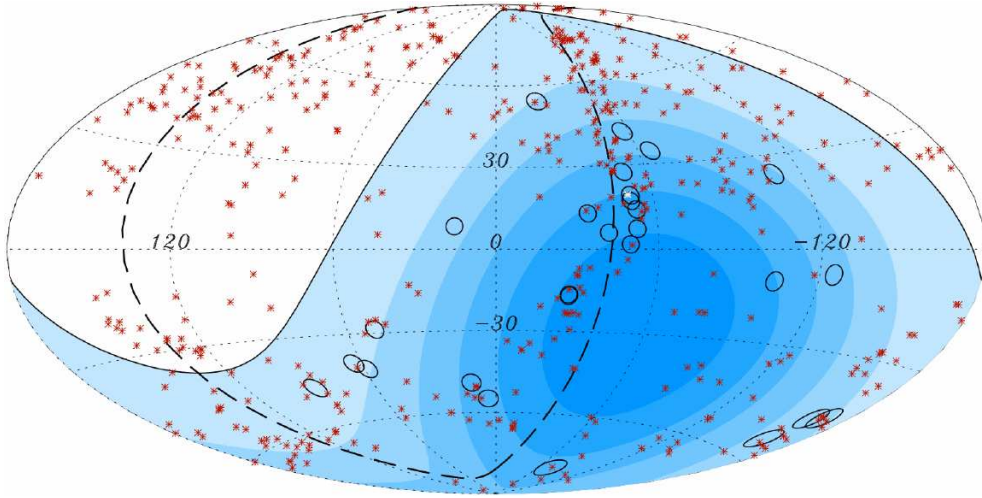


Figure 15: *A projection of the celestial sphere (plot adapted from Ref. [215]): the circles mark the arrival directions of the 27 UHECRs detected by the Pierre Auger Collaboration, and the asterisks the locations of 472 known nearby AGN. In particular for Centaurus A a white symbol is used. The dashed line follows the super-galactic plane. The darkness of the areas corresponds to the exposure (in the white area it vanishes).*

the AGASA Collaboration to perform a careful analysis of the directions where they found UHECRs [224]. They could see a slight clustering near the super-galactic plane,⁶⁴ but it was weaker than in the previous world data; otherwise they found consistence with isotropy. Not even their slight anisotropy signal was confirmed by HiRes, which reported full isotropy [225]. A new analysis referring to an updated definition of the super-galactic plane confirms a clustering of the 27 top UHECR directions observed by the Pierre Auger Collaboration, but for a similar number of previous world data events (in the same energy magnitude) clustering is still not evident [226].

With respect to part (b) of the AGN Hypothesis the statements about the C.L. are less striking in Ref. [215]. The analysis in Ref. [227] is more complete, for instance regarding the variation of the parameters (A.1) (see also Ref. [228]). First support for this Hypothesis beyond the Pierre Auger Observatory was provided by a new analysis of the Yakutsk data [229], but *not* by the HiRes data [230]: in that case, only 2 out of 13 events fulfil the correlation criterion for the parameter set (A.1).

⁶⁴The super-galactic plane is a sheet-like structure that contains the local super-clusters. It corresponds to the dash line in Figure 15.

Ref. [231] comments that the effect could reflect the property that the known AGN, as well as the detected nearby UHECR sources, are both preferentially located near the super-galactic plane.

Critics was also expressed in Ref. [232], which starts from the statement that the arriving flux of a source at distance R should be $\propto 1/R^2$. Hence according to the AGN Hypothesis the *nearest* AGN should contribute most. Therefore Ref. [232] expects Centaurus A and Virgo — which contain the two nearest AGN — to contribute each about 6 out of the 27 UHECR in the sky-map of Figure 15, if the AGN Hypothesis holds. The direction of the galaxy Centaurus A does contribute, and (with some tolerance about the angular window) it is compatible with this expectation,⁶⁵ but *nothing* is found in the direction of the Virgo cluster of galaxies (in Figure 15 it is located in the upper part near the dashed line, which follows the super-galactic plane). That deficit is the main point in the analysis of Ref. [232], which claims that the data *disfavour* the AGN Hypothesis with 99% C.L. One might remark that this reasoning seems to refer to a scenario where all AGN are UHECR sources with continuous luminosity. If AGN are episodic sources, then this argument might be circumvented.⁶⁶

For sure the matter distribution in the GZK-sphere is inhomogeneous. Therefore the AGN hypothesis could indeed lead to a new branch of astronomy based on cosmic rays, as we mentioned in the beginning of this appendix. A possible correlation of the nearby matter distribution with the magnetic field strength is another controversial issue [236]. The way it could affect the UHECR propagation is discussed — for various scenarios of the magnetic field structure — in Ref. [12].

Finally we add another interpretation put forward in Ref. [237], which concludes from the UHECR path limitation — according to the analysis in Ref. [215] — that the primary particles at source could be mostly nuclei heavier than protons. In fact the distance R_{\max} to the nearby AGN is a bit shorter than required for the maximal super-GZK path length of protons (eq. (1.15)), hence better suited for other nuclei. A new calculation of the effective energy loss of UHECRs in Ref. [231] supports the conjecture that these rays are mainly emitted as light nuclei, up to an atomic mass number $A \approx 24$. This interpretation caused a surge of interest in the CBR attenuation of nuclei, which has also been revisited in Refs. [238, 240].⁶⁷ Ref. [239] added that this could affect the magnitude to

⁶⁵See Ref. [233, 234] for discussions of the high energy radiation mechanism of Centaurus A.

⁶⁶Ref. [235] compares the scenarios of continuous vs. episodic UHECR sources, and arrives at different predictions for the energy dependence of the γ and ν flux.

⁶⁷One expects UHECRs to be accompanied by a neutrino flux generated in CMB

which LIV parameters are ruled out if the AGN Hypothesis holds, since possible LIV effects in the dispersion of N bound particles are amplified $\propto N^2$. On the other hand, for a given energy the Lorentz factor between the FRW laboratory frame and the ray rest frame shrinks $\propto 1/A$.

After a long journey, Ref. [240] expects either protons or Fe nuclei (or perhaps sub-Fe nuclei) to survive as UHECR primary particle. In this regard, a statistical analysis of the penetration depth into the atmosphere (cf. eq. (1.17)) suggests a mixed composition [241]. However, also that observation appears to be consistent only in part with the HiRes data [242] (a comparison is shown in Figure 4 of Ref. [243]).

In any case, more statistics will be needed to identify the nature of the UHECR primary particles directly. Above 10^{19} eV not much this is known in this respect. We may hope for new insight based on upcoming data, which the Pierre Auger Collaboration intends to release in 2009.

B Table of short-hand notations

For convenience we add an alphabetic list of the short-hand notations used in the text, with some hints where the corresponding terms are introduced and used:

AGN	Active Galactic Nuclei, see footnote 7. They play a central rôle in Appendix A.
C.L.	Confidence Level (for statistical results).
CPT	Charge conjugation combined with parity and time reflexion. Subsection 2.1 comments on its relation to LIV.
CMB	Cosmic Microwave Background, see Subsection 1.2.
DSL	Double Scaling Limit, see Subsection 3.3.2.
DSR	Doubly Special Relativity, see Subsection 3.3.
EFT	Effective Field Theory, see Subsection 3.5.
FRW	Friedmann-Robertson-Walker (or Friedmann-Lemaître-Robertson-Walker) A line element in the FRW metrics is given by $ds^2 = dt^2 - a(t)^2(dr^2 + \bar{r}^2 d\Omega)$ ($d\Omega$: spherical element) $a(t)$: scale factor of the Universe, \bar{r} : covariant distance $\bar{r} = r$ (no curvature), $\bar{r} = R \sin(r/R)$ ($\bar{r} = R \sinh(r/R)$) for positive (negative) curvature with radius R .
GRB	Gamma Ray Burst, see Subsection 3.2.
GRT	General Relativity Theory
GZK	Greisen-Zatsepin-Kuz'min

interactions (see *e.g.* Ref. [128]), which also depends on the atomic mass A [234].

	The GZK cutoff for the energy of cosmic rays, $E_{\text{GZK}} \simeq 6 \cdot 10^{19} \text{eV}$, is discussed in Subsection 1.3.
LI	Lorentz Invariance (or Lorentz Invariant)
LIV	Lorentz Invariance Violation, addressed in Sections 2 and 3.
MAV	Maximal Attainable Velocity, introduced in Subsection 2.4.
NC	Non-Commutative, see Subsection 3.3.
SSB	Spontaneous Symmetry Breaking
SME	Standard Model Extension, see Subsection 2.3.
SRT	Special Relativity Theory
SUSY	Supersymmetry
UHECR	Ultra High Energy Cosmic Ray, a cosmic ray with energy near (or above) the magnitude of E_{GZK}

For completeness we add that the literature often expresses the huge energies involved in cosmic rays in units of **PeV**, **EeV** and **ZeV**, where the initial capital letters mean Peta : 10^{15} , Exa : 10^{18} , Zetta : 10^{21} .

Acknowledgements : This review is based on talks presented at Humboldt-Universität zu Berlin, Universidad Central de Caracas, Universität Bern, IHEP (Beijing) and Beijing University. I thank Marco Panero for his careful reading of the draft version and many helpful comments. I am indebted to Maria Teresa Dova, Pedro Facal, Anamaria Font, Heinrich Rebel, Markus Risse, Markus Roth, Michael Unger and Luis Villaseñor for instructive information, and to Wolfram Schroers for technical support. Jorge Alfaro, Aiyalam Balachandran, Robert Bluhm, Anosh Joseph, Nikolaos Mavromatos, Richard Obousy, Albert Petrov and Alexander Sakharov attracted my attention to relevant references. I also benefitted from inspiring remarks by Brett Altschul, Dorothea Bahns, Yu Jia, Hermann Kolanowski, Bo-Qiang Ma, Uwe-Jens Wiese, Ulli Wolff and Zhi Xiao. Finally I thank my collaborators for their contributions to the joint works quoted here, and the authors of Refs. [10, 11, 41, 42, 50, 53, 113, 181, 215] for the kind permission to reproduce some of their plots.

References

- [1] K. Bergwitz, Habilitation Thesis, Braunschweig (1910).
- [2] A. Gockel, *Physik. Zeitschr.* **11** (1910) 280; *ibid.* **12** (1911) 595.
- [3] Th. Wulf, *Physik. Zeitschr.* **11** (1910) 811.
- [4] V.F. Hess, *Physik. Zeitschr.* **13** (1912) 1084.
- [5] W. Kolhörster, *Physik. Zeitschr.* **14** (1913) 1153.

- [6] V.F. Hess, *Physik. Zeitschr.* **14** (1913) 610.
- [7] P. Auger, R. Maze and T. Grivet-Mayer, *Compt. Rend. Acad. Sci.* **206** (1938) 1721.
- [8] W. Kolhörster, I. Mathes and E. Weber, *Naturwissenschaften* **26** (1938) 576.
- [9] P. Auger, P. Ehrenfest, R. Maze, J. Daudin and A. Fréon Robley, *Rev. Mod. Phys.* **11** (1939) 288.
- [10] <http://www.cosmic-ray.org/>
- [11] Pierre Auger Collaboration (J. Abraham *et al.*), *Phys. Rev. Lett.* **101** (2008) 061101.
- [12] G.A. Medina-Tanco, [astro-ph/0607543](https://arxiv.org/abs/astro-ph/0607543).
- [13] T. Antoni *et al.* (KASCADE Collaboration), *Astropart. Phys.* **24** (2005) 1.
- [14] E. Fermi, *Phys. Rev.* **75** (1949) 1169.
- [15] W.I. Axelford, E. Leer and G. Skadron, *Proc. 15th Int. Cosmic Ray Conference* **11** (1977) 132. G.F. Krymsky, *Dok. Acad. Nauk. USSR* **234** (1977) 1306. Supernovae as cosmic ray sources were suggested already by W. Baade and F. Zwicky, *Proc. Nat. Acad. Sci.* **20** (1934) 259. Shock wave acceleration in supernova remnants is now the most popular scenario for *galactic* cosmic rays, see *e.g.* S. Gabici, [arXiv:0811.0836](https://arxiv.org/abs/0811.0836) [[astro-ph](https://arxiv.org/abs/astro-ph)], which do, however, not include UHECRs.
- [16] A.V. Olinto, *Phys. Rept.* **333** (2000) 329. L. Anchordoqui, T. Paul, S. Reucroft and J. Swain, *Int. J. Mod. Phys. A* **18** (2003) 2229.
- [17] W. Bednarek and M. Bartosik, *Astron. Astrophys.* **423** (2004) 405.
- [18] G.R. Farrar and P.L. Biermann, *Phys. Rev. Lett.* **81** (1998) 3579.
- [19] A. Meli, J.K. Becker and J.J. Quenby, [arXiv:0709.3031](https://arxiv.org/abs/0709.3031) [[astro-ph](https://arxiv.org/abs/astro-ph)].
- [20] A. Dar and A. De Rújula, [hep-ph/0606199](https://arxiv.org/abs/hep-ph/0606199).
- [21] P. Bhattacharjee and G. Sigl, *Phys. Rept.* **327** (2000) 109.

- [22] V.S. Berezinsky and A. Vilenkin, *Phys. Rev.* **D 62** (2000) 083512. V.A. Kuz'min and I.I. Tkachev, *Phys. Rept.* **320** (1999) 199. S. Sarkar and R. Toldra, *Nucl. Phys.* **B 621** (2002) 495.
- [23] C.T. Hill, *Nucl. Phys.* **B 224** (1983) 469. P. Bhattacharjee and G. Sigl, *Phys. Rev.* **D 51** (1995) 4079. J.J. Blanco-Pillado and K.D. Olum, *Phys. Rev.* **D 60** (1999) 083001. E. Huguet and P. Peter, *Astropart. Phys.* **12** (2000) 277.
- [24] D.J.H. Chung, E.W. Kolb, A. Riotto and I.I. Tkachev, *Phys. Rev.* **D 62** (2000) 043508. H. Ziaeeepour, *Astropart. Phys.* **16** (2001) 101. E.W. Kolb and A.A. Starobinsky, *JCAP* **0707** (2007) 005.
- [25] Pierre Auger Collaboration (J. Abraham *et al.*), *Astropart. Phys.* **29** (2008) 243.
- [26] M. Risse and P. Homola, *Mod. Phys. Lett.* **A 22** (2007) 749. M. Kachelrieß, [arXiv:0810.3017](https://arxiv.org/abs/0810.3017) [astro-ph].
- [27] J.R. Hörandel, [arXiv:0803.3040](https://arxiv.org/abs/0803.3040) [astro-ph].
- [28] G.I. Rubtsov *et al.*, *Phys. Rev.* **D 73** (2006) 063009.
- [29] A.A. Penzias and R.W. Wilson, *Astrophys. J.* **142** (1965) 419.
- [30] M. Kamionkowski and A. Kosowsky, *Ann. Rev. Nucl. Part. Sci.* **49** (1999) 77. D. Samtleben, S. Staggs and B. Winstein, *Annu. Rev. Nucl. Part. Sci.* **57** (2007) 245. W. Hu, [arXiv:0802.3688](https://arxiv.org/abs/0802.3688) [astro-ph].
- [31] D.J. Fixsen, E.S. Cheng, J.M. Gales, J.C. Mather and R.A. Shafer, *Astrophys. J.* **473** (1996) 576.
- [32] W.-M. Yao *et al.* (Particle Data Group), *J. Phys.* **G 33** (2006) 1.
- [33] R. Durrer, “The cosmic microwave background”, Cambridge University Press, Cambridge U.K. (2008).
- [34] K. Greisen, *Phys. Rev. Lett.* **16** (1966) 748.
- [35] G.T. Zatsepin and V.A. Kuz'min, *Sov. Phys. JETP Lett.* **4** (1966) 78.
- [36] F.W. Stecker, *Phys. Rev. Lett.* **21** (1968) 1016.
- [37] R.R. Wilson, *Phys. Rev.* **110** (1958) 1212.

- [38] J.P. Rachen and P.L. Biermann, *Astron. Astrophys.* **272** (1993) 161.
- [39] F.W. Stecker and M.H. Salamon, *Astrophys. J.* **512** (1999) 521.
- [40] V. Berezhinsky, A.Z. Gazizov and S.I. Grigorieva, *Phys. Rev. D* **74** (2006) 043005.
- [41] D. Harari, S. Mollerach and E. Roulet, *JCAP* **0611** (2006) 012.
- [42] <http://www.auger.org/>
- [43] V. Berezhinsky, A.Z. Gazizov and S.I. Grigorieva, *Phys. Lett. B* **612** (2005) 147. R. Aloisio, V. Berezhinsky, P. Blasi, A. Gazizov and S. Grigorieva, *Astropart. Phys.* **27** (2007) 76.
- [44] J. Linsley, *Phys. Rev. Lett.* **10** (1963) 146.
- [45] K. Suga, H. Sakuyama, S. Kawaguchi and T. Hara, *Phys. Rev. Lett.* **27** (1971) 1604.
- [46] H. Sato, *Prog. Theor. (Phys. Suppl.)* **163** (2006) 163.
- [47] D.J. Bird *et al.*, *Phys. Rev. Lett.* **71** (1993) 3401.
- [48] S.P. Knurenko *et al.* (Yakutsk Collaboration), *Int. J. Mod. Phys. A* **20** (2005) 6878.
- [49] M.A. Lawrence, R.J.O. Reid and A.A. Watson, *J. Phys. G* **17** (1991) 733.
- [50] C.E. Navia, C.R.A. Augusto and K.H. Tsui, [arXiv:0707.1896](https://arxiv.org/abs/0707.1896) [astro-ph].
- [51] R. Abbasi *et al.* (HiRes Collaboration), *Phys. Rev. Lett.* **100** (2008) 101101.
- [52] K.-H. Kampert, *J. Phys. Conf. Ser.* **120** (2008) 062002.
- [53] D. De Marco, P. Blasi and A.V. Olinto, *JCAP* **0601** (2006) 002.
- [54] D. De Marco, P. Blasi and A.V. Olinto, *Astropart. Phys.* **20** (2003) 53.
- [55] J. Matthews, *Astropart. Phys.* **22** (2005) 387.
- [56] L. Anchordoqui, M.T. Dova, A. Mariuzzi, T. McCauley, T. Paul, S. Reucroft and J. Swain, *Annals Phys.* **314** (2004) 145. M.T. Dova, [astro-ph/0505583](https://arxiv.org/abs/astro-ph/0505583).

- [57] M. Roth (for the Pierre Auger Collaboration), [arXiv:0706.2096](#) [astro-ph].
- [58] T. Yamamoto (for the Pierre Auger Collaboration), [arXiv:0707.2638](#) [astro-ph].
- [59] G.J. Feldman and R.D. Cousins, *Phys. Rev.* **D 57** (1998) 3873.
- [60] P. Ramond, “Field Theory: A Modern Primer” (second edition), Frontiers in Physics V.74, Addison-Wesley (1980).
- [61] A. Shomer, [arXiv:0709.3555](#) [hep-th].
- [62] V.A. Kostelecký, *Phys. Rev.* **D 69** (2004) 105009. Q.G. Bailey and V.A. Kostelecký, *Phys. Rev.* **D 74** (2006) 045001.
- [63] J. Alfaro, *Phys. Rev. Lett.* **94** (2005) 221302.
- [64] R. Bluhm and V.A. Kostelecký, *Phys. Rev.* **D 71** (2005) 065008. R. Bluhm, S.-H. Fung and V.A. Kostelecký, *Phys. Rev.* **D 77** (2008) 065020.
- [65] J. Alfaro, *Phys. Rev.* **D 72** (2005) 024027.
- [66] P.A.M. Dirac, *Nature* **168** (1951) 906. J.D. Bjorken, *Annals Phys.* **24** (1963) 174. D.I. Blokhintsev and G.I. Kolerov, *Nuovo Cimento* **34** (1964) 163.
- [67] W. Pauli, *Nuovo Cimento* **6** (1957) 204. G. Lüders, *Ann. Phys.* **2** (1957) 1.
- [68] R. Jost, *Helv. Phys. Acta* **30** (1957) 409.
- [69] J. Fröhlich, [arXiv:0801.2724](#) [math-ph].
- [70] O.W. Greenberg, *Phys. Rev. Lett.* **89** (2002) 231602.
- [71] S.R. Coleman and S.L. Glashow, *Phys. Rev.* **D 59** (1999) 116008.
- [72] D. Mattingly, *Living Rev. Rel.* **8** (2005) 5.
- [73] M. Antonelli and G. D’Ambrosio, http://pdg.lbl.gov/2008/reviews/cpt_s011254.pdf
- [74] R. Bluhm, V.A. Kostelecký and N. Russell, *Phys. Rev. Lett.* **79** (1997) 1432. H. Belich, L.P. Colatto, T. Costa-Soares, J.A. Helayël-Neto and M.T.D. Orlando, [arXiv:0806.1253](#) [hep-th].

- [75] E. Fischbach, M.P. Haugan, D. Tadic and H.-Y. Cheng, *Phys. Rev. D* **32** (1985) 154.
- [76] T. Jacobson, S. Liberati and D. Mattingly, *Annals Phys.* **321** (2006) 150.
- [77] V.A. Kostelecký and N. Russell, [arXiv:0801.0287 \[hep-ph\]](#).
- [78] D. Mattingly, [arXiv:0802.1561 \[gr-qc\]](#).
- [79] N. Ishibashi, H. Kawai, Y. Kitazawa and A. Tsuchiya, *Nucl. Phys. B* **498** (1997) 467.
- [80] J. Nishimura and G. Vernizzi, *JHEP* **0004** (2000) 015; *Phys. Rev. Lett.* **85** (2000) 4664. J. Ambjørn, K.N. Anagnostopoulos, W. Bietenholz, T. Hotta and J. Nishimura, *JHEP* **0007** (2000) 011.
- [81] P. Bialas, Z. Burda, B. Petersson and J. Tabaczek, *Nucl. Phys. B* **592** (2001) 391. J. Ambjørn, K.N. Anagnostopoulos, W. Bietenholz and F. Hofheinz, *Phys. Rev. D* **65** (2002) 086001.
- [82] R.K. Obousy and G. Cleaver, [arXiv:0805.0019 \[gr-qc\]](#).
- [83] J. Alfaro and G. Palma, *Phys. Rev. D* **65** (2002) 103516; *Phys. Rev. D* **67** (2003) 083003.
- [84] D. Sudarsky, L. Urrutia and H. Vucetich, *Phys. Rev. Lett.* **89** (2002) 231301; *Phys. Rev. D* **68** (2003) 024010. G. Amelino-Camelia, C. Lämmerzahl, A. Macias and H. Müller, *AIP Conf. Proc.* **758** (2005) 30.
- [85] D. Lüst, S. Stieberger and T.R. Taylor, [arXiv:0807.3333 \[hep-th\]](#).
- [86] J.R. Ellis, G. Giudice, M.L. Mangano, I. Tkachev and U. Wiedemann, *J. Phys. G* **35** (2008) 115004.
- [87] D. Colladay and V.A. Kostelecký, *Phys. Rev. D* **58** (1998) 116002.
- [88] R. Bluhm, *Lect. Notes Phys.* **702** (2006) 191 [[hep-ph/0506054](#)].
- [89] V.A. Kostelecký and S. Samuel, *Phys. Rev. D* **39** (1989) 683.
- [90] V.A. Kostelecký, [hep-ph/0104227](#).
- [91] S.M. Carroll, G.B. Field and R. Jackiw, *Phys. Rev. D* **41** (1990) 1231.

- [92] M. Gomes, J.R. Nascimento, E. Passos, A.Yu. Petrov and A.J. da Silva, *Phys. Rev. D* **76** (2007) 047701. T. Mariz, J.R. Nascimento, A.Yu. Petrov, L.Y. Santos and A.J. da Silva, *Phys. Lett. B* **661** (2008) 312.
- [93] J. Gamboa, J. Lopez-Sarrion and A.P. Polychronakos, *Phys. Lett. B* **634** (2006) 471. J.-Q. Xia, H. Li, X.-L. Wang and X.-M. Zhang, *Astron. Astrophys.* **483** (2008) 715.
- [94] D. Colladay and V.A. Kostelecký, *Phys. Rev. D* **55** (1997) 6760.
- [95] V.A. Kostelecký and R. Lehnert, *Phys. Rev. D* **63** (2001) 065008.
- [96] V.A. Kostelecký and R. Potting, *Phys. Rev. D* **51** (1995) 3923.
- [97] J. Collins, A. Perez, D. Sudarsky, L. Urrutia and H. Vucetich, *Phys. Rev. Lett.* **93** (2004) 191301. J. Collins, A. Perez and D. Sudarsky, [hep-th/0603002](#).
- [98] E.E. Antonov, L.G. Dedenko, A.A. Kirillov, T.M. Roganova, G.F. Fedorova and E.Yu. Fedunin, *JETP Lett.* **73** (2001) 446.
- [99] B. Altschul, [arXiv:0805.0781](#) [hep-ph].
- [100] S.R. Coleman and S.L. Glashow, *Phys. Lett. B* **405** (1997) 249.
- [101] H. Sato and T. Tati, *Prog. Theor. Phys.* **47** (1972) 1788. D.A. Kirzhnits and V.A. Chechin, *Yad. Fiz.* **15** (1972) 1051.
- [102] O. Bertolami and C.S. Carvalho, *Phys. Rev. D* **61** (2000) 103002. J.W. Moffat, *Int. J. Mod. Phys. D* **12** (2003) 1279.
- [103] O. Gagnon and G.D. Moore, *Phys. Rev. D* **70** (2004) 065002.
- [104] B. Altschul, *Phys. Rev. D* **77** (2008) 105018.
- [105] S.L. Dubovsky and P.G. Tinyakov, *Astropart. Phys.* **18** (2002) 89.
- [106] A.M. Atoyan and C.D. Dermer, *Astrophys. J.* **586** (2003) 79. P.G. Tinyakov and I.I. Tkachev, *J. Exp. Theor. Phys.* **106** (2008) 481.
- [107] G. Gelmini, O. Kalashev and D.V. Semikoz, *Astropart. Phys.* **28** (2007) 390; *JCAP* **0711** (2007) 002.
- [108] J. Bordes, H.-M. Chan, J. Faridani, J. Pfaudler and S.T. Tsou, *Astropart. Phys.* **8** (1998) 135. P. Jain, D.W. McKay, S. Panda and J.P. Ralston, *Phys. Lett. B* **484** (2000) 267.

- [109] D.J.H. Chung, G.R. Farrar and E.W. Kolb, *Phys. Rev. D* **57** (1998) 4606.
- [110] V.A. Kostelecký and M. Mewes, *Phys. Rev. D* **70** (2004) 076002.
- [111] P. Lipari and M. Lusignoli, *Phys. Rev. D* **60** (1999) 013003.
- [112] G.L. Fogli, E. Lisi, A. Marrone and G. Scioscia, *Phys. Rev. D* **60** (1999) 053006.
- [113] G. Battistoni *et al.*, *Phys. Lett. B* **615** (2005) 14.
- [114] M.C. Gonzalez-Garcia and M. Maltoni, *Phys. Rev. D* **70** (2004) 033010.
- [115] L.B. Auerbach *et al.* (LSND Collaboration), *Phys. Rev. D* **72** (2005) 076004.
- [116] Z. Xiao and B.-Q. Ma, [arXiv:0805.2012 \[hep-ph\]](#).
- [117] T. Tanimori *et al.* (CANGAROO Collaboration), [astro-ph/9710272](#). S.V. Godambe *et al.*, [arXiv:0804.1473 \[astro-ph\]](#).
- [118] F.A. Aharonian *et al.* (HEGRA Collaboration), *Astron. Astrophys.* **349** (1999) 11.
- [119] F. Krennrich *et al.*, [astro-ph/9808333](#).
- [120] G. Amelino-Camelia, J.R. Ellis, N.E. Mavromatos, D.V. Nanopoulos and S. Sarkar, *Nature* **393** (1998) 763.
- [121] G. Amelino-Camelia and T. Piran, *Phys. Lett. B* **497** (2001) 265; *Phys. Rev. D* **64** (2001) 036005.
- [122] R.J. Protheroe and H. Meyer, *Phys. Lett. B* **493** (2000) 1.
- [123] A.K. Konopelko, A. Mastichiadis, J.G. Kirk, O.C. de Jager and F.W. Stecker, *Astrophys. J.* **597** (2003) 851. F.W. Stecker, *Astropart. Phys.* **20** (2003) 85. A. Franceschini, G. Rodighiero and M. Vaccari, [arXiv:0805.1841 \[astro-ph\]](#).
- [124] G. Amelino-Camelia, *New J. Phys.* **6** (2004) 188.
- [125] F.W. Stecker and S.L. Glashow, *Astropart. Phys.* **16** (2001) 97.
- [126] T. Jacobson, S. Liberati and D. Mattingly, *Phys. Rev. D* **67** (2003) 124011.

- [127] P. Mészáros, *Annual Rev. of Astronomy and Astrophysics* **40** (2002) 137. T. Piran, *Rev. Mod. Phys.* **76** (2004) 1143. Y.-Z. Fan and T. Piran, *Front. Phys. China* **3** (2008) 306. V.V. Sokolov, arXiv:0805.3262 [astro-ph].
- [128] E. Waxman, *Phil. Trans. Roy. Soc. Lond.* **A 365** (2007) 1323.
- [129] C.D. Dermer, arXiv:0711.2804 [astro-ph].
- [130] <http://www.eso.org>
- [131] R.J. Gleiser and C.N. Kozameh, *Phys. Rev.* **D 64** (2001) 083007.
- [132] C. Lämmerzahl, A. Macias and H. Müller, *Phys. Rev.* **D 71** (2005) 025007. T. Kahniashvili, G. Gogoberidze and B. Ratra, *Phys. Lett.* **B 643** (2006) 81. F.R. Klinkhamer and M. Risse, *Phys. Rev.* **D 77** (2008) 016002.
- [133] J. Magueijo, *Rept. Prog. Phys.* **66** (2003) 2025.
- [134] G. Amelino-Camelia, *Nature* **418** (2002) 34.
- [135] F.R. Klinkhamer, *JETP Lett.* **86** (2007) 73.
- [136] J. Madore, *Class. and Quant. Grav.* **9** (1992) 69.
- [137] T. Azuma, S. Bal, K. Nagao and J. Nishimura, *JHEP* **0405** (2004) 005. X. Martin, *JHEP* **0404** (2004) 077. M. Panero, *JHEP* **0705** (2007) 082. D. O'Connor and B. Ydri, *JHEP* **0611** (2006) 016. J. Medina, W. Bietenholz and D. O'Connor, *JHEP* **04** (2008) 041. W. Bietenholz, arXiv:0808.2387 [hep-th].
- [138] H.S. Snyder, *Phys. Rev.* **71** (1971) 38.
- [139] F. Dowker, J. Henson and R.D. Sorkin, *Mod. Phys. Lett.* **A 19** (2004) 1829.
- [140] W. Bietenholz, *Fortsch. Phys.* **56** (2008) 107.
- [141] D.B. Kaplan, *Phys. Lett.* **B 288** (1992) 342. W. Bietenholz, A. Gfeller and U.-J. Wiese, *JHEP* **0310** (2003) 018.
- [142] S. Doplicher, K. Fredenhagen and J.E. Roberts, *Phys. Lett.* **B 331** (1994) 39; *Commun. Math. Phys.* **172** (1995) 187.
- [143] D. Amati, M. Ciafaloni and G. Veneziano, *Phys. Lett.* **B 216** (1989) 41. K. Konishi, G. Paffuti and P. Provero, *Phys. Lett.* **B 234** (1990) 276. M. Maggiore, *Phys. Lett.* **B 304** (1993) 65.

- [144] C. Bambi and K. Freese, *Class. Quant. Grav.* **25** (2008) 195013.
- [145] D. Sudarsky, *Int. J. Mod. Phys. D* **17** (2008) 425.
- [146] M.R. Douglas and N.A. Nekrasov, *Rev. Mod. Phys.* **73** (2001) 977.
- [147] A.P. Balachandran, T.R. Govindarajan, G. Mangano, A. Pinzul, B.A. Qureshi and S. Vaidya, *Phys. Rev. D* **75** (2007) 045009. A.P. Balachandran, A. Pinzul, B.A. Qureshi and S. Vaidya, *Phys. Rev. D* **77** (2008) 025020.
- [148] M.M. Sheikh-Jabbari, *Phys. Rev. Lett.* **84** (2000) 5265.
- [149] L. Álvarez-Gaumé and M.A. Vázquez-Mozo, *Nucl. Phys. B* **668** (2003) 293.
- [150] E. Akofer, A.P. Balachandran, S.G. Jo and A. Joseph, *JHEP* **0708** (2007) 045.
- [151] T. Filk, *Phys. Lett. B* **376** (1996) 53.
- [152] S. Minwalla, M. Van Raamsdonk and N. Seiberg, *JHEP* **0002** (2000) 020.
- [153] X. Calmet, B. Jurco, P. Schupp and J. Wess, *Eur. Phys. J. C* **23** (2002) 363.
- [154] S.M. Carroll, J.A. Harvey, V.A. Kostelecký, C.D. Lane and T. Okamoto, *Phys. Rev. Lett.* **87** (2001) 141601.
- [155] N. Seiberg and E. Witten, *JHEP* **9909** (1999) 032. For earlier work along these lines, see *e.g.* A. Abouelsaood, C.G. Callan, C.R. Nappi and S.A. Yost, *Nucl. Phys. B* **280** (1987) 599.
- [156] M. Li and T. Yoneya *Phys. Rev. Lett.* **78** (1997) 1219. T. Yoneya, *Prog. Theor. Phys.* **103** (2000) 1081.
- [157] J. Ambjørn, K.N. Anagnostopoulos, W. Bietenholz, T. Hotta and J. Nishimura, *JHEP* **0007** (2000) 013.
- [158] A. Iorio, *J. Phys. (Conf. Ser.)* **67** (2007) 012008.
- [159] H.J. Groenewold, *Physica* **12** (1946) 405. J.E. Moyal, *Proc. Cambridge Phil. Soc.* **45** (1949) 99.
- [160] R.J. Szabo, *Phys. Rept.* **378** (2003) 207.
- [161] A. Matusis, L. Susskind and N. Toumbas, *JHEP* **0012** (2000) 002.

- [162] G. Amelino-Camelia, L. Doplicher, S.-K. Nam and Y.-S. Seo, *Phys. Rev. D* **67** (2003) 085008.
- [163] R.C. Helling and J. You, [arXiv:0707.1885](https://arxiv.org/abs/0707.1885) [hep-th].
- [164] W. Bietenholz, F. Hofheinz and J. Nishimura, *JHEP* **0405** (2004) 047.
- [165] F. Ruiz Ruiz, *Phys. Lett. B* **502** (2001) 274. K. Landsteiner, E. Lopez and M.H.G. Tytgat, *JHEP* **0106** (2001) 055. Z. Guralnik, R.C. Helling, K. Landsteiner and E. Lopez, *JHEP* **0205** (2002) 025. M. Van Raamsdonk, *JHEP* **0111** (2001) 006.
- [166] A. Sen, *JHEP* **9808** (1998) 012.
- [167] W. Bietenholz, F. Hofheinz and J. Nishimura, *JHEP* **0406** (2004) 042.
- [168] T. Azeyanagi, M. Hanada and T. Hirata, [arXiv:0806.3252](https://arxiv.org/abs/0806.3252) [hep-th].
- [169] W. Bietenholz, J. Nishimura, Y. Susaki and J. Volkholz, *JHEP* **0610** (2006) 042. W. Bietenholz, A. Bigarini, J. Nishimura, Y. Susaki and A. Torrielli, *PoS(LATTICE2007)049*.
- [170] K. Osterwalder and R. Schrader, *Commun. Math. Phys.* **31** (1973) 83; *Commun. Math. Phys.* **42** (1975) 281.
- [171] S. Majid and H. Ruegg, *Phys. Lett. B* **334** (1994) 348.
- [172] J. Ambjørn, Y. Makeenko, J. Nishimura and R.J. Szabo, *JHEP* **9911** (1999) 29; *Phys. Lett. B* **480** (2000) 399; *JHEP* **05** (2000) 023.
- [173] A. Gonzalez-Arroyo and M. Okawa, *Phys. Rev. D* **27** (1983) 2397. A. Gonzalez-Arroyo and C.P. Korthals Altes, *Phys. Lett. B* **131** (1983) 396.
- [174] W. Bietenholz, F. Hofheinz and J. Nishimura, *JHEP* **0209** (2002) 009. W. Bietenholz, A. Bigarini and A. Torrielli, *JHEP* **0708** (2007) 041.
- [175] D.J. Gross and E. Witten, *Phys. Rev. D* **21** (1980) 446.
- [176] R. Peierls, *Z. Phys.* **80** (1933) 763.

- [177] M. Teper and H. Vairinhos, *Phys. Lett.* **B 652** (2007) 359. T. Azeyanagi, M. Hanada, T. Hirata and T. Ishikawa, *JHEP* **0801** (2008) 025.
- [178] Q.-G. Huang and M. Li, *JHEP* **0306** (2003) 014; *JCAP* **0311** (2003) 001. S. Tsujikawa, R. Maartens and R. Brandenberger, *Phys. Lett.* **B 574** (2003) 141. A.H. Fatollahi and M. Hajirahimi, *Europhys. Lett.* **75** (2006) 542; *Phys. Lett.* **B 641** (2006) 381. A.P. Balachandran, A.R. Queiroz, A.M. Marques and P. Teotonio-Sobrinho, *Phys. Rev.* **D 77** (2008) 105032. E. Akofof, A.P. Balachandran, S.G. Jo, A. Joseph and B.A. Qureshi, *JHEP* **0805** (2008) 092. L. Barosi, F.A. Brito and A.R. Queiroz, *JCAP* **0804** (2008) 005. E. Akofof, A.P. Balachandran, A. Joseph, L. Pekowsky and B.A. Qureshi, [arXiv:0806.2458](https://arxiv.org/abs/0806.2458) [astro-ph].
- [179] R. Lehnert, *Phys. Rev.* **D 68** (2003) 085003.
- [180] A. Camacho and A. Macias, *Gen. Rel. Grav.* **39** (2007) 1175.
- [181] J.R. Ellis, N.E. Mavromatos, D.V. Nanopoulos, A.S. Sakharov and E.K.G. Sarkisyan, *Astropart. Phys.* **25** (2006) 402; Erratum [arXiv:0712.2781](https://arxiv.org/abs/0712.2781) [astro-ph].
- [182] S.E. Boggs, C.B. Wunderer, K. Hurley and W. Coburn, *Astrophys. J.* **611** (2004) L77.
- [183] M. Rodriguez Martinez and T. Piran, *JCAP* **0605** (2006) 017.
- [184] J. Albert *et al.* (MAGIC Collaboration), and J.R. Ellis, N.E. Mavromatos, D.V. Nanopoulos, A.S. Sakharov and E.K.G. Sarkisyan, *Phys. Lett.* **B 668** (2008) 253.
- [185] <http://glast.gsfc.nasa.gov/science/>
- [186] R. Lamon, *JCAP* **0808** (2008) 022.
- [187] J.R. Ellis, K. Farakos, N.E. Mavromatos, V.A. Mitsou, D.V. Nanopoulos, *Astrophys. J.* **535** (2000) 139.
- [188] J.R. Ellis, N.E. Mavromatos, D.V. Nanopoulos and G. Volkov, *Gen. Rel. Grav.* **32** (2000) 1777. V. Ammosov and G. Volkov, [hep-ph/0008032](https://arxiv.org/abs/hep-ph/0008032). U. Jacob and T. Piran, *Nature Phys.* **3** (2007) 87. M. Biesiada and A. Piórkowska, *JCAP* **05** (2007) 011. J.R. Ellis, N. Harries, A. Meregaglia, A. Rubbia and A. Sakharov, [arXiv:0805.0253](https://arxiv.org/abs/0805.0253) [hep-ph].

- [189] R.C. Myers and M. Pospelov, *Phys. Rev. Lett.* **90** (2003) 211601.
- [190] P.A. Bolokhov and M. Pospelov, *Phys. Rev. D* **77** (2008) 025022.
- [191] P.M. Crichigno and H. Vucetich, *Phys. Lett. B* **651** (2007) 313.
- [192] C.M. Reyes, L. Urrutia and J.D. Vergara, [arXiv:0806.2166](https://arxiv.org/abs/0806.2166) [hep-ph].
- [193] T.A. Jacobson, S. Liberati, D. Mattingly and F.W. Stecker, *Phys. Rev. Lett.* **93** (2004) 021101.
- [194] V.A. Kostelecký and A.G.M. Pickering, *Phys. Rev. Lett.* **91** (2003) 031801.
- [195] M. Galaverni and G. Sigl, *Phys. Rev. Lett.* **100** (2008) 021102.
- [196] L. Maccione and S. Liberati, [arXiv:0805.2548](https://arxiv.org/abs/0805.2548) [astro-ph].
- [197] L. Maccione, S. Liberati, A. Celotti and J.G. Kirk, *JCAP* **0710** (2007) 013.
- [198] R. Gambini and J. Pullin, *Phys. Rev. D* **59** (1999) 124021.
- [199] A.F. Ferrari, M. Gomes, J.R. Nascimento, E. Passos, A.Yu. Petrov and A.J. da Silva, *Phys. Lett. B* **652** (2007) 174.
- [200] V.A. Kostelecký and M. Mewes, *Phys. Rev. Lett.* **87** (2001) 251304.
- [201] S.A. Abel, J. Jaeckel, V.V. Khoze and A. Ringwald, *JHEP* **0609** (2006) 074.
- [202] T. Heinzl, B. Liesfeld, K.-U. Amthor, H. Schwöerer, R. Sauerbrey and A. Wipf, *Opt. Commun.* **267** (2006) 318.
- [203] K.R. Popper, “Conjectures and Refutations: The Growth of Scientific Knowledge”, Routledge, U.K. (1963).
- [204] <http://www.telescopearray.org/>
- [205] <http://euso.riken.go.jp/>
- [206] <http://owl.gsfc.nasa.gov/>
- [207] M. Pallavicini, R. Pesce, A. Petrolini and A. Thea, [arXiv:0810.5711](https://arxiv.org/abs/0810.5711) [astro-ph].
- [208] <http://agile.asdc.asi.it/>

- [209] <http://www.mpi-hd.mpg.de/hfm/HESS/>
- [210] A. De Angelis, O. Mansutti and M. Persic, *Riv. Nuovo Cim.* **31** (2008) 187.
- [211] S. Basa, J. Wei, J. Paul and S.N. Zhang (for the SVOM Collaboration), [arXiv:0811.1154](https://arxiv.org/abs/0811.1154) [astro-ph].
- [212] <http://www.icecube.wisc.edu/>
F. Halzen, A. Kappes and A. Ó Murchadha, *Phys. Rev. D* **78** (2008) 063004.
- [213] <http://amanda.uci.edu/~anita/>
<http://antares.in2p3.fr/>
<http://www.nestor.org.gr/>
- [214] H. Falcke *et al.* (LOPES Collaboration), *Nature* **435** (2005) 313.
- [215] Pierre Auger Collaboration (J. Abraham *et al.*), *Science* **318** (2007) 939.
- [216] V. Berezhinsky, A.Z. Gazizov and S.I. Grigorieva, [astro-ph/0210095](https://arxiv.org/abs/0811.0210).
- [217] S. Collin, [arXiv:0811.1731](https://arxiv.org/abs/0811.1731) [astro-ph]. P.L. Biermann *et al.*, [arXiv:0811.1848](https://arxiv.org/abs/0811.1848) [astro-ph].
- [218] S.T. Scully and F.W. Stecker, [arXiv:0811.2230](https://arxiv.org/abs/0811.2230) [astro-ph].
- [219] M.-P. Véron-Cetty and P. Véron, *Astron. and Astrophys.* **455** (2006) 773.
- [220] M.R. George, A.C. Fabian, W.H. Baumgartner, R.F. Mushotzky and J. Tueller, [arXiv:0805.2053](https://arxiv.org/abs/0805.2053) [astro-ph].
- [221] G. Ghisellini, G. Ghirlanda, F. Tavecchio, F. Fraternali and G. Pareschi, [arXiv:0806.2393](https://arxiv.org/abs/0806.2393) [astro-ph].
- [222] N.M. Nagar and J. Matulich, [arXiv:0806.3220](https://arxiv.org/abs/0806.3220) [astro-ph].
- [223] T. Stanev, P.L. Biermann, J. Lloyd-Evans, J.P. Rachen and A. Watson, *Phys. Rev. Lett.* **75** (1995) 3056.
- [224] N. Hayashida *et al.* (AGASA Collaboration), *Phys. Rev. Lett.* **77** (1996) 1000.
- [225] R.U. Abbasi *et al.* (High Resolution Fly's Eye Collaboration), *Astrophys. J.* **623** (2005) 164.

- [226] T. Stanev, [arXiv:0805.1746](#) [astro-ph].
- [227] Pierre Auger Collaboration (J. Abraham *et al.*), *Astropart. Phys.* **29** (2008) 188.
- [228] C.-C. Lu and G.-L. Lin, [arXiv:0804.3122](#) [astro-ph].
- [229] A.A. Ivanov (for the Yakutsk Array Group), *Pis'ma v ZhETF* **87** (2008) 215.
- [230] R.U. Abbasi *et al.* (HiRes Collaboration), [arXiv:0804.0382](#) [astro-ph].
- [231] C.D. Dermer, [arXiv:0804.2466](#) [astro-ph].
- [232] D. Gorbunov, P. Tinyakov, I. Tkachev and S. Troitsky, *JETP Letters* **87** (2008) 461; [arXiv:0804.1088](#) [astro-ph].
- [233] M. Kachelrieß, S. Ostapchenko and R. Tomàs, [arXiv:0805.2608](#) [astro-ph].
- [234] D. Allard, M. Ave, N. Busca, M.A. Malkan, A.V. Olinto, E. Parizot, F.W. Stecker and T. Yamamoto, *JCAP* **0609** (2006) 005.
- [235] G. Sigl, [arXiv:0803.3800](#) [astro-ph].
- [236] P.P. Kronberg, *Space Sci. Rev.* **75** (1996) 387.
- [237] D. Fargion, *Phys. Scripta* **78** (2008) 045901.
- [238] R. Aloisio, V. Berezhinsky and S. Grigorieva, [arXiv:0802.4452](#) [astro-ph]. R. Aloisio, V. Berezhinsky and A. Gazizov, [arXiv:0803.2494](#) [astro-ph].
- [239] L. Gonzalez-Mestres, [arXiv:0802.2536](#) [hep-ph].
- [240] D. Allard, N.G. Busca, G. Decerprit, A.V. Olinto and E. Parizot, [arXiv:0805.4779](#) [astro-ph].
- [241] M. Unger (for the Pierre Auger Collaboration), [arXiv:0706.1495](#) [astro-ph].
- [242] Y. Fedorova *et al.* (High Resolution Fly's Eye Collaboration), *Proc. 30th ICRC* (2007) 1236.
- [243] S. Petrerá, [arXiv:0810.4710](#) [astro-ph].